



HAL
open science

Evaluation of atrazine degradation processes in water by electrical discharges and high-frequency ultrasound: parametric optimization and study of reaction mechanisms

Junting Hong

► **To cite this version:**

Junting Hong. Evaluation of atrazine degradation processes in water by electrical discharges and high-frequency ultrasound: parametric optimization and study of reaction mechanisms. Chemical and Process Engineering. Université de Technologie de Compiègne, 2024. English. NNT : 2024COMP2804 . tel-04667989

HAL Id: tel-04667989

<https://theses.hal.science/tel-04667989>

Submitted on 6 Aug 2024

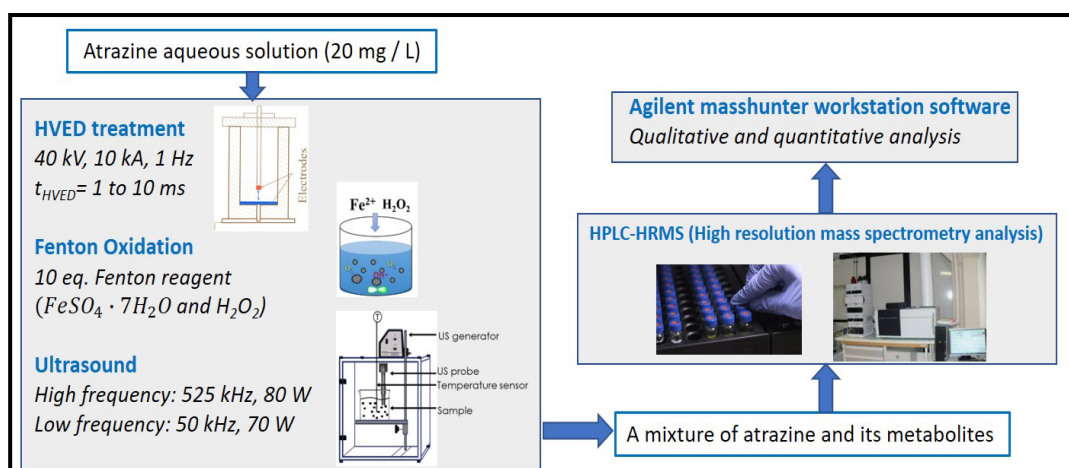
HAL is a multi-disciplinary open access archive for the deposit and dissemination of scientific research documents, whether they are published or not. The documents may come from teaching and research institutions in France or abroad, or from public or private research centers.

L'archive ouverte pluridisciplinaire **HAL**, est destinée au dépôt et à la diffusion de documents scientifiques de niveau recherche, publiés ou non, émanant des établissements d'enseignement et de recherche français ou étrangers, des laboratoires publics ou privés.

Par Junting HONG

Evaluation of atrazine degradation processes in water by electrical discharges and high-frequency ultrasound: parametric optimization and study of reaction mechanisms

Thèse présentée
pour l'obtention du grade
de Docteur de l'UTC



Soutenu le 15 avril 2024
Spécialité : Génie des Procédés et Chimie

Evaluation of atrazine degradation processes in water by electrical discharges and high- frequency ultrasound: parametric optimization and study of reaction mechanisms

Par **Junting HONG**

Spécialité : Génie des Procédés et Chimie

Soutenue le 15 avril 2024 devant le jury composé de :

M ^{me} . Laurie Barthe	Maitre de conférences HDR, INP-ENSIACET Toulouse	Rapporteur
M. Stéphane Baup	Professeur, Université de Grenoble alpes, Grenoble	Rapporteur
M ^{me} . Hélène Blanchoud	Maitre de conférences HDR, École Pratique des Hautes Études Paris	Examineur
M. Erwann Guénin	Professeur, UTC, Compiègne	Examineur
M. Franck Merlier	Ingénieur de recherche, UTC, Compiègne	Directeur de thèse
M. Nabil Grimi	Professeur, UTC, Compiègne	Directeur de thèse
M ^{me} . Nadia Boussetta	Maitre de conférences, UTC, Compiègne	Invitée
M. Gérald Enderlin	Enseignant-chercheur, ESCOM, Compiègne	Invité

Évaluation des procédés de dégradation de l'atrazine
dans l'eau par décharges électriques et par ultrasons
hautes fréquences : optimisation paramétrique et étude
des mécanismes réactionnels

Par **Junting HONG**

Spécialité : Génie des Procédés et Chimie

Soutenue le 15 avril 2024

Acknowledgements

This thesis work lasted for 42 months from 2020 to 2024 and was conducted in the laboratory of Integrated Transformations of Renewable Matter (TIMR), Agro-Industrial Technologies (TAI) team, and Enzyme and Cell Engineering Unit (GEC) at Université de Technologie de Compiègne (UTC). First of all, I would like to express my sincere gratitude to all those who contributed at various levels to the completion of this thesis.

I would like to thank the China Scholarship Council (CSC) for providing me with the scholarship, which enabled me to carry out my work under good conditions.

I am extremely grateful to my supervisors M. **Nabil Grimi** and M. **Franck Merlier** for providing research inspiration and academic guidance throughout my PhD studies. Their profound knowledge and professionalism greatly helped me complete my thesis. I am also thankful to my co-supervisors M^{me}. **Nadia Boussetta** and M. **Gérald Enderlin** for their help in the fields of high voltage electrical discharge technology and chemistry respectively. I am very grateful to all of them. They made careful corrections and suggestions for every article I published. Their patience, understanding, kindness and encouragement gave me enough courage to solve all difficulties in work and life.

I would like to express my appreciation to M^{me}. **Laurie Barthe**, M. **Stéphane Baup**, M^{me}. **Hélène Blanchoud** and M. **Erwann Guénin** for their valuable time as referees. Their useful suggestions further improved my thesis and gave me more inspiration for the future work.

Many thanks to my dear colleagues **Yuqi Huang, Shuli Liu, Adila Gherabli, Sarah Joe Salameh, Nicole Najjoun, Anissa Khelfa, Sara Mitri, Georgio Nemer, Etienne Diemer**. The memories of our working together and helping each other in the laboratory are unforgettable.

Finally, I would like to thank my parents and brother for their long-term companionship and firm support. I hope I can keep learning and become a better version of myself in the future.

Abstract

The main goal of this thesis is to develop an efficient technology for the degradation of pesticides. For this purpose, the widely used herbicide atrazine was studied as a model molecule. Atrazine was degraded in water by high voltage electrical discharge (HVED), and its degradation performance was compared with traditional water treatment technologies Fenton oxidation and ultrasound (US).

The detection and quantification of atrazine and its metabolites were achieved by high performance liquid chromatography-high resolution mass spectrometry (HPLC-HRMS). An online analysis method by HPLC-HRMS combined with automatic sampling was developed for real-time monitoring of the degradation process.

The HVED technology efficiently degraded atrazine and reduced toxic metabolites generated during Fenton oxidation and US processes. HVED process has less energy consumption than US process while achieving the same 89% atrazine degradation efficiency. The mechanism pathways of atrazine degradation for different technologies were proposed.

The effect of real matrix (tap water) versus model matrix (deionized water) on atrazine degradation was studied. Results showed that in HVED treatment, the degradation efficiency of atrazine in tap water was lower than that in deionized water, which may be related to the conductivity of the water and to the mechanism of electric arcs generation in a conductive medium. The acute toxicity (LC_{50}) in *Daphnia magna* was used to evaluate the toxicity of different treatment solutions initially containing atrazine. The toxicity of atrazine solution treated by Fenton oxidation is higher than that treated by HVED and US.

Keywords: Pesticide; Atrazine; High voltage electrical Discharge; Ultrasound; Fenton oxidation; Degradation metabolites; Mass spectrometry; Acute toxicity

Résumé

L'objectif principal de la thèse est de développer une technologie efficace pour la dégradation des pesticides. L'herbicide atrazine a été étudié comme molécule modèle. L'atrazine a été dégradée dans l'eau par décharge électrique de haute tension (DEHT), et ses performances de dégradation ont été comparées aux technologies traditionnelles d'oxydation de Fenton et d'ultrasons (US).

La détection et la quantification de l'atrazine et de ses métabolites ont été réalisées par chromatographie liquide haute performance et spectrométrie de masse à haute résolution (HPLC-HRMS). Une méthode d'analyse en ligne par HPLC-HRMS combinée à un échantillonnage automatique a été développée pour un suivi en temps réel du processus de dégradation.

La technologie DEHT a dégradé efficacement l'atrazine et a réduit les métabolites toxiques générés au cours des processus d'oxydation de Fenton et d'US. Le procédé de DEHT est moins consommateur d'énergie que le procédé d'US tout en atteignant la même efficacité de dégradation de l'atrazine de 89%. Les mécanismes de dégradation de l'atrazine pour les différentes technologies ont été proposés.

L'effet d'une matrice réelle (eau du robinet) par rapport à une matrice modèle (eau déminéralisée) sur la dégradation de l'atrazine a été étudié. Les résultats ont montré que dans le cas d'un traitement par DEHT, l'efficacité de dégradation de l'atrazine dans l'eau du robinet était inférieure à celle de l'eau déminéralisée, ce qui peut être lié à la conductivité de l'eau et au mécanisme de génération des arcs électriques dans un milieu conducteur. La toxicité aiguë (CL₅₀) chez la daphnie *Daphnia magna* a été utilisée pour évaluer la toxicité des différentes solutions de traitement contenant initialement de l'atrazine. La toxicité de la solution d'atrazine traitée par oxydation de Fenton est supérieure à celle traitée par DEHT et US.

Mots-clés: Pesticide; Atrazine; Décharge électrique à haute tension; Ultrason; Oxydation de Fenton; Métabolites de dégradation; Spectrométrie de masse; Toxicité aiguë

List of publications

I. Publications in international journals

- (1) Hong J., Boussetta N., Enderlin G., Merlier F., Grimi N. (2022). Degradation of Residual Herbicide Atrazine in Agri-Food and Washing Water. *Foods*, 11, 2416.
- (2) Hong J., Boussetta N., Enderlin G., Grimi N., Merlier F. (2022). Real-Time Monitoring of the Atrazine Degradation by Liquid Chromatography and High-Resolution Mass Spectrometry: Effect of Fenton Process and Ultrasound Treatment. *Molecules*, 27, 9021.
- (3) Hong J., Boussetta N., Enderlin G., Merlier F., Grimi, N. (2023). Degradation of herbicide atrazine in water by high voltage electrical discharge in comparison with Fenton oxidation and ultrasound treatments. *RSC Sustainability*, 1, 1462-1470.
- (4) Hong J., Revel M., Firmin S., Boussetta N., Enderlin G., Merlier F., Grimi, N. Degradation of atrazine in French tap water by high voltage electrical discharge (HVED) and high frequency ultrasound (HFUS), with normalized statistical analysis and acute *Daphnia magna* toxicity test. (prepared for publication).

II. Conferences « Oral presentation » :

- (1) Hong J., Boussetta N., Enderlin G., Merlier F., Grimi N. Degradation of pesticide atrazine by high voltage electrical discharges. Workshop "L'agroécologie au service d'une bioéconomie durable, mythe ou réalité ?". 19 November 2021, UniLaSalle, Beauvais, France.
- (2) Hong J., Boussetta N., Enderlin G., Merlier F., Grimi N. Etude de la dégradation d'atrazine par décharges électriques. Journées Formulation de la Société Chimique de France : « Substitution et Reformulation : défis d'aujourd'hui, produits de demain. 29 Novembre - 1 Décembre 2021, Université de Technologie de Compiègne.
- (3) Hong J., Boussetta N., Enderlin G., Merlier F., Grimi N. Impact of high voltage electrical discharges on the degradation of pesticides in water. École d'été « 8th School on Pulsed Electric Field Application in Food and Biotechnology», 30 Mai - 3 Juin 2022, Université de Technologie de

Compiègne.

- (4) Hong J., Boussetta N., Enderlin G., Merlier F., Grimi N. Impact des décharges électriques de hautes tensions sur la dégradation des pesticides dans l'eau. Congrès « 18ème congrès de la Société Française de Génie des Procédés, Sciences et solutions technologiques pour la transition ». 7-10 Novembre 2022, Centre de Congrès Pierre Baudis, Toulouse.
- (5) Hong J., Boussetta N., Enderlin G., Merlier F., Grimi N. Degradation of pesticide atrazine in water by high voltage electrical discharges. Le 2ème colloque interUT « Technological Systems, Sustainability and Safety ». 6-7 February 2024, Sorbonne Université, Paris.

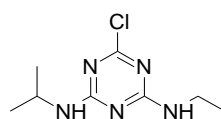
Table of contents

General Introduction	12
Chapter I. Literature review	17
I.1. Introduction	17
I.2. Chemical methods for atrazine degradation	19
I.3. Biological methods for atrazine degradation	27
I.4. Physicochemical methods for atrazine degradation	29
I.5. Atrazine degradation pathways, atrazine mineralization and metabolites toxicity	35
I.6. Conclusion and research objectives	40
I.7. References	44
Chapter II. Methods and protocols	44
II.1. Methodology	67
II.2. Development and validation of analytical methods for real-time monitoring atrazine degradation process by HPLC-HRMS	67
II.3. Effects of different technologies (HVED, US and Fenton oxidation) on atrazine degradation	70
II.4. Practical application of atrazine degradation in tap water & toxicity test of experimental wastewater	71
II.5. Organization of chapters III, IV, and V	72
Chapter III. Development and validation of analytical methods for real-time monitoring atrazine degradation process by HPLC-HRMS	73
III.1. Chapter introduction	73
III.2. Real-time monitoring of the atrazine degradation by liquid chromatography and high-resolution mass spectrometry: effect of Fenton process and ultrasound treatment	74
III.3. Chapter conclusion	97
III.4. References	98
Chapter IV. Effects of different technologies (HVED, US and Fenton oxidation) on atrazine degradation	103
IV.1. Chapter introduction	103
IV.2. Degradation of herbicide atrazine in water by high voltage electrical discharge in comparison with Fenton oxidation and ultrasound treatments	104
IV.3. Chapter conclusion	121
IV.4. References	122
Chapter V. Practical application of atrazine degradation in tap water & toxicity test of experimental wastewater	127

V.1. Chapter introduction.....	127
V.2. Degradation of atrazine in French tap water by high voltage electrical discharge (HVED) and high frequency ultrasound (HFUS), with normalized statistical analysis and acute <i>Daphnia magna</i> toxicity test.....	128
V.3. Chapter conclusion.....	143
V.4. References	145
General Conclusion and Prospects	149

General Introduction

Nowadays, in order to increase agricultural production, more and more pesticides are used. It is reported that the global average annual pesticide consumption is 2 million tons [1], and the average annual sales of pesticides in the EU is 360,000 tons [2]. France is the second largest pesticide consumer among EU member states, and the extensive use of pesticides has led to widespread pesticide residues in French soil [3]. There is pesticide contamination in French groundwater, including triazine herbicide (e.g. atrazine) and organochlorine pesticides (e.g. chloridazon) [4]. In this thesis, atrazine was chosen as the model molecule, and its chemical structure shows as follow.



Atrazine

(2-chloro-4-ethylamino-6-isopropylamino-1,3,5-triazine)

Atrazine is one of the commonly used herbicides for corn, sorghum and sugarcane cultivation in the United States, Brazil, China and other countries [5]. Although atrazine was withdrawn from the European market in 2003 [6], the concentration of atrazine in groundwater still exceeded 0.1 µg/L in some European areas [7-9]. As a general precautionary limit value, the quality standard of groundwater for each pesticide is set as 0.1 µg/L [10]. The French government "Ministry of Solidarity and Health" have collected the data of health control of water distributed commune by commune, updated on September 2023 [11], according to which the maximum concentrations of atrazine and its metabolites detected in tap water exceeded 0.1 µg/L in some French cities. It is reported that atrazine causes reproductive dysfunction [12] and disrupts the endocrine system [13], and may lead to breast cancer [14]. Due to its chemical stability, atrazine has a long half-life in water, 30-100 days [15]. Residues of atrazine in aquatic environment remain a concern.

There have been many attempts to degrade atrazine in aqueous environments. The existing atrazine degradation methods can be broadly divided into three categories: chemical methods, including Fenton oxidation [16, 17], ozone oxidation [18, 19], sulfate-radical-based oxidation [20, 21], etc; biological methods,

including microbial degradation [22, 23] and phytodegradation [24, 25]; physical and chemical methods, including ultrasound [26, 27], high voltage electrical discharges [28, 29], microwave [30], etc. However, these methods lead to diverse degradation pathways of atrazine and generate degradation metabolites with different toxicities, some of which are even more toxic than the substrate atrazine, causing greater harm to humans and the environment [15]. So, it is significant to study the degradation efficiency, metabolism, and toxicity of atrazine in different degradation processes.

Since atrazine has high antioxidant capacity and is resistant to some common reactive oxygen species such as hydrogen peroxide H_2O_2 and ozone O_3 , it is necessary to convert H_2O_2 and ozone O_3 into non-selective and highly reactive hydroxyl radicals $HO\cdot$ [31, 32]. Generally, hydroxyl radical $HO\cdot$ is the main reactive oxygen species responsible for the degradation of refractory pollutants [33]. As consequence, the advanced oxidation processes (AOPs) came into consideration, which was proposed in 1987 based on the emphasis on generating hydroxyl radicals $HO\cdot$ [34]. The following three AOPs were used in this thesis: Fenton oxidation, ultrasound (US) treatment and high voltage electrical discharges (HVED) treatment.

In Fenton oxidation, hydrogen peroxide H_2O_2 generates hydroxyl radicals $HO\cdot$ under the catalytic activation of Fe^{2+} ferrous ions [31]. In order to reduce the consumption of Fenton reagent and improve degradation efficiency, the combination processes of Fenton oxidation and other technologies are favored, such as sono-Fenton [35], photo-Fenton [36] and electro-Fenton [37]. In these combination processes, hydrogen peroxide H_2O_2 acts as a source of radicals through a dissociation process and also acts as a scavenger of the generated radicals [38]. Besides, for hydrogen peroxide H_2O_2 generated in situ in a system such as ultrasound, the additional addition of ferrous ions Fe^{2+} promotes degradation of contaminants [39]. So, in this thesis, the effect of hydrogen peroxide H_2O_2 and ferrous ion Fe^{2+} concentration during Fenton oxidation was studied, as was the effect of additional ferrous ions Fe^{2+} during US and HVED treatments.

In US treatment, bubbles in liquids cyclically form, grow and implode, which means that contaminant degradation occurs in reactional areas: the cavitation

bubble, the bubble/solution interface, and the bulk of the solution [40]. The chemical bonds of water molecules H_2O are homogeneously split under the high energy of ultrasonic cavitation bubble rupture, producing hydroxyl radicals $HO\cdot$ ejected towards the solution bulk to oxidize hydrophilic pollutants [41]. The solubility of atrazine is 34.7 mg/L in water [42]. In this thesis, the initial concentration of atrazine is fixed at 20 mg/L, so radicals $HO\cdot$ in the solution bulk play an important role in atrazine degradation. In addition, in 2017 & 2022, Barthe et al [43, 44]. have studied the effect of ultrasound frequency on sonochemistry and found that high frequency is the first choice because: although the cavitation threshold increases at high frequency (>100 kHz) and the energy released by cavity collapse decreases, the acoustic period required for bubble resonance becomes shorter, cavitation events occur more frequently; bubbles collapse faster, which is conducive to free radicals (e.g. $HO\cdot$) escaping before recombination. So, this thesis studies the effect of low and high frequency (50 kHz and 525 kHz) ultrasound on the degradation of atrazine.

In HVED treatment, the violent electrical discharges cause water molecules H_2O to dissociate under the bombardment of high-energy electrons, promoting the generation of highly reactive oxidative species such as hydroxyl radicals $HO\cdot$, singlet 1O_2 , ozone O_3 , UV photons, etc [45]. Although the reactive oxygen species generated during the electrical discharges process are complex, hydroxyl radicals $HO\cdot$ play a dominant role in the treatment of water solutions [46]. The degradation of atrazine by HVED is still under development. Most of the existing HVED treatments [47-49] focuses on the design of the electrical discharge reactor and atrazine degradation efficiency, without comparison with other technologies. So, in this thesis, a comparative study was conducted on atrazine degradation treated by HVED, US treatment and Fenton oxidation to evaluate the degradation performance during the processes, including atrazine degradation efficiency, metabolites formation kinetics, degradation mechanism pathways, toxicity and energy consumption.

In order to achieve the above evaluation of degradation performance, a good analytical method is necessary. The commonly used analytical method for tracking the evolution of atrazine and its metabolites is liquid chromatography-

mass spectrometry (LC-MS) with a UV detector [50, 51]. High-resolution mass spectrometry (HRMS) provides extra selectivity and high-resolution accurate-mass full-spectrum acquisition [52], which has enhanced performance in terms of confirmatory capabilities than low-resolution tandem mass spectrometry (MS/MS) [53]. So, in this thesis, HPLC-HRMS was adopted for analysis.

Therefore, the goal of this thesis is to develop an innovative and efficient technology for degrading pesticide atrazine, as well as a new analytical method for monitoring the evolution of atrazine and its metabolites during the degradation processes. This thesis is divided into five chapters and accompanied by four publications:

Chapter I provides a literature review on atrazine degradation technologies over the past two decades. This part of work has been published in journal *Foods* [15].

This chapter concludes the research works of atrazine degradation in aqueous solutions classified by chemical method, biodegradation and physicochemical methods. These methods are compared by their degradation performance (atrazine degradation efficiency, metabolites formation kinetics, degradation mechanism pathways, toxicity, treatment time and energy consumption). The research objectives are concluded.

Chapter II describes methods and protocols of this thesis.

Chapter III develops a new analytical method for monitoring the evolution of atrazine and its metabolites by HPLC-HRMS. The results of this chapter demonstrate the feasibility of HPLC-HRMS for real-time monitoring of the kinetics of atrazine and its metabolites during the Fenton oxidation and US processes. Automatic sampling coupled with the HPLC-HRMS system increased the sampling frequency and decreased the sample analysis time. The degradation of potentially unstable metabolites was prevented. The results of chapter III were published in the journal *Molecules* [54].

Chapter IV studies the effects of different technologies (HVED, US and Fenton oxidation) on atrazine degradation. The results of this study describe a comparative study on atrazine degradation by HVED treatment, US treatment and

Fenton oxidation, followed by the proposed atrazine degradation pathways. HVED treatment proved to be more advantageous due to the higher degradation efficiency, less-toxic generated metabolites and lower energy consumption. The results of the chapter IV were published on the international journal RSC Sustainability [55].

Chapter V describes the practical application of atrazine degradation in tap water and the toxicity test of experimental wastewater. This experimental study evaluates the effect of a real matrix (tap water) compared to the model matrix (deionized water) for atrazine degradation by HVED and US techniques, followed by the normalized statistical analysis of the differences in metabolites between different treatments. The results of the chapter V were summarized in an article and prepared for publication.

Chapter I. Literature review

Atrazine, an herbicide used to control grassy and broadleaf weed, has become an essential part of agricultural crop protection tools. It is widely sprayed on corn, sorghum and sugar cane, with the attendant problems of its residues in agri-food and washing water. If ingested into humans, this residual atrazine can cause reproductive harm, developmental toxicity and carcinogenicity. It is therefore important to find clean and economical degradation processes for atrazine. In recent years, many physical, chemical and biological methods have been proposed to remove atrazine from the aquatic environment.

In this chapter, works on atrazine degradation technology in the two decades are introduced by method classification. These methods are then compared by their advantages, disadvantages, and different degradation pathways of atrazine. Moreover, the existing toxicological experimental data for atrazine and its metabolites are summarized. Finally, the directions for future research and major challenges are proposed. This part of work has been published in journal "Foods" [15].

1.1. Introduction

Atrazine (Figure 1) is a triazine herbicide with a wide range of applications, for grassy and broadleaf weed control in corn, sugarcane, sorghum and certain other crops [56-59]. Due to its efficiency and low cost, its average consumption worldwide is 70,000 to 90,000 tons per year [60]. If shopping for conventional groceries, consumers are likely to have eaten food that has been sprayed with atrazine. Since atrazine is applied to crops used as livestock feed, its residues are found not only in crops, but also in milk and meat. According to the consumer risk assessment performed by the European Food Safety Authority [61], atrazine input values used for the dietary chronic exposure calculation of maize and other cereals except maize are 0.025 mg/kg and 0.05 mg/kg, respectively, based on the mean consumption data representative for 22 national diets. Although not considered acutely toxic to people, atrazine affects long term human health. Atrazine can act as the endocrine disrupting chemicals (EDC) [62] that can produce damage to the endocrine system, and cause a series of pathological changes and reproductive

abnormalities [13]. Additionally, atrazine is also a potential carcinogen due to negative impact on human health such as tumors, breast, ovarian, and uterine cancers as well as leukemia and lymphoma [63]. For these reasons, atrazine was banned in the European Union (EU) in 2003 [6]. However, the commercial formulations of the herbicide atrazine (such as Gesaprim 90% WG) are still widely employed in Latin America. For example, herbicides were the main pesticide class used in Brazil between 2009 and 2018, with oscillations from 52.4% (2011) to 62.5% (2012), and atrazine was the top two active ingredient in this period [64]. Brazil is the world's third biggest exporter of agricultural products and organic food market leader in Latin America [65]. In addition, Brazil's main export markets are the European Union and the United States [66]. So, the residual problem of atrazine still remains a concern. Atrazine is chemically stable with long half-life in water (30–100 days) [67, 68], and its microbial degradation in soil environments is a relatively slow process (the range of field half-lives is 18 to 148 days [69, 70]). It is also slightly soluble in water (33 mg.L⁻¹ at 22 °C) and has low adsorption in soil [71]. Thus, it contaminates both surface and ground water [72]. The upper limit for atrazine in drinking water is 3 µg/L in America whereas in Europe, it is fixed as 1 µg/L [73, 74]. However, investigations [75-77] have shown that concentrations of atrazine exceed the authorized limit of water contamination in surface water and ground water. Lots of works [78-83] have been conducted on the detection and quantification of atrazine in water, which is important to the food safety and quality control. Controlling the pollution of residual atrazine in agri-food and washing water has become a major issue.

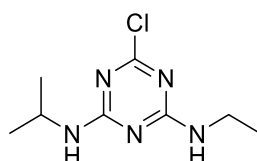


Figure 1. Atrazine (2-chloro-4-ethylamino-6-isopropylamino-1,3,5-triazine).

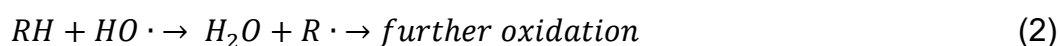
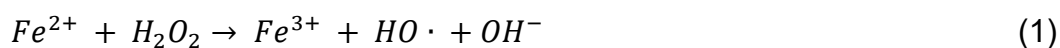
So far, many treatment technologies of aqueous atrazine have been developed, including microwave assisted photo reactions, advanced oxidation processes (AOPs), bioremediation, etc. This review summarizes recent degradation progress of atrazine in water, with an emphasis on current chemical methods (Fenton/Fenton-Like Method [17, 31, 84-88], Sulfate Radical Oxidation

[20, 89-94], Photocatalytic Method [95-99], Electrocatalytic Method [100-104], Ozone Oxidation Method [105-109]), Biodegradation (Microbial Degradation [110-114] and Phytodegradation [115-119]) and physicochemical methods (High Voltage Electrical Discharges [45, 47-49, 120-122], Ultrasound [41, 123, 124], Microwave [125-127] and Ionizing Radiation [128-130]). Although two recently published reviews [131, 132] also describe atrazine degradation techniques, they do not cover degradation methods comprehensively. This review not only expands the atrazine degradation techniques, but also compares them in terms of degradation pathways, atrazine mineralization, and metabolite toxicity.

I.2. Chemical methods for atrazine degradation

I.2.1. Fenton/Fenton-Like Method

The classical Fenton reaction describes the activation of hydrogen peroxide (H_2O_2) by ferrous (Fe^{2+}) ions to generate hydroxyl radicals ($HO\cdot$) [58]. The hydroxyl radical abstracts a hydrogen atom from organic substrate ($R-H$), and generates an organic radical ($R\cdot$), which subsequently undergoes a series of chemical transformation to form various oxidation products. The reactions are as follows:



Although the classic Fenton oxidation achieves the generation of free radicals and has strong oxidizing ability under ambient conditions, insoluble ferric hydroxide precipitates are generated during the process, which reduces the overall oxidation efficiency and requires continuous addition of Fe^{2+} salt. Therefore, Fenton-like methods with higher oxidation efficiency have been developed. For example, photo-Fenton, electro-Fenton and sono-Fenton are improvements of Fenton oxidation combined with photochemistry, electrochemistry, and ultrasound, respectively, and they have been used for the degradation of aqueous atrazine. In 2002, Ventura et al. [31] designed an electro-Fenton system and used it for the degradation of atrazine. The electro-Fenton system could continuously produce the ferrous iron and the hydrogen peroxide, thereby allowing more efficient generation of $HO\cdot$, which led to a more thorough oxidation of atrazine. In the same

year, Saltmiras et al. [84] published a similar work using anodic Fenton treatment to degrade 70% of atrazine in 3 min.

In 2020, Yang et al. [133] prepared a heterogeneous Fenton catalyst Fe/TiO_2 using TiO_2 synthesized by sol-gel method as carrier and ferric nitrate as Fe source, which could effectively remove atrazine under visible light, achieving over 95% removal efficiency within 30 min. In 2020, Shi et al. [134] reported Fe_3S_4 Fenton oxidation of atrazine using visible light, and atrazine was completely degraded within 35 min. In 2021, Fareed et al. [135] adopted the $UV/FeCl_3/H_2O_2$ system and achieved a 97% degradation rate of atrazine. In addition, the use of iron-modified mesoporous molecular sieve materials to degrade atrazine using UV-vis irradiation was reported by Benzaquén et al. [136]. Additionally, there are other related photo-Fenton systems, using tantalum (oxy)nitrides to prepare photocatalytic materials, on the degradation of aqueous atrazine [86, 87, 137, 138]. In the past two years, there have been new attempts at photocatalysts on atrazine degradation by photo-Fenton. In 2023, Cai et al. [17] used Iron-doped bismuth oxybromides Fe-BiOBr to degrade atrazine under visible light (97% degradation efficiency in 120 min). In the same year, Carmelo da Rocha et al. [88] used basalt powder as a natural heterogeneous catalyst for degrading atrazine under ultra-violet irradiation (96% degradation efficiency in 180 min).

The stepwise-Fenton's processes for the degradation of atrazine were developed by Chu et al. in 2007 [85]. And according to the system models built through the examination of reaction kinetics, they found that the performance of stepwise- Fenton's processes was better than that of conventional Fenton's processes.

1.2.2. Sulfate Radical (SO_4^-) Oxidation Method

Compared with OH , the sulfate radical SO_4^- has a higher redox potential, longer half-life, and higher selectivity for electron transport reactions, receiving increasing attention on the degradation of pollutants [89]. So far, there are many generation methods of SO_4^- for atrazine removal (Table 1).

Table 1. Generation methods of SO_4^- for atrazine removal.

Generation Methods	Removal Effect
Carbon sheet fabricated from corn straw and potassium oxalate activated persulfate.	97.2% of atrazine was removed by the system within 20 min, when the concentration of persulfate was 2 mM [89].
Biochar supported nZVI composites (nZVI@BC) activated persulfate.	The atrazine removal rate was up to 93.8% [90].
Siderite/ $CaSO_3$ system was used to provide Fe^{2+} to activate sulfite.	>90% atrazine was removed within 6 min at 45 °C [91].
Pyrite activated persulfate.	100% of atrazine was degraded in 45 min and the TOC(total organic carbon) removal efficiency was 26% within 7 h [92].
Mechano chemically synthesized S-ZVI ^{bm} composites activated persulfate.	The degradation of atrazine was up to 90%, which was pH-independent [93].
Nanoscale $LaFe_{1-x}Cu_xO_{3-\delta}$ perovskite activated peroxymonosulfate.	Atrazine (23 μ M) was removed completely within 60 min in the presence of 0.5 g/L catalyst and 0.5 mM peroxymonosulfate [139].
Composite of nanoscale zero valent iron and graphene activated persulfate.	92.1% of atrazine was removed within 21 min using mass ratio of 5:1 nanoscale zero-valent iron (nZVI) to graphene (GR) [140].
Natural negatively-charged kaolinite with abundant hydroxyl groups activated peroxymonosulfate.	When the kaolinite dosage increased to 1.0 g/L, the degradation of atrazine exceeded 90% at 60 min [141].
Cobalt-impregnated biochar activated peroxymonosulfate.	99% of atrazine was degraded within 6 min [142].
Co-doped mesoporous $FePO_4$ activated peroxymonosulfate.	100% of atrazine was degraded for CoFeP-0.1 after 30 min at pH = 7 [143].
$LaCoO_3/Al_2O_3$ activated peroxymonosulfate.	Under the optimal conditions, the removal rate and mineralization efficiency of ATZ reached 100% and 30.8%, respectively [144].
Copper sulfide activated persulfate.	The degradation of atrazine was up to 91.6% [145]
Hydroxylamine drinking water treatment residuals activated peroxymonosulfate.	The removal efficiency of atrazine was 95.5% in 30 min [146].
Fe_3O_4 -sepiolite activated persulfate.	71.6% of atrazine and 20% of solution TOC were removed after 60 min [147].
CoMgAl layered double oxides activated	The degradation of atrazine was up to

peroxymonosulfate.	98.7% [148].
Cysteine and Fe ₃ O ₄ activated persulfate.	The atrazine removal was 72.3 % in 360 min [20].
Hydrangea-like NiCo ₂ S ₄ heterogeneous catalyst activated peroxymonosulfate (PMS).	Atrazine was degraded into intermediates with reduced toxicity in NiCo ₂ S ₄ /PMS [94].

In addition, there are processes that combine sulfate radical oxidation with other technologies such as UV-vis [149-151]. The photocatalysis technology is needed for the activation of sulfite to generate SO_4^- effectively at the neutral pH condition without any precipitation of metal-hydroxyl species, thus greatly improving the degradation rate of atrazine.

1.2.3. Photocatalytic Method

Photocatalysis generally refers to a photochemical reaction with the participation of a catalyst. Under the irradiation of ultraviolet or visible light, electron-hole pairs are created by photocatalysts, which generate free radicals such as OH able to oxidize and decompose organic pollutants. The image below (Figure 2) refers to reference [152].

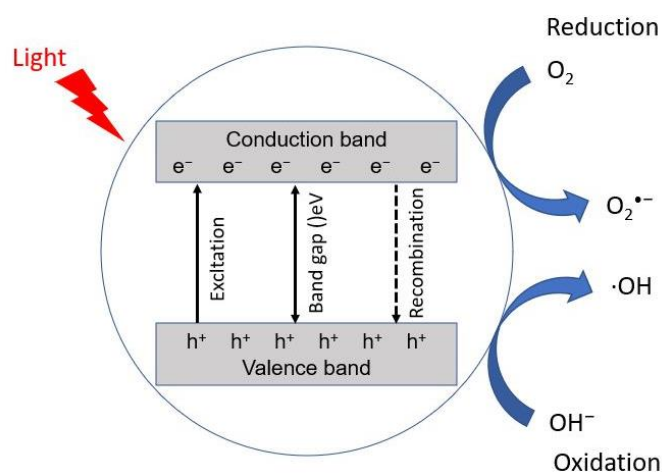


Figure 2. Schematic representation of mechanism of photocatalysis.

The general photocatalysts are N-type semiconductor materials, which have the characteristics of low band gap, such as TiO_2 , ZrO_2 , ZnO , CdS , WO_3 , Fe_2O_3 , Bi_2O_3 , etc. Among them, Ti -based, W -based, and Bi -based materials and their oxides are commonly used in the photodegradation of aqueous atrazine (Table 2).

In addition, photoelectrocatalysis (PEC), which combines both electrochemistry and photocatalysis, has also been used in the degradation of aqueous atrazine. In 2018, Fernández-Domene et al. [153] reported the degradation of atrazine by photo-electrocatalysis using a photoanode based on WO_3 nanosheets. Atrazine was completely degraded after 180 min. In 2021, Xie et al. [154] used the bias potential applied on the photo-anode to achieve a 96.8% removal efficiency of atrazine.

The photocatalytic method has received widespread attention because of its high efficiency, non-toxicity, and lack of secondary pollution. It is recommended to use visible light catalytic process to degrade atrazine, because the use of solar energy is sustainable and environmentally friendly.

Table 2. Photodegradation of aqueous atrazine.

Photocatalyst	Preparation	Light Source	Removal Effect
In, S-TiO ₂ @rGO nanocomposite	TiO ₂ @rGO nanocomposites were synthesized based on a new ultrasonic-assisted hydrothermal method.	Visible-light, a 300 W tungsten xenon lamp.	The complete degradation and 95.5% mineralization of atrazine was achieved within 20 min [95].
Boron-doped TiO ₂	Used a one-step calcination method.	Visible-light, a 350 W (15 A) Xenon lamp with a 300 nm cutoff filter (CHF-XM-350 W, Beijing Trusttech. Co., Beijing, China).	The degradation of atrazine was up to 95% [96].
Metalloporphyrins supported on TiO ₂	Tetra (4-carboxyphenyl) porphyrin with different metal centers and metal-free was adsorbed on TiO ₂ surface.	Visible-light, an open borosilicate (Pyrex) glass cell with an optical window of 11 cm ² area.	82% of atrazine was degraded using Cu(II) porphyrin within 1 h [97].
Crystal TiO ₂ nanowires with high specific surface area	Use a PEG-assisted hydrothermal method.	UV irradiation, two 15 W Philips UV light lamps (365 nm wavelength, intensity: 2.47 ± 0.16 mW cm ⁻²).	The degradation of atrazine is up to 60% in 1 h [98].

Photocatalyst	Preparation	Light Source	Removal Effect
TiO ₂ nanoparticles involved boron enrichment waste		UV irradiation, a UV lamp (400 W, $\lambda = 250\text{--}570$ nm).	The degradation of atrazine is up to 60% in 70 min. The removal of atrazine followed a pseudo-first-order reaction kinetic [99].
Mesoporous Ag-WO ₃ /SBA-15 composite		Visible-light, a broadband light source (450 W Xe arc lamp) fitted with a neutral density optical filter to allow light of wavelength above 400 nm.	70% of atrazine was degraded in 18 min [155].
Heterojunction BiVO ₄ -Bi ₂ O ₃	Platelet-like BiVO ₄ was synthesized by hyperbranched polyethyleneimine [156].	Visible-light, a mercury 250 W High-Pressure lamp.	The heterojunction efficiently removed >90% of atrazine [157].
CdS/BiOBr/Bi ₂ O ₂ CO ₃ ternary heterostructure materials	Used a simple one pot hydrothermal method.	Visible-light, a 250 W xenon lamp with a 400 nm cutoff filter.	The degradation of atrazine was up to 95% in 30 min [158].
BiOBr/UiO-66 composite	Used an in situ growth method.	Visible-light, a 300 W Xe lamp (Beijing Zhongjiaojinyuan, CEL-HXF300) with a 400 nm cut-off glass filter.	The degradation of atrazine was up to 90% in 3 h [159].
Cu-BiOCl	Used a one-pot solvothermal method.	UV irradiation, a Steripen Mercury UV lamp with emission wavelength of 254 nm.	29% of atrazine was degraded [160].

1.2.4. Electrocatalytic Method

Electrocatalysis is a catalytic process involving oxidation and reduction reactions through the direct transfer of electrons, which requires electrocatalysts to lower the overpotential of the reactions [161]. Electrocatalytic oxidation

technology can produce $\cdot\text{OH}$ in situ and no additional chemical reagent is required, which can remove atrazine from wastewater efficiently and environmental-friendly [100]. Electrode materials play an essential role in the progress of electrocatalytic oxidation. Various types of electrodes have been exploited for the degradation of atrazine in water (Table 3).

Table 3. Electrocatalytic oxidation of aqueous atrazine.

Electrodes	Removal Effect
Co/Sm-modified Ti/PbO ₂ anode	The maximum degradation rate of 92.6% and the chemical oxygen demand (COD) removal rate of 84.5% are achieved in electrolysis time 3 h [100].
Fly ash-red mud particle electrode	90.1 % atrazine was degraded in 30 min [101].
Bifunctional nickel foam composite cathode co-modified with CoFe@NC and CNTs	The removal of atrazine reached 100% in 105 min under the given conditions, the removal efficiency of TOC after 420 min was $78.7 \pm 2.6\%$ [102].
Boron Doped Diamond (BDD) anode	Around 100% removal rate of atrazine was achieved in 4 h [103].
BDD anode	Permanganate was in situ electrochemical generated for the treatment of atrazine. Atrazine degradation increased significantly with permanganate production [104].
BDD anode	A high mineralization rate of 82% was obtained [71].
BDD, Carbon Felt, and Mixed Metal Oxides Anodes with Iridium and Ruthenium	BDD completely removes atrazine, and rest of anodes reached approximately 75% atrazine removal [162].

In addition, electrochemistry has also been combined with ozone oxidation to degrade aqueous atrazine [163]. In 2016, Zhou et al. proposed a novel oxidation process using iron electrodes and ozone in atrazine degradation [164]. Moreover, atrazine degradation by in situ electrochemically generated ozone was reported by Vera et al. in 2009 [165]. The combination of electrochemistry and ozonation exhibited higher removal efficiency for ATZ than ozonation and electrocoagulation [164].

Moreover, Electrochemical Advanced Oxidation Processes (EAOPs) is also an efficient method to remove recalcitrant molecules. Atrazine is a very stable molecule with a relative resistance to microbial attack. Therefore, EAOPs can be used for pretreatment, before the biodegradation of atrazine [162].

1.2.5. Ozone Oxidation Method

Ozone is a strong oxidant, which can oxidize organic or inorganic substances in wastewater, thereby disinfecting, oxidizing or decolorizing. Because atrazine is resistant to the degradation by ozone, additional catalysts are required for the ozonation of atrazine [166]. In recent years, the ozonation of aqueous atrazine has been reported (Table 4).

In addition, using ozone oxidation combined with other oxidation processes can improve the degradation efficiency and mineralization rate of atrazine. In 2006, Bianchi et al., [167] studied the mechanism of atrazine degradation in aqueous phase under sonolysis at 20 kHz, ozonation, photolysis at 254 nm and photocatalysis in the presence of TiO₂, employed either separately or in combination. Ozonation and photocatalysis induced atrazine de-alkylation, followed by slower de-chlorination, and simultaneous sonolysis increased the rate of photocatalytic de-alkylation. The highest degradation rate of atrazine was achieved when photolysis at 254 nm was combined with ozonation.

Table 4. Ozonation of aqueous atrazine.

Catalyst	Removal Effect
Manganese	The presence of humic substances has a substantial influence on the Mn-catalysed ozonation of atrazine [105].
A non-ionic surfactant, Brij35 (polyoxyethylene (23) lauryl ether)	Atrazine was completely removed after a reaction time of 2 h [106].
Nano-ZnO	The degradation efficiency of atrazine was 99% after 5 min reaction at pH 6 [107].
Mesoporous Fe ₃ O ₄	The removal rate of atrazine was up to 97% [108]
Hydroxylamine	80% of atrazine was degraded by ozonation in the presence of hydroxylamine [109].

Catalyst	Removal Effect
Rutile TiO ₂	The removal rate and the mineralization of atrazine was 93% and 56%, respectively [168].
Oxygen functionalized graphitic carbon nitrideO@g-C ₃ N ₄	The removal rate of atrazine was 93%, after 5 min reaction at pH 6 [169].
Three-dimensional Co/Ni bimetallic organic frameworks	94% of atrazine were removed [170].

I.3. Biological methods for atrazine degradation

Biodegradation refers to the partial, and sometimes total, transformation or detoxification of contaminants by microbial, plants or enzymes [171]. It has advantages over physical and chemical methods in terms of low costs and environmental friendliness [172]. Since the discovery of biotic atrazine degradation [173, 174], biodegradation has been a major method for atrazine catabolism [56].

I.3.1. Microbial Degradation

Microbial degradation exploits the ability of microorganisms for removal of pollutants from contaminated sites [175]. That is because indigenous microorganisms that are already present in polluted environments may transform pollutants to harmless products via reactions that take place as a part of their metabolic processes [176]. Generally, isolated microbes are selected for the degradation due to nature and type of pollutants. Different atrazine-degrading bacteria and fungi have been isolated (Table 5). Because microorganisms are easily drained in water making their effectiveness greatly reduced, Yu et al. [114] developed a self-immobilized biomixture (SIB) with biosorption and biodegradation properties, that can obtain better atrazine removal rate.

Table 5. Microbial degradation of aqueous atrazine.

Strain	Origin	Removal Effect
<i>Arthrobacter</i> sp. DNS10	Black soil [110]	The removal rate of 100 mg/L atrazine reached 95% and 86% in 0.05 mM Zn ²⁺ and 1.0 mM Zn ²⁺ , respectively at 48 h. [111].
<i>Bacillus badius</i>	Maize fields	Response-surface-methodology (RSM) was used to optimize environmental factors such as pH,

ABP6		temperature, agitation speed and atrazine-concentration on atrazine degradation by utilizing <i>Bacillus badius</i> ABP6 strain. In the optimum conditions (pH 7.05, temperature 30.4 °C, agitation speed 145.7 rpm, and atrazine-concentration 200.9 ppm), the degradation rate of atrazine reaches a maximum value of 90% [112].
<i>Bjerkanderaadusta</i>	Rotten wood surfaces	In the optimum conditions (pH 4, temperature 28 °C, biomass 2 g, and atrazine-concentration 50 ppm), the removal rate of atrazine was up to 92% in 5 days [113].
<i>Agrobacterium</i> sp. WL-1, <i>Arthrobacter</i> sp. ZXY-2	Jilin Pesticide Plant	After adding biochar ZXY-2 pellets, the removal rate of atrazine reached 61% within 1 h, higher than that treated by ZXY-2 pellets without biochar. The addition of biochar could enhance the connection between ZXY-2 and pellets-based carrier, and the favorable biodegradation pH of ZXY-2 changed to 6 and 10 [114].
<i>Chlorella</i> sp.	The Freshwater Algae Culture Collection at the Institute of Hydrobiology, China	Atrazine with initial concentration of 5 mg/L was photocatalytic degraded for 60 min with degradation ratio of 31%. After an 8 d exposure of the microalga <i>Chlorella</i> sp., 83% and 64% of the atrazine were removed from the degraded solutions containing 40 µg/L and 80 µg/L of atrazine, respectively [177].
<i>Myriophyllum spicatum</i>	Wuhan Botanical Garden	<i>Myriophyllum spicatum</i> absorbed more than 18-fold the amount of atrazine in sediments and degraded atrazine to hydroxyatrazine (HA), deethylatrazine (DEA), didealkylatrazine (DDA), cyanuric acid (CYA) and biuret. The formation of biuret suggested for the first time, the ring opening of atrazine in an aquatic plant. The residual rate of atrazine was $6.5 \pm 2.0\%$ in <i>M. spicatum</i> -grown sediment on day 60 [178].

1.3.2. Phytodegradation

The phytodegradation of organic compounds take place inside the plant or within the rhizosphere of the plant [179]. Rhizosphere, the immediate vicinity of plant roots, is a zone of intense microbial activity, and the use of vegetation at the waste sites can overcome the inherent limitations such as low microbial population or inadequate microbial activity [115]. It has been reported that atrazine can be degraded or detoxified in crops [116, 117], and the molecular mechanism for catabolism and detoxification of atrazine in plants is a major research topic (Table

6).

Table 6. Phytodegradation of aqueous atrazine.

Plant	Gene/Enzymes	Result
Pennisetum clandestinum	Soil dehydrogenase	Within 80 days, nearly 45% of atrazine was degraded [115].
Rice	Two novel methyltransferases LOC_Os04g09604, LOC_Os11g15040	Atrazine degradation and detoxification are regulated [118]
Alfalfa (Medicago sativa)	Genes encoding glycosyltransferases, glutathione S-transferases or ABC transporters	Atrazine in alfalfa can be detoxified through different pathways [119].

Generally, atrazine may be degraded within the plant biomass by plant enzymes as well as in its rhizosphere by microbial biotransformation [180, 181].

1.4. Physicochemical methods for atrazine degradation

1.4.1. High Voltage Electrical Discharges (HVED)

High Voltage Electrical Discharges (HVED) is one of the advanced oxidation processes that has been used for the treatment of wastewater. During the discharge processes of gas and liquid system, the low-temperature plasma, high-energy electrons and UV-radiation are generated to degrade wastewater. The generated plasma is a conductive fluid that is electrically neutral and consists of electrons, positive and negative ions, free radicals, neutral particles and excited-state atoms [182]. Among them, the high-energy electrons bombard water molecules to ionize and generate oxidants such as $\cdot OH$ and H_2O_2 , which can efficiently degrade organic substances. The main reactions include:





The plasma reactors can be divided into three types. One is the non-thermalizing electrical discharge applied in the air above an aqueous solution, generating an atmospheric plasma. The second is the discharge applied into the water, creating high-temperature plasma channels. In addition, the hybrid reactors utilize both gas phase nonthermal plasma formed above the water solution and direct liquid phase corona-like discharge in water [183].

In 1997, Houben et al. [120] reported a research work on the degradation of atrazine by pulsed corona discharges above the water surface, in which 0.12 mM atrazine was oxidized for 5 h and the degradation rate was 57%. This is the earliest work using plasma reactors to degrade atrazine. Several years later, in 2005, Karpel Vel Leitner et al. [48] applied the pulsed arc electrohydraulic discharge (PAED) system on the degradation of atrazine. PAED was generated by a spark gap type power supply (0.5 kJ/pulse) with rod-to-rod type electrodes in water. The removal rate of atrazine (0.5 μ mol/L) achieved 80% with inter-electrode gap of 4 mm when the input energies were higher than 10 kJ/L. In 2007, Mededovic and Locke [47] present an investigation of the atrazine degradation by pulsed electrical discharge in water. Different electrolytes and electrode materials were studied. An initial pH 3 (adjusted with H₂SO₄) 90% of the atrazine (2×10^{-5} M) was degraded in 1 h, and the final degradation product was ammeline. When ferrous ions were used as an electrolyte, atrazine was degraded within 10 min due to the hydrogen peroxide produced by the discharge which reacted with ferrous ions. In addition, they compared their work with the above two pulsed electrical discharge works. The comparison of energy efficiency showed that the underwater pulsed electrical discharge had higher atrazine conversion for the same energy input than discharge above the water surface and pulsed arc discharge (Table 7).

Table 7. Comparison of energy efficiency for the three pulsed electrical discharge processes.

Technology	Concentration of Atrazine (M)	Energy Efficiency (mol/J)
Pulsed electrical discharge in water [47]	2×10^{-5}	3×10^{-9}
Pulsed corona discharges above the water surface [120]	0.12×10^{-3}	7.67×10^{-10}
Pulsed arc electrohydraulic discharge in water [48]	2×10^{-6}	1.56×10^{-10}

Moreover, there are four other works using dielectric barrier discharge (DBD), a typical non-equilibrium high-voltage gas discharge. In 2014, Zhu et al. [49] designed a novel wire–cylinder DBD plasma reactor for atrazine degradation, and the degradation rate was up to 93.7%, and 12.7% of total organic carbon (TOC) was removed after 18 min of discharge at the optimum conditions (input power = 50 W, air flow rate = 140 L.h⁻¹). In 2015, Patrick Vanraes et al. combined DBD with absorption of activated carbon [45] or nanofiber membrane [121] on the degradation of atrazine. In 2021, Wang et al. [184] combined DBD with microbubbles (MBs) for persulfate (PS) activation and atrazine removal in water. Under these DBD/MBs/PS systems, the degradation efficiency reached 89% after 75 min of treatment at a discharge power of 85 W, a PS concentration of 1 mM, and an air flow rate of 30 mL/min. And according to the calculated energy yield (EY 41.8 mg/kWh at a discharge power of 85 W), they supposed that DBD/MBs/PS system was economically viable in treating large scale atrazine wastewater.

In addition, there is another report on the remediation of atrazine in a plasma reactor. In 2018, Aggelopoulou et al. [185] used DBD plasma at atmospheric air pressure to treat a sandy soil polluted with atrazine. The atrazine degradation rates of 87% and 98% were achieved after 60 min of plasma treatment, starting from initial pollutant concentrations of 100 and 10 mg/kg, respectively. In 2023, many works have used DBD plasma to remediate atrazine-contaminated soil [28, 122, 186].

HVED is an innovative technique, which combines sonochemistry, high-energy electron radiation, photochemistry, etc., and can effectively decompose

organic pollutants. Nevertheless, the use of HVED for wastewater treatment is still under development, and further research is needed. The research on the degradation behavior of aqueous atrazine by plasma deserves more attention.

1.4.2. Ultrasound

The main principles of ultrasonic degradation of pollutants in water are cavitation effect and free radical oxidation. The high energy generated by the collapse of the ultrasonic cavitation bubble is sufficient to break the chemical bond and generate hydroxyl radicals $\cdot OH$ and hydrogen radicals $\cdot H$, which oxidize organic substances and transform into CO_2 , H_2O , inorganic ions or low-toxic organic compounds. At the same time, the rupture of bubbles enhances the purification. In wastewater treatment, ultrasound technique is often combined with other techniques [187] (ozone oxidation, ultraviolet irradiation, biodegradation, etc.) to achieve efficient degradation.

The earliest report on ultrasonic treatment of aqueous atrazine was reported by W.C. Koskinen et al. in 1994 [188], and the kinetic of sonochemical decomposition of atrazine in water was determined. In 1996, Petrier et al. [123] used two frequencies (20 kHz and 500 kHz) to degrade atrazine in aqueous solution. The degradation rate of atrazine was nearly 100% after 80 min at 500 kHz and 55% after 120 min at 20 kHz.

Later, ultrasonic treatment was combined with other techniques to degrade aqueous atrazine, and it is common to combine US and UV, or US and ozonation. In 2001, A. Hiskia et al. [189] published a report on US/UV decomposition of atrazine in the presence of polyoxometalates (POM) within a few minutes, giving common intermediates, namely, 2-hydroxy-4-(isopropylamino)-6-(ethylamino)-s-triazine (HA), 2-chloro-4-(isopropylamino)-6-amino-s-triazine (DEA), 2-chloro-4-amino-6-(ethylamino)-s-triazine (DIA), ammeline (AM) among others. The final products for both methods, US and UV with POM, were cyanuric acid, NO_3^- , Cl^- , CO_2 , and H_2O . In 2012, R. Kidak and S. Dogan [190] investigated the efficiency of O_3 and US and also of their combined application (US + O_3) for the degradation and potential mineralization of atrazine in water, leading to 95% removal for O_3 and 78% for US after 90 min of treatment, and 100% for US + O_3 after 20 min of treatment. In 2014, Xu et al. [41] reported sonophotolysis (US/UV) for the

degradation of atrazine. After 60 min of sonophotolysis treatment, the complete degradation of atrazine and 60% total organic carbon (TOC) removal rate were achieved. In 2017, Jing et al. [124] used a pilot-scale UV/O₃/US flow-through system to remove atrazine from wastewater. The optimal atrazine removal rate (98%) was obtained at the conditions of 75 W UV power, 10.75 g.h⁻¹ O₃ flow rate and 142.5 W ultrasound power. In 2023, Jia et al. [26] use the Chinese medicinal residue of *Acanthopanax senticosus* to activate persulfate, coupled with 45 kHz US, and atrazine was degraded 70% in 50 min.

Ultrasonic treatment has a strong effect on the degradation of organic substances, but it has the problem of high energy consumption. For the degradation of aqueous atrazine, more consideration can be given to combine ultrasonic treatment with other techniques, such as biodegradation, electrochemistry, Fenton oxidation, etc.

1.4.3. Microwave

Microwave treatment is a breakthrough, innovative, and broad-spectrum water treatment technique. It achieves the effect of decontamination and sterilization through the selective heating, low-temperature catalysis, and rapid penetration by the microwave field. The principle is that microwave heating generates efficient internal heat-transfer by penetrating subjects and causing uniform energy distribution throughout the material irradiated, which leads to an even chemical reaction [191]. Microwave irradiation can cause atrazine degradation through formation of micro-scale “hot spots” on the pore wall surface that pyrolyze the absorbed organic molecules [192].

In existing reports, microwave is often used as an auxiliary technique for the treatment of atrazine. The earliest work was on the microwave-assisted extraction of atrazine from soil, reported by Xiong et al. [125] in 1998. The combination of microwave (MW) power and ultraviolet (UV) light can improve the photochemical process, thereby making the degradation of atrazine more efficient. In 2006, Ta et al. [126] reported the degradation of atrazine by microwave-assisted electrode less discharge mercury lamp (MW-EDML) in aqueous solution. Microwave improved the photolysis of atrazine under UV-vis irradiation, so that it was completely degraded in a relatively short time (i.e., $t_{1/2} = 1.2$ min for 10 mg/L). Additionally, the

main degradation products during atrazine degradation process were identified by gas chromatography mass spectrometry (GC–MS) and liquid chromatography mass spectrometry (LC–MS), according to which the degradation mechanism including four possible pathways for atrazine degradation was proposed. In 2007, Gao et al. [127] reported a method of microwave-assisted photocatalysis on TiO_2 nanotubes for the degradation of aqueous atrazine. Atrazine was completely degraded in 5 min and the mineralization efficiency was 98% in 20 min, which superior to many other atrazine degradation works (they cannot achieve complete atrazine degradation with the formation of many toxic intermediates such as Deethylatrazine, Deisopropylatrazine, ammeline, etc.). High mineralization efficiency means that atrazine was released in soluble inorganic forms such as CO_2 , H_2O , NH_4^+ and small acids, which is beneficial to the non-toxic treatment of wastewater. Therefore, for the degradation of atrazine, not only a high degradation efficiency, but also a high mineralization rate is very important. In 2011, Chen et al. [193] used a microwave photochemical reactor to degrade atrazine in the presence of hydrogen peroxide H_2O_2 . The optimal condition of atrazine degradation by MW/UV/ H_2O_2 process was 53 °C, 300 mg/L H_2O_2 , MW power $P_{appl} = 30 \pm 0.3$ W (half-life $t_{1/2} = 1.1$ min for 20.8 mg/L initial concentration). Comparing with other processes such as UV alone [193] (half-life $t_{1/2} = 9.9$ min for 20 mg/L initial concentration), UV/ H_2O_2 [194] (half-life $t_{1/2} = 1.2$ min for 8.4 mg/L initial concentration with 343.4 mg/L H_2O_2) and MW/UV [193] (half-life $t_{1/2} = 2.2$ min for 20.8 mg/L initial concentration), microwave-assisted photocatalytic method is better than traditional photocatalytic methods, and adding H_2O_2 can achieve high-efficiency degradation of aqueous atrazine.

In addition, for traditional adsorption, its degradation efficiency highly depends on the adsorbent, while microwave heating can modify the adsorbent to bring about highly efficient adsorbent performance. Therefore, the adsorption and degradation of aqueous atrazine under microwave heating has attracted attention. Hu et al. [192, 195] reported the adsorption and degradation of atrazine in transition metal-loaded microporous under microwave induction. In 2017, Wei et al. [196] enhanced adsorption of atrazine using a coal-based activated carbon modified with sodium dodecyl benzene sulfonate under microwave heating. In the same year, Sivarajasekar et al. reported a fixed-bed column towards sorptive removal of

Atrazine from aqueous solutions using microwave irradiated Aegle marmelos Correa fruit shell.

1.4.4. Ionizing Radiation (γ -Rays, Electron Beams)

In recent years, due to environmental protection, ionizing radiation treatment of pollutants has received more and more attention. Ionizing radiation can cause displacement of electrons from atoms and breaks in chemical bonds, and γ -rays and electron beams are most commonly employed forms [197].

In 2009, Basfaret al. [128, 129] reported the degradation of atrazine herbicide in humic substances (HS) aqueous solutions and distilled water solutions on a laboratory scale upon γ -irradiation from a ^{60}Co source, which can achieve 90% degradation rate of atrazine. And they later use γ -irradiation to degrade atrazine present in natural ground waters on a laboratory scale.

In 2015, Khanet al. [130, 198] studied the kinetics, degradation pathways, influence of hydrated electron and radical scavengers in the degradation of aqueous atrazine by γ -irradiation, and the degradation rate can reach 69% under optimal conditions.

In addition, electron beams induced degradation of atrazine in aqueous solution was reported by Xu et al. [199] in 2015. Atrazine can be almost completely degraded (95%) and completely mineralized without any residue of cyanuric acid in aqueous solution.

1.5. Atrazine degradation pathways, atrazine mineralization and metabolites toxicity

The degradation of atrazine is a complex process with different pathways through different biotic or abiotic water treatment processes. Regarding the biotic degradation processes, there are two stages [200] (Figure 3). In the first stage, hydrolytic dichlorination and *N*-dealkylation of atrazine generate cyanuric acid in the role of the enzymes that have broad substrate specificity [201]. For hydrolytic dichlorination of atrazine, enzyme atrazine chlorohydrolase (AtzA) [202] or hydrolase triazine (TrzN) [203] catalyzes hydrolytic dichlorination of atrazine, but they display substantial differences in their substrate ranges: AtzA is restricted to atrazine analogs with a chlorine substituent at carbon 2 and *N*-alkyl groups, ranging

in size from methyl to t-butyl[204], and TrzN hydrolyzes a range of leaving groups (e.g., OCH₃, -SCH₃, -Cl, -F, -CN) from both triazines and pyrimidines [203]. For *N*-dealkylation of atrazine, hydroxyatrazine *N*-ethylaminohydrolase (AtzB) [205] catalyzes the hydrolytic conversion of hydroxyatrazine to *N*-isopropylammelide, and *N*-isopropylammelide isopropylaminohydrolase (AtzC) [206] catalyzes the hydrolysis of *N*-isopropylammelide to cyanuric acid. In the second stage, cyanuric acid is converted to ammonium and carbon dioxide by a set of enzymes AtzDEF [207, 208] and TrzD [207, 209].

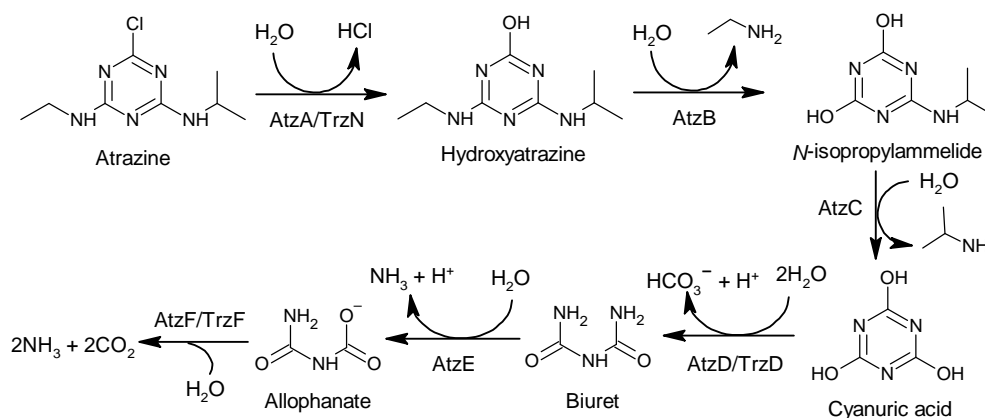


Figure 3. Degradation pathway of atrazine through biotic treatment process.

The above discussion is based on the enzymatic steps catalyzed by the gene products. In actual operation, atrazine degradation may be achieved by a consortium of organisms harboring the appropriate combination of enzymes, for example, the enriched mixed culture as well as the isolated strain, designated as *Arthrobacter* sp. strain GZK-1, mineralized ¹⁴C-ring-labeled atrazine up to 88% to ¹⁴CO₂ in a liquid culture within 14 d. [210].

In addition, for abiotic water treatment processes, as shown in Sections 2 and 3 of this article, many advanced oxidation processes (AOPs) have been involved in the degradation of atrazine in water. These AOPs can be used individually or in combination to improve efficiency such as US/UV [41, 211], US/UV/O₃ [167, 212], electrochemistry (EC)/O₃ [164], UV/H₂O₂ [213], UV/US/PS [214], UV/MW [215, 216], UV/Fenton [135], etc. Generally, AOPs rely on the in situ formation of reactive species[130], such as hydroxyl radical ([•]OH) [217], sulfate radical (SO₄^{-•}) [218, 219], singlet oxygen (¹O₂) [185], superoxide radical anions (O₂^{-•}) [92], hydrated electron (e_{aq}⁻) [130] and hydrogen radical (H[•]) [130]. These

reactive species have different redox potential and reaction selectivity. Therefore, the degradation pathways of atrazine vary from different AOPs. The general involved mechanisms were de-chlorination, hydroxylation of the s-triazine ring, de-alkylation of the amino groups, oxidation of the amino groups, de-amination and the opening of the s-triazine ring [41] (Figure 4). In most previous works [41, 144, 167, 185, 219], the final products of atrazine degradation tend to be cyanuric acid, ammelide and ammeline, because it is difficult to cleave the s-triazine ring [220]. At present, few studies [101, 127, 133, 221, 222] have reported the complete mineralization of atrazine, in which s-triazine ring-cleavage produced the less toxic compound biuret [221], and biuret hydrolyzed to allophanate, followed by the final generation of CO_2 , H_2O , NH_4^+ and small acids. The complete mineralization of atrazine thus reduces the toxicity of the treated wastewater for subsequent release.

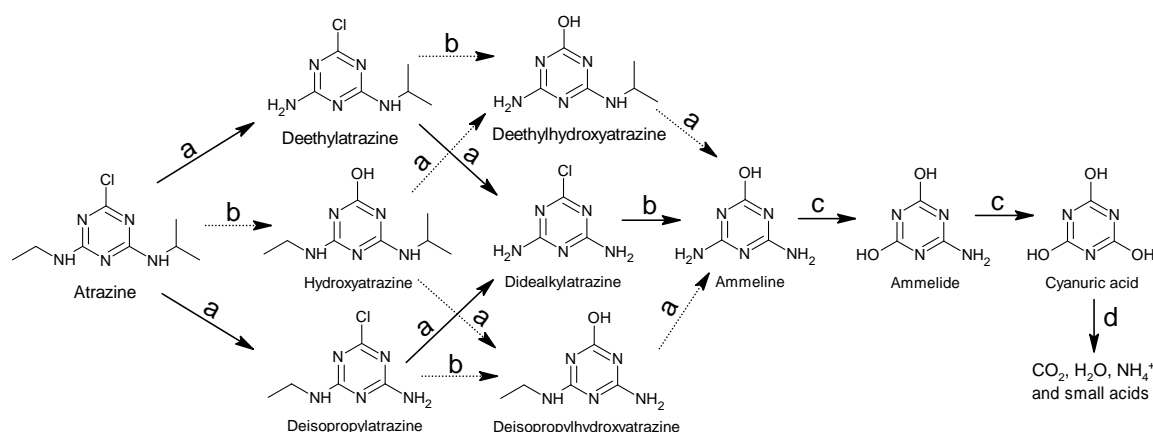


Figure 4. General involved degradation mechanisms of atrazine: (a) dealkylation of the amino groups; (b) dechlorination and hydroxylation of the s-triazine ring; (c) oxidation of the amino groups and deamination; (d) the opening of the s-triazine ring.

Toxicity studies on atrazine degradation are still incomplete, because some atrazine metabolites such as ammeline lack toxicological data. According to the book “Pesticide residues in food: 2007, toxicological evaluations”, published by the World Health Organization [223], atrazine, and its chloro-s-triazine metabolites are of moderate or low acute oral toxicity in male rats (LD_{50}), 1870–3090, 1890, 2290 and 3690 mg/kg bw for ATZ, DEA, DIA and DDA, respectively; and the acute oral toxicity of hydroxyatrazine in male rats (LD_{50} , >5050 mg/kg bw) is lower than that of atrazine or its chlorometabolites. However, toxicity comparisons based on these LD_{50} values are still inaccurate, as the results of toxicity tests vary based on

different subjects (plants, animals, human cells, etc.) or different concerns (reproductive or developmental toxicity, liver toxicity, etc.). More toxicity tests data are shown above (Table 8). Combining these data, the following toxicity ranking can be roughly obtained: atrazine (ATZ) > deethylatrazine (DEA) > deisopropylatrazine (DIA) > ammeline (AM) > didealkylatrazine (DDA) > hydroxyatrazine (HA).

Table 8. Chemical structures and toxicity tests data of atrazine and its metabolites.

Name	Atrazine (ATZ)	Deethylatrazine (DEA)	Deisopropylatrazine (DIA)	Ammeline (AM)	Cyanuric Acid	Didealkylatrazine (DDA)	Hydroxyatrazine (HA)
Chemical structure							
Acute oral toxicity in male rats (LD ₅₀) [223]	1870–3090 mg/kg	1890 mg/kg	2290 mg/kg			3690 mg/kg	>5050 mg/kg
Median lethal concentrations (LC ₅₀) for <i>Pseudokirchneriella subcapitata</i> in 96 h of exposure [224]	1600 µg/L	2000 µg/L	>3000 µg/L				
Concentration for 50% of maximal effect (EC ₅₀) on algal photosynthesis for <i>A. variabilis</i> [225]	0.1 ppm	0.7 ppm	4.7 ppm			100 ppm	>100 ppm
Acute oral toxicity in rats (LD ₅₀) [225]					>5000 mg/kg		
Adverse effects in sheep [226]				An average daily intake of ammeline No adverse effects at 296 mg/kg body weight 198 to 600 mg/kg body weight per day for 42 days for sheep caused half death.			

In addition, Banghai Liu et.al. [142] used the ECOSAR program to predict the acute and chronic toxicity of atrazine and its transformation intermediates, and it was found that although the vast majority of detected products possessed lower toxicity compared to atrazine, they remained classified as very toxic compounds to aquatic organisms.

The degradation mechanism, atrazine degradation rate, mineralization rate and main products are different for different treatment process. For better elaboration, the following discussion is based on treatment process type.

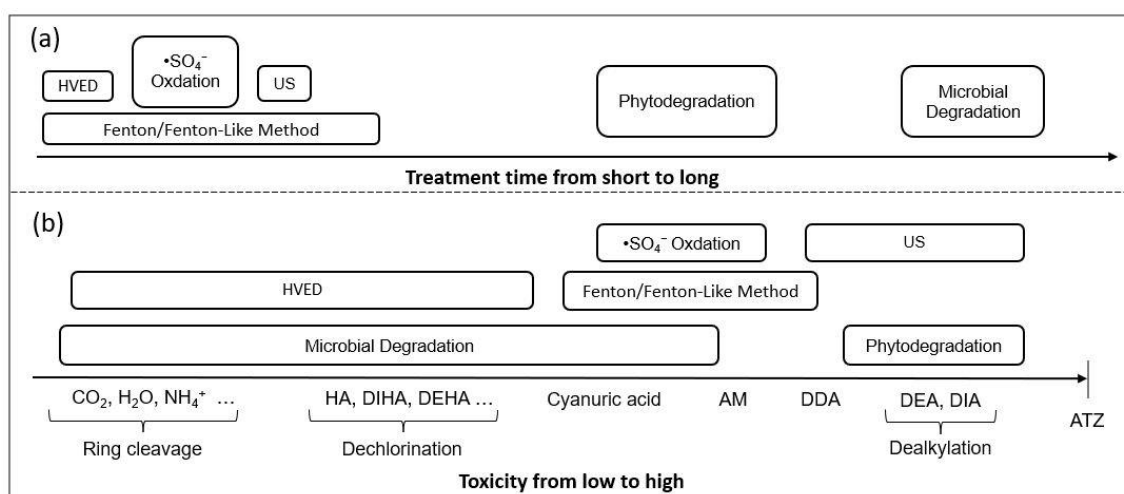


Figure 5. Comparison of different methods: (a) treatment time (b) product distribution.

As the Table 9 shows, generally, different methods can achieve high degradation rates (>90%) of atrazine by filtering the optimal conditions, but the treatment time needed and atrazine degrading capacity vary. Figure 5 is a comparison of treatment time and atrazine product distribution of different methods based on the data listed in Table A1. We can see that the processing time required for biodegradation is significantly more than other methods, while HVED and Fenton/Fenton-like method take less time (Figure 5a). In addition, ring cleavage can be achieved by microbial degradation as well as HVED (Figure 5b). Compared with the Fenton method, HVED has the advantages of short processing time, high atrazine degrading capacity and low toxic product distribution.

I.6. Conclusion and research objectives

As a widely used herbicide, atrazine is widely sprayed on many crops. Atrazine remaining in agri-food can cause physiological toxicity for a long time if it is ingested by humans. Additionally, because of chemical stability, atrazine in agri-food washing water flows into surface or groundwater and persists to be difficult to degrade. It is therefore of significant interest to develop clean and economical degradation processes for atrazine.

At present, biological processes are the common methods for the degradation of aqueous atrazine due to environmental protection, but biodegradation has its own limitations, such as slow degradation kinetics, and low remediation efficiency. Therefore, many studies have been focused on more highly efficient treatment technologies of aqueous atrazine, especially advanced oxidation processes (AOPs) that generate powerful nonspecific oxidant, hydroxyl radicals $\cdot OH$. Previous research reported the treatment of aqueous atrazine using $\cdot OH$ generated by physicochemical methods and chemical methods. In these methods, a single technology processing or a co-processing of two or more technologies will be used, and often the latter can achieve a more ideal degradation rate. In addition to pursuing a high atrazine degradation rate, it is also significant to improve the degradation ability to achieve full mineralization. Therefore, more and more innovative technologies have been investigated, especially High Voltage Electrical Discharge (HVED). However, these new methods for the degradation of atrazine are still being explored, and further research is needed.

Atrazine is a widely used herbicide. Although the European Union has banned it, it is still used in other countries such as Brazil and the United States. Atrazine has a long half-life in water and low adsorption in soil, causing residual contamination of groundwater and surface water. The detection and quantification of atrazine in water is of great significance for quality control. In addition, because atrazine acts as an endocrine disruptor and is harmful to human health, the development of efficient atrazine degradation technology is a research focus. However, the antioxidant capacity of atrazine makes its degradation challenging. The advanced oxidation process (AOP), which generates the powerful nonspecific oxidant hydroxyl radical $HO\cdot$, is more favored in atrazine degradation. High voltage

electrical discharge (HVED) technology, which is still in the development stage, has good research prospects because of its rapid degradation kinetics, efficient degradation ability, and low-toxic degradation metabolites.

Therefore, this thesis focuses on the degradation of atrazine in water by HVED technology. The research objectives include:

- 1) Develop and validate an online monitoring analysis method for the detection and quantification of atrazine and its metabolites.
- 2) Study and compare the impact of different degradation techniques (HVED, Fenton oxidation and sonication) on atrazine degradation.
- 3) Propose the degradation mechanism pathways of atrazine under different technologies, based on the formation kinetics of degradation metabolites.
- 4) Study the effect of real matrices such as tap water on atrazine degradation.
- 5) Perform toxicity analysis of treatment solutions on atrazine degradation by different technologies.

Table 9. Comparison of different methods (degradation mechanism, atrazine degradation rate, atrazine mineralization rate and main products).

Method	Degradation Mechanism	Strain/Plant/Generated Reactive Species	Initial Atrazine Concentration and Some Notes	Treatment Time	Atrazine Degradation Rate	Atrazine Degrading Capacity	Products	References
Microbial Degradation	Microbes' express atrazine-degrading enzymes that degrade atrazine.	<i>Chelatobacter heintzii</i> Cit1	The initial atrazine concentration is 0.5 mg per kg of soil. The bacteria described were isolated from 12 cultivated and grassland soils from different areas in France.	131 days	No residual atrazine detected	Ring cleavage	CO ₂ , H ₂ O ...	[227]
		<i>Chelatobacter heintzii</i> Sal1-3						
		<i>Chelatobacter heintzii</i> LR3-3						
		<i>Chelatobacter heintzii</i> LRA						
		<i>Chelatobacter heintzii</i> SalB			56%	Dechlorination	Dechlorination products	
		<i>Chelatobacter heintzii</i> Lous2-3						
		<i>Chelatobacter heintzii</i> Sal2						
		<i>Pseudomonas</i> sp. ADP			No residual atrazine detected	Ring cleavage	CO ₂ , H ₂ O ...	
		<i>Arthrobacter cristallopoietes</i> Cit2						
<i>Nocardioides</i> sp. SP12	Cyanuric acid production	Cyanuric acid						
Phytodegradation	Phytoextraction: atrazine in soil and groundwater can be taken up inside plant tissues; Phytotransformation: atrazine inside plant tissues can be transformed by plant enzymes; Rhizoremediation: pollutants in soil	Tall fescue Ryegrass Barley Maize	49 days after planting, the soils were spiked with aqueous solutions of atrazine to achieve concentrations of 2, 5 and 10 mg of atrazine per kg of soil. The plants were harvested after 65 days, that	16 days	88.6–96.7%	Dealkylation	DIA and DEA	[228]
					96.6–99.6%			
					96.4–99.4%			

	can be degraded by microbes in the root zone.		is, 16 days after atrazine application.		97.2–98.6%			
Fenton/Fenton-Like Method	H ₂ O ₂ reacts with Fe ²⁺ to generate reactive radicals $\cdot\text{OH}$, which degrade atrazine.	$\cdot\text{OH}$	The optimal mixture, 2.69 mM (1:1) FeSO ₄ :H ₂ O ₂ , degraded [2,4,6- ¹⁴ C]-atrazine (140 μmol).	≤ 30 s	100%	Dealkylation	DDA	[229]
			The photo-Fenton process: 10 mg/L atrazine was degraded, using 1g/L Heterogeneous Fenton catalyst Fe/TiO ₂ , 1.6 mM H ₂ O ₂ and pH = 3. The light intensity at 420 nm was 30 W/m ² .	30 min	95%	Ring cleavage (TOC removal rate 18%)	DDA, Cyanuric acid ...	[230]
			The initial concentration of atrazine was 23 $\mu\text{mol/L}$. The electro-Fenton process: the simultaneous reduction in ferric ions and oxygen at a simple electrode allowed the subsequent production of $\cdot\text{OH}$.	4 h	100%	Dealkylation	DDA	[231]
Sulfate Radical (SO ₄ ^{•-}) Oxidation	With the activation of persulfate (PS), sulfate radical (SO ₄ ^{•-}) can be generated by the cleavage of O–O bond of PS. Meanwhile, SO ₄ ^{•-} could react with water and OH ⁻ to produce hydroxyl radicals ($\cdot\text{OH}$).	SO ₄ ^{•-} and $\cdot\text{OH}$	The initial concentration of atrazine was 50 $\mu\text{mol/L}$. Copper sulfide (CuS)/persulfate (PS)	40 min	91.6%	Dealkylation and Dechlorination	AM	[232]
			The initial concentration of atrazine was 10 mmol/L. Magnetite Fe ₃ O ₄ -sepiolite/ persulfate (PS)	1 h	72.3%			[233]
			The initial concentration of atrazine was 20 mg/L. Pyrite (FeS ₂)/persulfate (PS)	45 min	100 %			[234]
High Voltage Electrical Discharges (HVED)	HVED can not only generate radical species, such as $\cdot\text{OH}$, HO ₂ [•] , and H [•] ions, and free electrons (e ⁻), but also generate physical agents, such as UV, shock waves, and heat.	$\cdot\text{OH}$	The initial concentration of atrazine was 11.9 mg/L. Dielectric barrier discharge (DBD)	18 min	93.7%	Ring cleavage (TOC removal rate 12.7%)	Dechlorination products, CO ₂ , H ₂ O ...	[235]
Ultrasound (US)	The high energy generated by the collapse of the ultrasonic cavitation bubble leads to the generation of hydroxyl radicals ($\cdot\text{OH}$) and hydrogen radicals ($\cdot\text{H}$).	$\cdot\text{OH}$	The initial concentration of atrazine was 0.1 mmol/L. Ultrasound frequency: 500 kHz	80 min	100%	Dealkylation	DEA, DIA, DDA	[236]

I.7. References

- [1] A. Sharma, V. Kumar, B. Shahzad, M. Tanveer, G.P.S. Sidhu, N. Handa, S.K. Kohli, P. Yadav, A.S. Bali, R.D. Parihar, O.I. Dar, K. Singh, S. Jasrotia, P. Bakshi, M. Ramakrishnan, S. Kumar, R. Bhardwaj, A.K. Thukral, Worldwide pesticide usage and its impacts on ecosystem, *SN Applied Sciences* 1(11) (2019) 1446. <https://doi.org/10.1007/s42452-019-1485-1>.
- [2] M. Désert, S. Ravier, G. Gille, A. Quinapallo, A. Armengaud, G. Pochet, J.-L. Savelli, H. Wortham, E. Quivet, Spatial and temporal distribution of current-use pesticides in ambient air of Provence-Alpes-Côte-d'Azur Region and Corsica, France, *Atmospheric Environment* 192 (2018) 241-256. <https://doi.org/https://doi.org/10.1016/j.atmosenv.2018.08.054>.
- [3] C. Froger, C. Jolivet, H. Budzinski, M. Pierdet, G. Caria, N.P.A. Saby, D. Arrouays, A. Bispo, Pesticide Residues in French Soils: Occurrence, Risks, and Persistence, *Environmental Science & Technology* 57(20) (2023) 7818-7827. <https://doi.org/10.1021/acs.est.2c09591>.
- [4] N. Baran, N. Surdyk, C. Auterives, Pesticides in groundwater at a national scale (France): Impact of regulations, molecular properties, uses, hydrogeology and climatic conditions, *Science of The Total Environment* 791 (2021) 148137. <https://doi.org/10.1016/j.scitotenv.2021.148137>.
- [5] Y. Liu, M. Li, J. Wu, W. Liu, Y. Li, F. Zhao, H. Tan, Characterization and novel pathway of atrazine catabolism by *Agrobacterium rhizogenes* AT13 and its potential for environmental bioremediation, *Chemosphere* 319 (2023) 137980. <https://doi.org/https://doi.org/10.1016/j.chemosphere.2023.137980>.
- [6] J. Bethsass, A. Colangelo, European Union Bans Atrazine, While the United States Negotiates Continued Use, *International Journal of Occupational and Environmental Health* 12(3) (2006) 260-267. <https://doi.org/10.1179/oeh.2006.12.3.260>.
- [7] X. Morvan, C. Mouvet, N. Baran, A. Gutierrez, Pesticides in the groundwater of a spring draining a sandy aquifer: Temporal variability of concentrations and fluxes, *Journal of Contaminant Hydrology* 87(3) (2006) 176-190. <https://doi.org/https://doi.org/10.1016/j.jconhyd.2006.05.003>.
- [8] B. Lopez, P. Ollivier, A. Togola, N. Baran, J.-P. Ghestem, Screening of French groundwater for regulated and emerging contaminants, *Science of The Total Environment* 518-519 (2015) 562-573. <https://doi.org/https://doi.org/10.1016/j.scitotenv.2015.01.110>.
- [9] N. Chen, D. Valdes, C. Marlin, H. Blanchoud, R. Guerin, M. Rouelle, P. Ribstein, Water, nitrate and atrazine transfer through the unsaturated zone of the Chalk aquifer in northern France, *Science of The Total Environment* 652 (2019) 927-938. <https://doi.org/https://doi.org/10.1016/j.scitotenv.2018.10.286>.
- [10] European Union, Directive 2006/118/EC of the European Parliament and of the Council of 12 December 2006 on the protection of groundwater against pollution and deterioration, *Official Journal of the European Communities* L 372 (2006) 19-31.

- [11] Ministère des Solidarités et de la Santé, Résultats du contrôle sanitaire de l'eau distribuée commune par commune, 2024. <https://www.data.gouv.fr/fr/datasets/resultats-du-contrôle-sanitaire-de-leau-distribuee-commune-par-commune/>. (Accessed 24 January 2024).
- [12] S.E. Wirbisky, G.J. Weber, M.S. Sepúlveda, T.-L. Lin, A.S. Jannasch, J.L. Freeman, An embryonic atrazine exposure results in reproductive dysfunction in adult zebrafish and morphological alterations in their offspring, *Scientific Reports* 6(1) (2016) 21337. <https://doi.org/10.1038/srep21337>.
- [13] T.B. Hayes, V. Khoury, A. Narayan, M. Nazir, A. Park, T. Brown, L. Adame, E. Chan, D. Buchholz, T. Stueve, S. Gallipeau, Atrazine induces complete feminization and chemical castration in male African clawed frogs (*Xenopus laevis*), *Proceedings of the National Academy of Sciences* 107(10) (2010) 4612-4617. <https://doi.org/10.1073/pnas.0909519107>.
- [14] M. Wang, J. Chen, S. Zhao, J. Zheng, K. He, W. Liu, W. Zhao, J. Li, K. Wang, Y. Wang, J. Liu, L. Zhao, Atrazine promotes breast cancer development by suppressing immune function and upregulating MMP expression, *Ecotoxicology and Environmental Safety* 253 (2023) 114691. <https://doi.org/https://doi.org/10.1016/j.ecoenv.2023.114691>.
- [15] J. Hong, N. Boussetta, G. Enderlin, F. Merlier, N. Grimi, Degradation of Residual Herbicide Atrazine in Agri-Food and Washing Water, *Foods* 11(16) (2022) 2416. <https://doi.org/https://doi.org/10.3390/foods11162416>.
- [16] Y. Yoon, M. Cho, Understanding atrazine elimination via treatment of the enzyme-based Fenton reaction: Kinetics, mechanism, reaction pathway, and metabolites toxicity, *Chemosphere* 349 (2024) 140982. <https://doi.org/https://doi.org/10.1016/j.chemosphere.2023.140982>.
- [17] Y.-L. Cai, Y.-H. Xu, J.-Z. Xiang, Z.-Q. Zhang, Q.-X. He, Y.-F. Li, J. Lü, Iron-doped bismuth oxybromides as visible-light-responsive Fenton catalysts for the degradation of atrazine in aqueous phases, *Journal of Environmental Sciences* 137 (2024) 321-332. <https://doi.org/https://doi.org/10.1016/j.jes.2023.01.005>.
- [18] S. Liu, Z. Chen, Y. Shen, H. Chen, Z. Li, L. Cai, H. Yang, C. Zhu, J. Shen, J. Kang, P. Yan, Simultaneous regeneration of activated carbon and removal of adsorbed atrazine by ozonation process: From laboratory scale to pilot studies, *Water Research* 251 (2024) 121113. <https://doi.org/https://doi.org/10.1016/j.watres.2024.121113>.
- [19] Y. He, L. Wang, Z. Chen, X. Huang, X. Wang, X. Zhang, X. Wen, Novel catalytic ceramic membranes anchored with MnMe oxide and their catalytic ozonation performance towards atrazine degradation, *Journal of Membrane Science* 648 (2022) 120362. <https://doi.org/https://doi.org/10.1016/j.memsci.2022.120362>.
- [20] M. Zheng, Y. Li, M. Cao, Y. Guo, G. Qiu, S. Tu, S. Xiong, D. Fang, Amino acid promoted oxidation of atrazine by Fe₃O₄/persulfate, *Heliyon* 10(1) (2024) e23371. <https://doi.org/https://doi.org/10.1016/j.heliyon.2023.e23371>.

- [21] E.A. El-Bestawy, M. Gaber, H. Shokry, M. Samy, Effective degradation of atrazine by spinach-derived biochar via persulfate activation system: Process optimization, mechanism, degradation pathway and application in real wastewater, *Environmental Research* 229 (2023) 115987. <https://doi.org/https://doi.org/10.1016/j.envres.2023.115987>.
- [22] S. Han, Y. Tao, L. Zhao, Y. Cui, Y. Zhang, Metabolic insights into how multifunctional microbial consortium enhances atrazine removal and phosphorus uptake at low temperature, *Journal of Hazardous Materials* 461 (2024) 132539. <https://doi.org/https://doi.org/10.1016/j.jhazmat.2023.132539>.
- [23] H. Wang, X. Long, X. Cao, L. Li, J. Zhang, Y. Zhao, D. Wang, Z. Wang, H. Meng, W. Dong, C. Jiang, J. Li, X. Li, Stimulation of atrazine degradation by activated carbon and cathodic effect in soil microbial fuel cell, *Chemosphere* 320 (2023) 138087. <https://doi.org/https://doi.org/10.1016/j.chemosphere.2023.138087>.
- [24] G.M. Barroso, E.A. dos Santos, F.R. Pires, L. Galon, C.M. Cabral, J.B. dos Santos, Phytoremediation: A green and low-cost technology to remediate herbicides in the environment, *Chemosphere* 334 (2023) 138943. <https://doi.org/https://doi.org/10.1016/j.chemosphere.2023.138943>.
- [25] X. Wang, W. Wang, L. Wang, G. Wang, Y. You, F. Ma, Process analysis of asymmetric interaction between copper and atrazine in a system of macrophytes, *Science of The Total Environment* 857 (2023) 159652. <https://doi.org/https://doi.org/10.1016/j.scitotenv.2022.159652>.
- [26] W. Jia, H. Wang, Q. Wu, L. Sun, Q. Si, Q. Zhao, Y. Wu, N. Ren, W. Guo, Insight into Chinese medicine residue biochar combined with ultrasound for persulfate activation in atrazine degradation: *Acanthopanax senticosus* precursors, synergistic effects and toxicity assessment, *Science of The Total Environment* 880 (2023) 163054. <https://doi.org/10.1016/j.scitotenv.2023.163054>.
- [27] M. Dehvari, A.A. Babaei, S. Esmaeili, Amplification of oxidative elimination of atrazine by Ultrasound/Ultraviolet-assisted Sono/Photocatalyst using a spinel cobalt ferrite-anchored MWCNT as peroxymonosulfate activator, *Journal of Photochemistry and Photobiology A: Chemistry* 437 (2023) 114452. <https://doi.org/https://doi.org/10.1016/j.jphotochem.2022.114452>.
- [28] N. Jiang, Y. Qu, J. Zhu, H. Wang, J. Li, Y. Shu, Y. Cui, Y. Tan, B. Peng, J. Li, Remediation of atrazine-contaminated soil in a fluidized-bed DBD plasma reactor, *Chemical Engineering Journal* 464 (2023) 142467. <https://doi.org/https://doi.org/10.1016/j.cej.2023.142467>.
- [29] Y. Shang, N. Jiang, Z. Liu, C. Li, H. Sun, H. Guo, B. Peng, J. Li, Pulsed discharge plasma assisted with Z-scheme graphene-TiO₂-MnFe₂O₄ for simultaneous removal of atrazine and Cr (VI): Performance and mechanism, *Chemical Engineering Journal* 452 (2023) 139342. <https://doi.org/https://doi.org/10.1016/j.cej.2022.139342>.
- [30] I.M.D. Gonzaga, A.R. Dória, R.S.S. Castro, M.R.R. Souza, M.A. Rodrigo, K.I.B. Eguiluz, G.R. Salazar-Banda, Microwave-prepared Ti/RuO₂-IrO₂ anodes: Influence of IrO₂ content on

atrazine removal, *Electrochimica Acta* 426 (2022) 140782.
<https://doi.org/https://doi.org/10.1016/j.electacta.2022.140782>.

[31] A. Ventura, G. Jacquet, A. Bermond, V. Camel, Electrochemical generation of the Fenton's reagent: application to atrazine degradation, *Water Research* 36(14) (2002) 3517-3522.
[https://doi.org/https://doi.org/10.1016/S0043-1354\(02\)00064-7](https://doi.org/https://doi.org/10.1016/S0043-1354(02)00064-7).

[32] C.A. Guzman-Perez, J. Soltan, J. Robertson, Kinetics of catalytic ozonation of atrazine in the presence of activated carbon, *Separation and Purification Technology* 79(1) (2011) 8-14.
<https://doi.org/https://doi.org/10.1016/j.seppur.2011.02.035>.

[33] Y. Guo, Y. Zhang, G. Yu, Y. Wang, Revisiting the role of reactive oxygen species for pollutant abatement during catalytic ozonation: The probe approach versus the scavenger approach, *Applied Catalysis B: Environmental* 280 (2021) 119418.
<https://doi.org/https://doi.org/10.1016/j.apcatb.2020.119418>.

[34] W.H. Glaze, J.-W. Kang, D.H. Chapin, The Chemistry of Water Treatment Processes Involving Ozone, Hydrogen Peroxide and Ultraviolet Radiation, *Ozone: Science & Engineering* 9(4) (1987) 335-352. <https://doi.org/10.1080/01919518708552148>.

[35] M. Naderi, S. Asadpour, M. Nekoeinia, M. Kooravand, Ultrasound assisted Sono-Fenton process including FeMnO₃ nanocatalysts for degradation of phenazopyridine, *Journal of Molecular Liquids* 390 (2023) 122916.
<https://doi.org/https://doi.org/10.1016/j.molliq.2023.122916>.

[36] S. Wang, D. Hu, Y. Liu, H. Xiong, Synthesis of ferrihydrite/polyaniline composite using waste Fe(III)/EPS-cultures with polyaniline and its application for tetracycline photo-Fenton degradation, *Journal of Environmental Chemical Engineering* 12(2) (2024) 112180.
<https://doi.org/https://doi.org/10.1016/j.jece.2024.112180>.

[37] Q. Zhuo, J. Lu, K. Lu, T. Li, L. Tian, Z. Yang, Y. Liu, B. Yang, S. Lv, Y. Qiu, Efficient degradation of carbamazepine using a modified nickel-foam cathode (Ni-FM/CNTs) in penetrating electro-Fenton process, *Process Safety and Environmental Protection* 178 (2023) 381-391.
<https://doi.org/https://doi.org/10.1016/j.psep.2023.08.026>.

[38] P.R. Gogate, A.B. Pandit, A review of imperative technologies for wastewater treatment II: hybrid methods, *Advances in Environmental Research* 8(3) (2004) 553-597.
[https://doi.org/https://doi.org/10.1016/S1093-0191\(03\)00031-5](https://doi.org/https://doi.org/10.1016/S1093-0191(03)00031-5).

[39] S. Papoutsakis, S. Miralles-Cuevas, N. Gondrexon, S. Baup, S. Malato, C. Pulgarin, Coupling between high-frequency ultrasound and solar photo-Fenton at pilot scale for the treatment of organic contaminants: An initial approach, *Ultrasonics Sonochemistry* 22 (2015) 527-534. <https://doi.org/https://doi.org/10.1016/j.ultsonch.2014.05.003>.

[40] S. Dalhatou, S. Laminsi, C. Pétrier, S. Baup, Competition in sonochemical degradation of Naphthol Blue Black: Presence of an organic (nonylphenol) and a mineral (bicarbonate ions) matrix, *Journal of Environmental Chemical Engineering* 7(1) (2019) 102819.
<https://doi.org/https://doi.org/10.1016/j.jece.2018.102819>.

- [41] L.J. Xu, W. Chu, N. Graham, Atrazine degradation using chemical-free process of USUV: Analysis of the micro-heterogeneous environments and the degradation mechanisms, *Journal of Hazardous Materials* 275 (2014) 166-174. <https://doi.org/https://doi.org/10.1016/j.jhazmat.2014.05.007>.
- [42] M.A. Baghapour, S. Nasser, Z. Derakhshan, Atrazine removal from aqueous solutions using submerged biological aerated filter, *Journal of Environmental Health Science and Engineering* 11(1) (2013) 6. <https://doi.org/10.1186/2052-336X-11-6>.
- [43] S. Adityosulindro, L. Barthe, K. González-Labrada, U.J. Jáuregui Haza, H. Delmas, C. Julcour, Sonolysis and sono-Fenton oxidation for removal of ibuprofen in (waste)water, *Ultrasonics Sonochemistry* 39 (2017) 889-896. <https://doi.org/https://doi.org/10.1016/j.ultsonch.2017.06.008>.
- [44] Y. Lan, C. Causserand, L. Barthe, Practical insights into ultrasound-assisted heterogeneous Fenton membrane reactors for water treatment, *Journal of Water Process Engineering* 45 (2022) 102523. <https://doi.org/https://doi.org/10.1016/j.jwpe.2021.102523>.
- [45] P. Vanraes, G. Willems, A. Nikiforov, P. Surmont, F. Lynen, J. Vandamme, J. Van Durme, Y.P. Verheust, S.W.H. Van Hulle, A. Dumoulin, C. Leys, Removal of atrazine in water by combination of activated carbon and dielectric barrier discharge, *Journal of Hazardous Materials* 299 (2015) 647-655. <https://doi.org/https://doi.org/10.1016/j.jhazmat.2015.07.075>.
- [46] F. Tampieri, M.-P. Ginebra, C. Canal, Quantification of Plasma-Produced Hydroxyl Radicals in Solution and their Dependence on the pH, *Analytical Chemistry* 93(8) (2021) 3666-3670. <https://doi.org/10.1021/acs.analchem.0c04906>.
- [47] S. Mededovic, B.R. Locke, Side-Chain Degradation of Atrazine by Pulsed Electrical Discharge in Water, *Industrial & Engineering Chemistry Research* 46(9) (2007) 2702-2709. <https://doi.org/10.1021/ie070020a>.
- [48] N. Karpel Vel Leitner, G. Syoen, H. Romat, K. Urashima, J.S. Chang, Generation of active entities by the pulsed arc electrohydraulic discharge system and application to removal of atrazine, *Water Research* 39(19) (2005) 4705-4714. <https://doi.org/https://doi.org/10.1016/j.watres.2005.09.010>.
- [49] D. Zhu, L. Jiang, R.-I. Liu, P. Chen, L. Lang, J.-w. Feng, S.-j. Yuan, D.-y. Zhao, Wire-cylinder dielectric barrier discharge induced degradation of aqueous atrazine, *Chemosphere* 117 (2014) 506-514. <https://doi.org/https://doi.org/10.1016/j.chemosphere.2014.09.031>.
- [50] S.M. Arnold, R.E. Talaat, W.J. Hickey, R.F. Harris, Identification of Fenton's reagent-generated atrazine degradation products by high-performance liquid chromatography and megafLOW electrospray ionization tandem mass spectrometry, *Journal of Mass Spectrometry* 30(3) (1995) 452-460. <https://doi.org/https://doi.org/10.1002/jms.1190300309>.
- [51] Z.-H. Diao, W. Qian, Z.-W. Zhang, J.-C. Jin, Z.-L. Chen, P.-R. Guo, F.-X. Dong, L. Yan, L.-J. Kong, W. Chu, Removals of Cr(VI) and Cd(II) by a novel nanoscale zero valent iron/peroxydisulfate process and its Fenton-like oxidation of pesticide atrazine: Coexisting

effect, products and mechanism, *Chemical Engineering Journal* 397 (2020) 125382. <https://doi.org/https://doi.org/10.1016/j.cej.2020.125382>.

[52] F. Hernández, J.V. Sancho, M. Ibáñez, E. Abad, T. Portolés, L. Mattioli, Current use of high-resolution mass spectrometry in the environmental sciences, *Analytical and Bioanalytical Chemistry* 403(5) (2012) 1251-1264. <https://doi.org/10.1007/s00216-012-5844-7>.

[53] P. Herrero, N. Cortés-Francisco, F. Borrull, J. Caixach, E. Pocurull, R.M. Marcé, Comparison of triple quadrupole mass spectrometry and Orbitrap high-resolution mass spectrometry in ultrahigh performance liquid chromatography for the determination of veterinary drugs in sewage: benefits and drawbacks, *Journal of Mass Spectrometry* 49(7) (2014) 585-596. <https://doi.org/https://doi.org/10.1002/jms.3377>.

[54] J. Hong, N. Boussetta, G. Enderlin, N. Grimi, F. Merlier, Real-Time Monitoring of the Atrazine Degradation by Liquid Chromatography and High-Resolution Mass Spectrometry: Effect of Fenton Process and Ultrasound Treatment, *Molecules* 27(24) (2022). <https://doi.org/10.3390/molecules27249021>.

[55] J. Hong, N. Boussetta, G. Enderlin, F. Merlier, N. Grimi, Degradation of herbicide atrazine in water by high voltage electrical discharge in comparison with Fenton oxidation and ultrasound treatments, *RSC Sustainability* 1(6) (2023) 1462-1470. <https://doi.org/10.1039/d3su00103b>.

[56] N. Udiković-Kolić, C. Scott, F. Martin-Laurent, Evolution of atrazine-degrading capabilities in the environment, *Applied Microbiology and Biotechnology* 96(5) (2012) 1175-1189. <https://doi.org/10.1007/s00253-012-4495-0>.

[57] X. Fan, F. Song, Bioremediation of atrazine: recent advances and promises, *Journal of Soils and Sediments* 14(10) (2014) 1727-1737. <https://doi.org/10.1007/s11368-014-0921-5>.

[58] H. He, Y. Liu, S. You, J. Liu, H. Xiao, Z. Tu, A Review on Recent Treatment Technology for Herbicide Atrazine in Contaminated Environment, *International Journal of Environmental Research and Public Health* 16(24) (2019). <https://doi.org/10.3390/ijerph16245129>.

[59] T. Komang Ralebitso, E. Senior, H.W. van Verseveld, Microbial aspects of atrazine degradation in natural environments, *Biodegradation* 13(1) (2002) 11-19. <https://doi.org/10.1023/A:1016329628618>.

[60] P.N. Chandra, K. Usha, Removal of atrazine herbicide from water by polyelectrolyte multilayer membranes, *Materials Today: Proceedings* 41 (2021) 622-627. <https://doi.org/https://doi.org/10.1016/j.matpr.2020.05.263>.

[61] A. European Food Safety, Reasoned opinion on the setting of a new maximum residue level for atrazine in cereals, *EFSA Journal* 13(6) (2015) 4126. <https://doi.org/https://doi.org/10.2903/j.efsa.2015.4126>.

- [62] S.E. Wirbisky, J.L. Freeman, Atrazine Exposure and Reproductive Dysfunction through the Hypothalamus-Pituitary-Gonadal (HPG) Axis, *Toxics* 3(4) (2015) 414-450. <https://doi.org/10.3390/toxics3040414>.
- [63] R.K. Pathak, A.K. Dikshit, Atrazine and Human Health, *International Journal of Ecosystem* 1(1) (2011) 14-23. <https://doi.org/https://doi.org/10.5923/j.jje.20110101.03>.
- [64] F.T. Farruggia, C.M. Rossmeisl, J.A. Hetrick, M. Biscoe, M. Branch III, Refined ecological risk assessment for atrazine, US Environmental Protection Agency, Office of Pesticide Programs: Washington, DC (2016).
- [65] R.C. Esteves, A.L. do Amaral Vendramini, F. Accioly, A qualitative meta-synthesis study of the convergence between organic crop regulations in the United States, Brazil, and Europe, *Trends in Food Science & Technology* 107 (2021) 343-357. <https://doi.org/https://doi.org/10.1016/j.tifs.2020.10.044>.
- [66] E.I. Megiato, A. Massuquetti, A.F.Z. de Azevedo, Impacts of integration of Brazil with the European Union through a general equilibrium model, *EconomiA* 17(1) (2016) 126-140. <https://doi.org/https://doi.org/10.1016/j.econ.2015.10.001>.
- [67] S. Wu, H. Li, X. Li, H. He, C. Yang, Performances and mechanisms of efficient degradation of atrazine using peroxymonosulfate and ferrate as oxidants, *Chemical Engineering Journal* 353 (2018) 533-541. <https://doi.org/https://doi.org/10.1016/j.cej.2018.06.133>.
- [68] S.U. Khan, W.J. Saidak, Residues of atrazine and its metabolites after prolonged usage, *Weed Research* 21(1) (1981) 9-12. <https://doi.org/https://doi.org/10.1111/j.1365-3180.1981.tb00090.x>.
- [69] T.K. James, H. Ghanizadeh, K.C. Harrington, N.S. Bolan, Degradation of atrazine and bromacil in two forestry waste products, *Scientific Reports* 11(1) (2021) 3284. <https://doi.org/10.1038/s41598-021-83052-z>.
- [70] R.D. Wauchope, T.M. Buttler, A.G. Hornsby, P.W.M. Augustijn-Beckers, J.P. Burt, The SCS/ARS/CES Pesticide Properties Database for Environmental Decision-Making, in: G.W. Ware (Ed.), *Reviews of Environmental Contamination and Toxicology: Continuation of Residue Reviews*, Springer New York, New York, NY, 1992, pp. 1-155. https://doi.org/10.1007/978-1-4612-2862-2_1.
- [71] B. Balci, N. Oturan, R. Cherrier, M.A. Oturan, Degradation of atrazine in aqueous medium by electrocatalytically generated hydroxyl radicals. A kinetic and mechanistic study, *Water Research* 43(7) (2009) 1924-1934. <https://doi.org/https://doi.org/10.1016/j.watres.2009.01.021>.
- [72] D.A. Belluck, S.L. Benjamin, T. Dawson, Groundwater Contamination by Atrazine and Its Metabolites, *Pesticide Transformation Products*, American Chemical Society 1991, pp. 254-273. <https://doi.org/doi:10.1021/bk-1991-0459.ch018>

10.1021/bk-1991-0459.ch018.

- [73] J. Mahía, A. Martín, T. Carballas, M. Díaz-Raviña, Atrazine degradation and enzyme activities in an agricultural soil under two tillage systems, *Science of The Total Environment* 378(1) (2007) 187-194. <https://doi.org/https://doi.org/10.1016/j.scitotenv.2007.01.036>.
- [74] T. Bohn, E. Cocco, L. Gourdol, C. Guignard, L. Hoffmann, Determination of atrazine and degradation products in Luxembourgish drinking water: origin and fate of potential endocrine-disrupting pesticides, *Food Additives & Contaminants: Part A* 28(8) (2011) 1041-1054. <https://doi.org/10.1080/19440049.2011.580012>.
- [75] W.E. Pereira, C.E. Rostad, Occurrence, distributions, and transport of herbicides and their degradation products in the Lower Mississippi River and its tributaries, *Environmental Science & Technology* 24(9) (1990) 1400-1406. <https://doi.org/10.1021/es00079a015>.
- [76] D.-h. Yan, Y. He, H. Wang, Environmental characteristics of the atrazine in the waters in East Liaohe River Basin, *Huan Jing Ke Xue* 26(3) (2005) 203-208.
- [77] N. Antić, M. Radišić, T. Radović, T. Vasiljević, S. Grujić, A. Petković, M. Dimkić, M. Laušević, Pesticide Residues in the Danube River Basin in Serbia – a Survey during 2009–2011, *CLEAN – Soil, Air, Water* 43(2) (2015) 197-204. <https://doi.org/https://doi.org/10.1002/clen.201200360>.
- [78] C. Steffens, S.C. Ballen, E. Scapin, D.M. da Silva, J. Steffens, R.A. Jacques, Advances of nanobiosensors and its application in atrazine detection in water: A review, *Sensors and Actuators Reports* 4 (2022) 100096. <https://doi.org/https://doi.org/10.1016/j.snr.2022.100096>.
- [79] Z. Salahshoor, K.-V. Ho, S.-Y. Hsu, C.-H. Lin, M. Fidalgo de Cortalezzi, Detection of Atrazine and its metabolites by photonic molecularly imprinted polymers in aqueous solutions, *Chemical Engineering Journal Advances* 12 (2022) 100368. <https://doi.org/https://doi.org/10.1016/j.cej.2022.100368>.
- [80] S. Farooq, H. Wu, J. Nie, S. Ahmad, I. Muhammad, M. Zeeshan, R. Khan, M. Asim, Application, advancement and green aspects of magnetic molecularly imprinted polymers in pesticide residue detection, *Science of The Total Environment* 804 (2022) 150293. <https://doi.org/https://doi.org/10.1016/j.scitotenv.2021.150293>.
- [81] S. Farooq, J. Nie, Y. Cheng, Z. Yan, J. Li, S.A.S. Bacha, A. Mushtaq, H. Zhang, Molecularly imprinted polymers' application in pesticide residue detection, *Analyst* 143(17) (2018) 3971-3989. <https://doi.org/10.1039/C8AN00907D>.
- [82] Z. Wen, P. Qin, C. Wan, G. Peng, L. Ding, G. Yang, K. Wang, A novel dual-signal amplification photofuel cells aptasensor for atrazine ultrasensitive detection in grapes and tomatoes, *Sensors and Actuators B: Chemical* 400 (2024) 134940. <https://doi.org/https://doi.org/10.1016/j.snb.2023.134940>.
- [83] S.A.G. Krishnan, M.B. Gumpu, G. Arthanareeswaran, P.S. Goh, F. Aziz, A.F. Ismail, Electrochemical quantification of atrazine-fulvic acid and removal through bismuth tungstate

photocatalytic hybrid membranes, *Chemosphere* 311 (2023) 137016. <https://doi.org/https://doi.org/10.1016/j.chemosphere.2022.137016>.

[84] D.A. Saltmiras, A.T. Lemley, Atrazine degradation by anodic Fenton treatment, *Water Research* 36(20) (2002) 5113-5119. [https://doi.org/https://doi.org/10.1016/S0043-1354\(02\)00223-3](https://doi.org/https://doi.org/10.1016/S0043-1354(02)00223-3).

[85] W. Chu, K.H. Chan, C.Y. Kwan, K.Y. Choi, Degradation of atrazine by modified stepwise-Fenton's processes, *Chemosphere* 67(4) (2007) 755-761. <https://doi.org/https://doi.org/10.1016/j.chemosphere.2006.10.039>.

[86] Y. Du, L. Zhao, Y. Su, Tantalum (oxy)nitrides: Preparation, characterisation and enhancement of photo-Fenton-like degradation of atrazine under visible light, *Journal of Hazardous Materials* 195 (2011) 291-297. <https://doi.org/https://doi.org/10.1016/j.jhazmat.2011.08.042>.

[87] Y. Du, L. Zhao, Y. Chang, Y. Su, Tantalum (oxy)nitrides nanotube arrays for the degradation of atrazine in vis-Fenton-like process, *Journal of Hazardous Materials* 225-226 (2012) 21-27. <https://doi.org/https://doi.org/10.1016/j.jhazmat.2012.04.058>.

[88] A. Carmelo da Rocha, Á. de Oliveira Sampaio Dantas, P. Angélica Vieira, V. Luiz Cardoso, Evaluation of basalt powder as a natural heterogeneous catalyst in photo-Fenton like treatment of atrazine, *Journal of Photochemistry and Photobiology A: Chemistry* 446 (2024) 115149. <https://doi.org/https://doi.org/10.1016/j.jphotochem.2023.115149>.

[89] Q. Jiang, Y. Zhang, S. Jiang, Y. Wang, H. Li, W. Han, J. Qu, L. Wang, Y. Hu, Graphene-like carbon sheet-supported nZVI for efficient atrazine oxidation degradation by persulfate activation, *Chemical Engineering Journal* 403 (2021) 126309. <https://doi.org/https://doi.org/10.1016/j.cej.2020.126309>.

[90] Y. Zhang, Q. Jiang, S. Jiang, H. Li, R. Zhang, J. Qu, S. Zhang, W. Han, One-step synthesis of biochar supported nZVI composites for highly efficient activating persulfate to oxidatively degrade atrazine, *Chemical Engineering Journal* 420 (2021) 129868. <https://doi.org/https://doi.org/10.1016/j.cej.2021.129868>.

[91] G. Li, Y. Guo, Y. Jin, W. Tan, F. Liu, H. Yin, Intrinsic mechanisms of calcium sulfite activation by siderite for atrazine degradation, *Chemical Engineering Journal* 426 (2021) 131917. <https://doi.org/https://doi.org/10.1016/j.cej.2021.131917>.

[92] X. Wang, Y. Wang, N. Chen, Y. Shi, L. Zhang, Pyrite enables persulfate activation for efficient atrazine degradation, *Chemosphere* 244 (2020) 125568. <https://doi.org/https://doi.org/10.1016/j.chemosphere.2019.125568>.

[93] S. Deng, L. Liu, G. Cagnetta, J. Huang, G. Yu, Mechanochemically synthesized S-ZVIbm composites for the activation of persulfate in the pH-independent degradation of atrazine: Effects of sulfur dose and ball-milling conditions, *Chemical Engineering Journal* 423 (2021) 129789. <https://doi.org/https://doi.org/10.1016/j.cej.2021.129789>.

- [94] Z. Zhu, J. Yan, M. Wang, H. Zhu, X. Li, L. Wu, Insights into hydrangea-like NiCo₂S₄ activating peroxymonosulfate for efficient degradation of atrazine, *Chemical Engineering Journal* 477 (2023) 146876. <https://doi.org/https://doi.org/10.1016/j.cej.2023.146876>.
- [95] A.H.C. Khavar, G. Moussavi, A.R. Mahjoub, M. Satari, P. Abdolmaleki, Synthesis and visible-light photocatalytic activity of In₂S₃-TiO₂@rGO nanocomposite for degradation and detoxification of pesticide atrazine in water, *Chemical Engineering Journal* 345 (2018) 300-311. <https://doi.org/https://doi.org/10.1016/j.cej.2018.03.095>.
- [96] W.-K. Wang, J.-J. Chen, M. Gao, Y.-X. Huang, X. Zhang, H.-Q. Yu, Photocatalytic degradation of atrazine by boron-doped TiO₂ with a tunable rutile/anatase ratio, *Applied Catalysis B: Environmental* 195 (2016) 69-76. <https://doi.org/https://doi.org/10.1016/j.apcatb.2016.05.009>.
- [97] G. Granados-Oliveros, E.A. Páez-Mozo, F.M. Ortega, C. Ferronato, J.-M. Chovelon, Degradation of atrazine using metalloporphyrins supported on TiO₂ under visible light irradiation, *Applied Catalysis B: Environmental* 89(3) (2009) 448-454. <https://doi.org/https://doi.org/10.1016/j.apcatb.2009.01.001>.
- [98] Y. Zhang, C. Han, G. Zhang, D.D. Dionysiou, M.N. Nadagouda, PEG-assisted synthesis of crystal TiO₂ nanowires with high specific surface area for enhanced photocatalytic degradation of atrazine, *Chemical Engineering Journal* 268 (2015) 170-179. <https://doi.org/https://doi.org/10.1016/j.cej.2015.01.006>.
- [99] M.L. Yola, T. Eren, N. Atar, A novel efficient photocatalyst based on TiO₂ nanoparticles involved boron enrichment waste for photocatalytic degradation of atrazine, *Chemical Engineering Journal* 250 (2014) 288-294. <https://doi.org/https://doi.org/10.1016/j.cej.2014.03.116>.
- [100] S. Chen, P. He, X. Wang, F. Xiao, P. Zhou, Q. He, L. Jia, F. Dong, H. Zhang, B. Jia, H. Liu, B. Tang, Co/Sm-modified Ti/PbO₂ anode for atrazine degradation: Effective electrocatalytic performance and degradation mechanism, *Chemosphere* 268 (2021) 128799. <https://doi.org/https://doi.org/10.1016/j.chemosphere.2020.128799>.
- [101] X. Teng, J. Li, J. Wang, J. Liu, X. Ge, T. Gu, Effective degradation of atrazine in wastewater by three-dimensional electrochemical system using fly ash-red mud particle electrode: Mechanism and pathway, *Separation and Purification Technology* 267 (2021) 118661. <https://doi.org/https://doi.org/10.1016/j.seppur.2021.118661>.
- [102] X. Sun, H. Qi, Z. Sun, Bifunctional nickel foam composite cathode co-modified with CoFe@NC and CNTs for electrocatalytic degradation of atrazine over wide pH range, *Chemosphere* 286 (2022) 131972. <https://doi.org/https://doi.org/10.1016/j.chemosphere.2021.131972>.
- [103] T. Wang, T. Huang, H. Jiang, R. Ma, Electrochemical degradation of atrazine by BDD anode: Evidence from compound-specific stable isotope analysis and DFT simulations, *Chemosphere* 273 (2021) 129754. <https://doi.org/https://doi.org/10.1016/j.chemosphere.2021.129754>.

- [104] S.T. McBeath, N.J.D. Graham, In-situ electrochemical generation of permanganate for the treatment of atrazine, *Separation and Purification Technology* 260 (2021) 118252. <https://doi.org/https://doi.org/10.1016/j.seppur.2020.118252>.
- [105] J. Ma, N.J.D. Graham, Degradation of atrazine by manganese-catalysed ozonation: Influence of humic substances, *Water Research* 33(3) (1999) 785–793. [https://doi.org/https://doi.org/10.1016/S0043-1354\(98\)00266-8](https://doi.org/https://doi.org/10.1016/S0043-1354(98)00266-8).
- [106] W. Chu, K.H. Chan, N.J.D. Graham, Enhancement of ozone oxidation and its associated processes in the presence of surfactant: Degradation of atrazine, *Chemosphere* 64(6) (2006) 931–936. <https://doi.org/https://doi.org/10.1016/j.chemosphere.2006.01.028>.
- [107] X. Yuan, X. Yan, H. Xu, D. Li, L. Sun, G. Cao, D. Xia, Enhanced ozonation degradation of atrazine in the presence of nano-ZnO: Performance, kinetics and effects, *Journal of Environmental Sciences* 61 (2017) 3–13. <https://doi.org/https://doi.org/10.1016/j.jes.2017.04.037>.
- [108] S. Zhu, B. Dong, Y. Yu, L. Bu, J. Deng, S. Zhou, Heterogeneous catalysis of ozone using ordered mesoporous Fe₃O₄ for degradation of atrazine, *Chemical Engineering Journal* 328 (2017) 527–535. <https://doi.org/https://doi.org/10.1016/j.cej.2017.07.083>.
- [109] J. Yang, J. Li, W. Dong, J. Ma, J. Cao, T. Li, J. Li, J. Gu, P. Liu, Study on enhanced degradation of atrazine by ozonation in the presence of hydroxylamine, *Journal of Hazardous Materials* 316 (2016) 110–121. <https://doi.org/https://doi.org/10.1016/j.jhazmat.2016.04.078>.
- [110] Y. Zhang, Z. Jiang, B. Cao, M. Hu, Z. Wang, X. Dong, Metabolic ability and gene characteristics of *Arthrobacter* sp. strain DNS10, the sole atrazine-degrading strain in a consortium isolated from black soil, *International Biodeterioration & Biodegradation* 65(8) (2011) 1140–1144. <https://doi.org/https://doi.org/10.1016/j.ibiod.2011.08.010>.
- [111] Z. Jiang, J. Chen, J. Li, B. Cao, Y. Chen, D. Liu, X. Wang, Y. Zhang, Exogenous Zn²⁺ enhance the biodegradation of atrazine by regulating the chlorohydrolase gene *trzN* transcription and membrane permeability of the degrader *Arthrobacter* sp. DNS10, *Chemosphere* 238 (2020) 124594. <https://doi.org/https://doi.org/10.1016/j.chemosphere.2019.124594>.
- [112] H. Khatoon, J.P.N. Rai, Optimization studies on biodegradation of atrazine by *Bacillus badius* ABP6 strain using response surface methodology, *Biotechnology Reports* 26 (2020) e00459. <https://doi.org/https://doi.org/10.1016/j.btre.2020.e00459>.
- [113] N. Dhiman, T. Jasrotia, P. Sharma, S. Negi, S. Chaudhary, R. Kumar, M.H. Mahnashi, A. Umar, R. Kumar, Immobilization interaction between xenobiotic and *Bjerkandera adusta* for the biodegradation of atrazine, *Chemosphere* 257 (2020) 127060. <https://doi.org/https://doi.org/10.1016/j.chemosphere.2020.127060>.
- [114] T. Yu, L. Wang, F. Ma, Y. Wang, S. Bai, A bio-functions integration microcosm: Self-immobilized biochar-pellets combined with two strains of bacteria to remove atrazine in

water and mechanisms, *Journal of Hazardous Materials* 384 (2020) 121326. <https://doi.org/https://doi.org/10.1016/j.jhazmat.2019.121326>.

[115] N. Singh, M. Megharaj, R.S. Kookana, R. Naidu, N. Sethunathan, Atrazine and simazine degradation in Pennisetum rhizosphere, *Chemosphere* 56(3) (2004) 257-263. <https://doi.org/https://doi.org/10.1016/j.chemosphere.2004.03.010>.

[116] J.J. Zhang, Y.C. Lu, H. Yang, Chemical Modification and Degradation of Atrazine in *Medicago sativa* through Multiple Pathways, *Journal of Agricultural and Food Chemistry* 62(40) (2014) 9657-9668. <https://doi.org/10.1021/jf503221c>.

[117] Y.C. Lu, S.J. Feng, J.J. Zhang, F. Luo, S. Zhang, H. Yang, Genome-wide identification of DNA methylation provides insights into the association of gene expression in rice exposed to pesticide atrazine, *Scientific Reports* 6(1) (2016) 18985. <https://doi.org/10.1038/srep18985>.

[118] Y.C. Lu, F. Luo, Z.J. Pu, S. Zhang, M.T. Huang, H. Yang, Enhanced detoxification and degradation of herbicide atrazine by a group of O-methyltransferases in rice, *Chemosphere* 165 (2016) 487-496. <https://doi.org/https://doi.org/10.1016/j.chemosphere.2016.09.025>.

[119] J.J. Zhang, Y.C. Lu, S.H. Zhang, F.F. Lu, H. Yang, Identification of transcriptome involved in atrazine detoxification and degradation in alfalfa (*Medicago sativa*) exposed to realistic environmental contamination, *Ecotoxicology and Environmental Safety* 130 (2016) 103-112. <https://doi.org/https://doi.org/10.1016/j.ecoenv.2016.04.009>.

[120] W. Hoeben, E. Van Veldhuizen, H. Classens, W. Rutgers, The Degradation of Phenol and Atrazine in Water by Pulsed Corona Discharges, 13th International Symposium on Plasma Chemistry, 1997, pp. 18-22.

[121] P. Vanraes, G. Willems, N. Daels, S.W.H. Van Hulle, K. De Clerck, P. Surmont, F. Lynen, J. Vandamme, J. Van Durme, A. Nikiforov, C. Leys, Decomposition of atrazine traces in water by combination of non-thermal electrical discharge and adsorption on nanofiber membrane, *Water Research* 72 (2015) 361-371. <https://doi.org/https://doi.org/10.1016/j.watres.2014.11.009>.

[122] X. Gao, X. Shen, J. Gu, J. Zhang, Experimental degradation of atrazine in soil by dielectric barrier discharge and optimization, *Chemical Engineering and Processing - Process Intensification* 191 (2023) 109485. <https://doi.org/https://doi.org/10.1016/j.cep.2023.109485>.

[123] C. Petrier, B. David, S. Laguian, Ultrasonic degradation at 20 kHz and 500 kHz of atrazine and pentachlorophenol in aqueous solution: Preliminary results, *Chemosphere* 32(9) (1996) 1709-1718. [https://doi.org/https://doi.org/10.1016/0045-6535\(96\)00088-4](https://doi.org/https://doi.org/10.1016/0045-6535(96)00088-4).

[124] L. Jing, B. Chen, D. Wen, J. Zheng, B. Zhang, Pilot-scale treatment of atrazine production wastewater by UV/O₃/ultrasound: Factor effects and system optimization, *Journal of Environmental Management* 203 (2017) 182-190. <https://doi.org/https://doi.org/10.1016/j.jenvman.2017.07.027>.

- [125] G. Xiong, J. Liang, S. Zou, Z. Zhang, Microwave-assisted extraction of atrazine from soil followed by rapid detection using commercial ELISA kit, *Analytica Chimica Acta* 371(1) (1998) 97-103. [https://doi.org/https://doi.org/10.1016/S0003-2670\(98\)00266-9](https://doi.org/https://doi.org/10.1016/S0003-2670(98)00266-9).
- [126] N. Ta, J. Hong, T. Liu, C. Sun, Degradation of atrazine by microwave-assisted electrodeless discharge mercury lamp in aqueous solution, *Journal of Hazardous Materials* 138(1) (2006) 187-194. <https://doi.org/https://doi.org/10.1016/j.jhazmat.2006.05.050>.
- [127] G. Zhanqi, Y. Shaogui, T. Na, S. Cheng, Microwave assisted rapid and complete degradation of atrazine using TiO₂ nanotube photocatalyst suspensions, *Journal of Hazardous Materials* 145(3) (2007) 424-430. <https://doi.org/https://doi.org/10.1016/j.jhazmat.2006.11.042>.
- [128] A.A. Basfar, K.A. Mohamed, A.J. Al-Abduly, A.A. Al-Shahrani, Radiolytic degradation of atrazine aqueous solution containing humic substances, *Ecotoxicology and Environmental Safety* 72(3) (2009) 948-953. <https://doi.org/https://doi.org/10.1016/j.ecoenv.2008.05.006>.
- [129] K.A. Mohamed, A.A. Basfar, A.A. Al-Shahrani, Gamma-ray induced degradation of diazinon and atrazine in natural groundwaters, *Journal of Hazardous Materials* 166(2) (2009) 810-814. <https://doi.org/https://doi.org/10.1016/j.jhazmat.2008.11.081>.
- [130] J.A. Khan, N.S. Shah, S. Nawaz, M. Ismail, F. Rehman, H.M. Khan, Role of eaq⁻, OH and H in radiolytic degradation of atrazine: A kinetic and mechanistic approach, *Journal of Hazardous Materials* 288 (2015) 147-157. <https://doi.org/https://doi.org/10.1016/j.jhazmat.2014.11.026>.
- [131] K. Poonia, V. Hasija, P. Singh, A.A. Parwaz Khan, S. Thakur, V.K. Thakur, S. Mukherjee, T. Ahamad, S.M. Alshehri, P. Raizada, Photocatalytic degradation aspects of atrazine in water: Enhancement strategies and mechanistic insights, *Journal of Cleaner Production* 367 (2022) 133087. <https://doi.org/https://doi.org/10.1016/j.jclepro.2022.133087>.
- [132] S. Rostami, S. Jafari, Z. Moeini, M. Jaskulak, L. Keshtgar, A. Badeenezhad, A. Azhdarpoor, M. Rostami, K. Zorena, M. Dehghani, Current methods and technologies for degradation of atrazine in contaminated soil and water: A review, *Environmental Technology & Innovation* 24 (2021) 102019. <https://doi.org/https://doi.org/10.1016/j.eti.2021.102019>.
- [133] N. Yang, Y. Liu, J. Zhu, Z. Wang, J. Li, Study on the efficacy and mechanism of Fe-TiO₂ visible heterogeneous Fenton catalytic degradation of atrazine, *Chemosphere* 252 (2020) 126333. <https://doi.org/https://doi.org/10.1016/j.chemosphere.2020.126333>.
- [134] Y. Shi, X. Wang, X. Liu, C. Ling, W. Shen, L. Zhang, Visible light promoted Fe₃S₄ Fenton oxidation of atrazine, *Applied Catalysis B: Environmental* 277 (2020) 119229. <https://doi.org/https://doi.org/10.1016/j.apcatb.2020.119229>.
- [135] A. Fareed, A. Hussain, M. Nawaz, M. Imran, Z. Ali, S.U. Haq, The impact of prolonged use and oxidative degradation of Atrazine by Fenton and photo-Fenton processes, *Environmental Technology & Innovation* 24 (2021) 101840. <https://doi.org/https://doi.org/10.1016/j.eti.2021.101840>.

- [136] T.B. Benzaquén, N.I. Cuello, O.M. Alfano, G.A. Eimer, Degradation of Atrazine over a heterogeneous photo-fenton process with iron modified MCM-41 materials, *Catalysis Today* 296 (2017) 51-58. <https://doi.org/https://doi.org/10.1016/j.cattod.2017.04.021>.
- [137] Y. Du, L. Zhao, Y. Zhang, Roles of TaON and Ta₃N₅ in the visible-Fenton-like degradation of atrazine, *Journal of Hazardous Materials* 267 (2014) 55-61. <https://doi.org/https://doi.org/10.1016/j.jhazmat.2013.12.042>.
- [138] Y. Zhang, Y. Du, D. Liu, W. Bian, The role of dissolved oxygen in the Ta(O)N-driven visible Fenton-like degradation of atrazine, *Journal of Environmental Chemical Engineering* 2(3) (2014) 1691-1698. <https://doi.org/https://doi.org/10.1016/j.jece.2014.06.005>.
- [139] G. Wang, C. Cheng, J. Zhu, L. Wang, S. Gao, X. Xia, Enhanced degradation of atrazine by nanoscale LaFe_{1-x}Cu_xO_{3-δ} perovskite activated peroxydisulfate: Performance and mechanism, *Science of The Total Environment* 673 (2019) 565-575. <https://doi.org/https://doi.org/10.1016/j.scitotenv.2019.04.098>.
- [140] S. Wu, H. He, X. Li, C. Yang, G. Zeng, B. Wu, S. He, L. Lu, Insights into atrazine degradation by persulfate activation using composite of nanoscale zero-valent iron and graphene: Performances and mechanisms, *Chemical Engineering Journal* 341 (2018) 126-136. <https://doi.org/https://doi.org/10.1016/j.cej.2018.01.136>.
- [141] C. Li, Y. Huang, X. Dong, Z. Sun, X. Duan, B. Ren, S. Zheng, D.D. Dionysiou, Highly efficient activation of peroxydisulfate by natural negatively-charged kaolinite with abundant hydroxyl groups for the degradation of atrazine, *Applied Catalysis B: Environmental* 247 (2019) 10-23. <https://doi.org/https://doi.org/10.1016/j.apcatb.2019.01.079>.
- [142] B. Liu, W. Guo, H. Wang, Q. Si, Q. Zhao, H. Luo, N. Ren, Activation of peroxydisulfate by cobalt-impregnated biochar for atrazine degradation: The pivotal roles of persistent free radicals and ecotoxicity assessment, *Journal of Hazardous Materials* 398 (2020) 122768. <https://doi.org/https://doi.org/10.1016/j.jhazmat.2020.122768>.
- [143] J. Zhu, J. Wang, C. Shan, J. Zhang, L. Lv, B. Pan, Durable activation of peroxydisulfate mediated by Co-doped mesoporous FePO₄ via charge redistribution for atrazine degradation, *Chemical Engineering Journal* 375 (2019) 122009. <https://doi.org/https://doi.org/10.1016/j.cej.2019.122009>.
- [144] R. Zhang, Y. Wan, J. Peng, G. Yao, Y. Zhang, B. Lai, Efficient degradation of atrazine by LaCoO₃/Al₂O₃ catalyzed peroxydisulfate: Performance, degradation intermediates and mechanism, *Chemical Engineering Journal* 372 (2019) 796-808. <https://doi.org/https://doi.org/10.1016/j.cej.2019.04.188>.
- [145] J. Peng, X. Lu, X. Jiang, Y. Zhang, Q. Chen, B. Lai, G. Yao, Degradation of atrazine by persulfate activation with copper sulfide (CuS): Kinetics study, degradation pathways and mechanism, *Chemical Engineering Journal* 354 (2018) 740-752. <https://doi.org/https://doi.org/10.1016/j.cej.2018.08.038>.

- [146] H. Zhang, X. Liu, C. Lin, X. Li, Z. Zhou, G. Fan, J. Ma, Peroxymonosulfate activation by hydroxylamine-drinking water treatment residuals for the degradation of atrazine, *Chemosphere* 224 (2019) 689–697. <https://doi.org/https://doi.org/10.1016/j.chemosphere.2019.02.186>.
- [147] X. Xu, W. Chen, S. Zong, X. Ren, D. Liu, Atrazine degradation using Fe₃O₄-sepiolite catalyzed persulfate: Reactivity, mechanism and stability, *Journal of Hazardous Materials* 377 (2019) 62–69. <https://doi.org/https://doi.org/10.1016/j.jhazmat.2019.05.029>.
- [148] Y. Hong, J. Peng, X. Zhao, Y. Yan, B. Lai, G. Yao, Efficient degradation of atrazine by CoMgAl layered double oxides catalyzed peroxydisulfate: Optimization, degradation pathways and mechanism, *Chemical Engineering Journal* 370 (2019) 354–363. <https://doi.org/https://doi.org/10.1016/j.cej.2019.03.127>.
- [149] Y. Huang, C. Han, Y. Liu, M.N. Nadagouda, L. Machala, K.E. O'Shea, V.K. Sharma, D.D. Dionysiou, Degradation of atrazine by ZnxCu_{1-x}Fe₂O₄ nanomaterial-catalyzed sulfite under UV-vis light irradiation: Green strategy to generate SO₄⁻, *Applied Catalysis B: Environmental* 221 (2018) 380–392. <https://doi.org/https://doi.org/10.1016/j.apcatb.2017.09.001>.
- [150] S. Popova, G. Matafonova, V. Batoev, Simultaneous atrazine degradation and *E. coli* inactivation by UV/S₂O₈²⁻/Fe²⁺ process under KrCl excilamp (222 nm) irradiation, *Ecotoxicology and Environmental Safety* 169 (2019) 169–177. <https://doi.org/https://doi.org/10.1016/j.ecoenv.2018.11.014>.
- [151] X. Yu, X. Jin, H. Liu, Y. Yu, J. Tang, R. Zhou, A. Yin, J. Sun, L. Zhu, Enhanced degradation of atrazine through UV/bisulfite: Mechanism, reaction pathways and toxicological analysis, *Science of The Total Environment* 856 (2023) 159157. <https://doi.org/https://doi.org/10.1016/j.scitotenv.2022.159157>.
- [152] N. Noah, Chapter 6 - Green synthesis: Characterization and application of silver and gold nanoparticles, in: A.K. Shukla, S. Irvani (Eds.), *Green Synthesis, Characterization and Applications of Nanoparticles*, Elsevier 2019, pp. 111–135. <https://doi.org/https://doi.org/10.1016/B978-0-08-102579-6.00006-X>.
- [153] R.M. Fernández-Domene, R. Sánchez-Tovar, B. Lucas-granados, M.J. Muñoz-Portero, J. García-Antón, Elimination of pesticide atrazine by photoelectrocatalysis using a photoanode based on WO₃ nanosheets, *Chemical Engineering Journal* 350 (2018) 1114–1124. <https://doi.org/https://doi.org/10.1016/j.cej.2018.06.015>.
- [154] S. Xie, C. Tang, H. Shi, G. Zhao, Highly efficient photoelectrochemical removal of atrazine and the mechanism investigation: Bias potential effect and reactive species, *Journal of Hazardous Materials* 415 (2021) 125681. <https://doi.org/https://doi.org/10.1016/j.jhazmat.2021.125681>.
- [155] M.A. Gondal, M.A. Suliman, M.A. Dastageer, G.-K. Chuah, C. Basheer, D. Yang, A. Suwaiyan, Visible light photocatalytic degradation of herbicide (Atrazine) using surface plasmon resonance induced in mesoporous Ag-WO₃/SBA-15 composite, *Journal of*

Molecular Catalysis A: Chemical 425 (2016) 208-216.
<https://doi.org/https://doi.org/10.1016/j.molcata.2016.10.015>.

[156] L.C. Mahlalela, C. Casado, J. Marugán, S. Septien, T. Ndlovu, L.N. Dlamini, Synthesis of platelet-like BiVO₄ using hyperbranched polyethyleneimine for the formation of heterojunctions with Bi₂O₃, *Applied Nanoscience* 9(7) (2019) 1501-1514.
<https://doi.org/10.1007/s13204-019-00977-8>.

[157] L.C. Mahlalela, C. Casado, J. Marugán, S. Septien, T. Ndlovu, L.N. Dlamini, Photocatalytic degradation of atrazine in aqueous solution using hyperbranched polyethyleneimine templated morphologies of BiVO₄ fused with Bi₂O₃, *Journal of Environmental Chemical Engineering* 8(5) (2020) 104215. <https://doi.org/https://doi.org/10.1016/j.jece.2020.104215>.

[158] D. Majhi, K. Das, A. Mishra, R. Dhiman, B.G. Mishra, One pot synthesis of CdS/BiOBr/Bi₂O₂CO₃: A novel ternary double Z-scheme heterostructure photocatalyst for efficient degradation of atrazine, *Applied Catalysis B: Environmental* 260 (2020) 118222.
<https://doi.org/https://doi.org/10.1016/j.apcatb.2019.118222>.

[159] Y. Xue, P. Wang, C. Wang, Y. Ao, Efficient degradation of atrazine by BiOBr/UiO-66 composite photocatalyst under visible light irradiation: Environmental factors, mechanisms and degradation pathways, *Chemosphere* 203 (2018) 497-505.
<https://doi.org/https://doi.org/10.1016/j.chemosphere.2018.04.017>.

[160] M.A. Moyet, R.B. Arthur, E.E. Lueders, W.P. Breeding, H.H. Patterson, The role of Copper (II) ions in Cu-BiOCl for use in the photocatalytic degradation of atrazine, *Journal of Environmental Chemical Engineering* 6(4) (2018) 5595-5601.
<https://doi.org/https://doi.org/10.1016/j.jece.2018.08.057>.

[161] R. Li, C. Li, Chapter One - Photocatalytic Water Splitting on Semiconductor-Based Photocatalysts, in: C. Song (Ed.), *Advances in Catalysis*, Academic Press 2017, pp. 1-57.
<https://doi.org/https://doi.org/10.1016/bs.acat.2017.09.001>.

[162] M.B. Carboneras Contreras, J. Villaseñor Camacho, F.J. Fernández-Morales, P.C. Cañizares, M.A. Rodrigo Rodrigo, Biodegradability improvement and toxicity reduction of soil washing effluents polluted with atrazine by means of electrochemical pre-treatment: Influence of the anode material, *Journal of Environmental Management* 255 (2020) 109895.
<https://doi.org/https://doi.org/10.1016/j.jenvman.2019.109895>.

[163] G.L. Saylor, C. Zhao, M.J. Kupferle, Synergistic enhancement of oxidative degradation of atrazine using combined electrolysis and ozonation, *Journal of Water Process Engineering* 21 (2018) 154-162. <https://doi.org/https://doi.org/10.1016/j.jwpe.2017.12.010>.

[164] S. Zhou, L. Bu, Z. Shi, C. Bi, Q. Yi, A novel advanced oxidation process using iron electrodes and ozone in atrazine degradation: Performance and mechanism, *Chemical Engineering Journal* 306 (2016) 719-725.
<https://doi.org/https://doi.org/10.1016/j.cej.2016.08.001>.

- [165] Y.M. Vera, R.J.d. Carvalho, M.L. Torem, B.A. Calfa, Atrazine degradation by in situ electrochemically generated ozone, *Chemical Engineering Journal* 155(3) (2009) 691-697. <https://doi.org/https://doi.org/10.1016/j.cej.2009.09.001>.
- [166] J.L. Acero, K. Stemmler, U. von Gunten, Degradation Kinetics of Atrazine and Its Degradation Products with Ozone and OH Radicals: A Predictive Tool for Drinking Water Treatment, *Environmental Science & Technology* 34(4) (2000) 591-597. <https://doi.org/10.1021/es990724e>.
- [167] C.L. Bianchi, C. Pirola, V. Ragaini, E. Selli, Mechanism and efficiency of atrazine degradation under combined oxidation processes, *Applied Catalysis B: Environmental* 64(1) (2006) 131-138. <https://doi.org/https://doi.org/10.1016/j.apcatb.2005.11.009>.
- [168] Y. Yang, H. Cao, P. Peng, H. Bo, Degradation and transformation of atrazine under catalyzed ozonation process with TiO₂ as catalyst, *Journal of Hazardous Materials* 279 (2014) 444-451. <https://doi.org/https://doi.org/10.1016/j.jhazmat.2014.07.035>.
- [169] X. Yuan, R. Xie, Q. Zhang, L. Sun, X. Long, D. Xia, Oxygen functionalized graphitic carbon nitride as an efficient metal-free ozonation catalyst for atrazine removal: Performance and mechanism, *Separation and Purification Technology* 211 (2019) 823-831. <https://doi.org/https://doi.org/10.1016/j.seppur.2018.10.052>.
- [170] G. Ye, P. Luo, Y. Zhao, G. Qiu, Y. Hu, S. Preis, C. Wei, Three-dimensional Co/Ni bimetallic organic frameworks for high-efficient catalytic ozonation of atrazine: Mechanism, effect parameters, and degradation pathways analysis, *Chemosphere* 253 (2020) 126767. <https://doi.org/https://doi.org/10.1016/j.chemosphere.2020.126767>.
- [171] S. Gouma, S. Fragoeiro, A.C. Bastos, N. Magan, 13 - Bacterial and Fungal Bioremediation Strategies, in: S. Das (Ed.), *Microbial Biodegradation and Bioremediation*, Elsevier, Oxford, 2014, pp. 301-323. <https://doi.org/https://doi.org/10.1016/B978-0-12-800021-2.00013-3>.
- [172] J.-P. Lasserre, F. Fack, D. Revets, S. Planchon, J. Renaut, L. Hoffmann, A.C. Gutleb, C.P. Muller, T. Bohn, Effects of the Endocrine Disruptors Atrazine and PCB 153 on the Protein Expression of MCF-7 Human Cells, *Journal of Proteome Research* 8(12) (2009) 5485-5496. <https://doi.org/10.1021/pr900480f>.
- [173] C. Yanze-Kontchou, N. Gschwind, Mineralization of the herbicide atrazine as a carbon source by a *Pseudomonas* strain, *Applied and Environmental Microbiology* 60(12) (1994) 4297-4302. <https://doi.org/10.1128/aem.60.12.4297-4302.1994>.
- [174] J.K. Struthers, K. Jayachandran, T.B. Moorman, Biodegradation of Atrazine by *Agrobacterium radiobacter* J14a and Use of This Strain in Bioremediation of Contaminated Soil, *Applied and Environmental Microbiology* 64(9) (1998) 3368-3375. <https://doi.org/10.1128/AEM.64.9.3368-3375.1998>.
- [175] P. Bhatt, V.M. Pathak, S. Joshi, T.S. Bisht, K. Singh, D. Chandra, Chapter 12 - Major metabolites after degradation of xenobiotics and enzymes involved in these pathways, in: P.

Bhatt (Ed.), Smart Bioremediation Technologies, Academic Press 2019, pp. 205-215. <https://doi.org/https://doi.org/10.1016/B978-0-12-818307-6.00012-3>.

[176] M. Vidali, Bioremediation. An overview, Pure and Applied Chemistry 73(7) (2001) 1163-1172. <https://doi.org/doi:10.1351/pac200173071163>.

[177] N. Hu, Y. Xu, C. Sun, L. Zhu, S. Sun, Y. Zhao, C. Hu, Removal of atrazine in catalytic degradation solutions by microalgae *Chlorella* sp. and evaluation of toxicity of degradation products via algal growth and photosynthetic activity, Ecotoxicology and Environmental Safety 207 (2021) 111546. <https://doi.org/https://doi.org/10.1016/j.ecoenv.2020.111546>.

[178] M. Qu, N. Li, H. Li, T. Yang, W. Liu, Y. Yan, X. Feng, D. Zhu, Phytoextraction and biodegradation of atrazine by *Myriophyllum spicatum* and evaluation of bacterial communities involved in atrazine degradation in lake sediment, Chemosphere 209 (2018) 439-448. <https://doi.org/https://doi.org/10.1016/j.chemosphere.2018.06.055>.

[179] L.A. Newman, C.M. Reynolds, Phytodegradation of organic compounds, Current Opinion in Biotechnology 15(3) (2004) 225-230. <https://doi.org/https://doi.org/10.1016/j.copbio.2004.04.006>.

[180] I.J. Murphy, J.R. Coats, The capacity of switchgrass (*Panicum virgatum*) to degrade atrazine in a phytoremediation setting, Environmental Toxicology and Chemistry 30(3) (2011) 715-722. <https://doi.org/https://doi.org/10.1002/etc.437>.

[181] D.J. Pérez, W.J. Doucette, M.T. Moore, Atrazine uptake, translocation, bioaccumulation and biodegradation in cattail (*Typha latifolia*) as a function of exposure time, Chemosphere 287 (2022) 132104. <https://doi.org/https://doi.org/10.1016/j.chemosphere.2021.132104>.

[182] Zhu Xinyan, Study on wastewater treatment and process intensification by Pulsed high-voltage discharge, Beijing University of Chemical Technology, 2017.

[183] E. Marotta, E. Ceriani, M. Schiorlin, C. Ceretta, C. Paradisi, Comparison of the rates of phenol advanced oxidation in deionized and tap water within a dielectric barrier discharge reactor, Water Research 46(19) (2012) 6239-6246. <https://doi.org/https://doi.org/10.1016/j.watres.2012.08.022>.

[184] Q. Wang, A. Zhang, P. Li, P. Héroux, H. Zhang, X. Yu, Y. Liu, Degradation of aqueous atrazine using persulfate activated by electrochemical plasma coupling with microbubbles: removal mechanisms and potential applications, Journal of Hazardous Materials 403 (2021) 124087. <https://doi.org/https://doi.org/10.1016/j.jhazmat.2020.124087>.

[185] C.A. Aggelopoulos, D. Tataraki, G. Rassias, Degradation of atrazine in soil by dielectric barrier discharge plasma – Potential singlet oxygen mediation, Chemical Engineering Journal 347 (2018) 682-694. <https://doi.org/https://doi.org/10.1016/j.cej.2018.04.111>.

[186] Y. Zhang, H. Zhang, A. Zhang, P. Héroux, Z. Sun, Y. Liu, Remediation of atrazine-polluted soil using dielectric barrier discharge plasma and biochar sequential batch experimental

technology, Chemical Engineering Journal 458 (2023) 141406.
<https://doi.org/https://doi.org/10.1016/j.cej.2023.141406>.

[187] J. Wang, Z. Wang, C.L.Z. Vieira, J.M. Wolfson, G. Pingtian, S. Huang, Review on the treatment of organic pollutants in water by ultrasonic technology, Ultrason Sonochem 55 (2019) 273-278. <https://doi.org/https://doi.org/10.1016/j.ultsonch.2019.01.017>.

[188] W.C. Koskinen, K.E. Sellung, J.M. Baker, B.L. Barber, R.H. Dowdy, Ultrasonic decomposition of atrazine and alachlor in water, Journal of Environmental Science and Health, Part B 29(3) (1994) 581-590.
<https://doi.org/https://doi.org/10.1080/03601239409372895>.

[189] A. Hiskia, M. Ecke, A. Troupis, A. Kokorakis, H. Hennig, E. Papaconstantinou, Sonolytic, Photolytic, and Photocatalytic Decomposition of Atrazine in the Presence of Polyoxometalates, Environmental Science & Technology 35(11) (2001) 2358-2364.
<https://doi.org/https://doi.org/10.1021/es000212w>.

[190] R. Kidak, S. Dogan, Degradation of atrazine by advanced oxidation processes, Sixteenth International Water Technology Conference, Citeseer, Istanbul, Turkey, 2012.

[191] N. Sivarajasekar, K. Balasubramani, N. Mohanraj, J. Prakash Maran, S. Sivamani, P. Ajmal Koya, V. Karthik, Fixed-bed adsorption of atrazine onto microwave irradiated Aegle marmelos Correa fruit shell: Statistical optimization, process design and breakthrough modeling, Journal of Molecular Liquids 241 (2017) 823-830.
<https://doi.org/https://doi.org/10.1016/j.molliq.2017.06.064>.

[192] E. Hu, Y. Hu, H. Cheng, Performance of a novel microwave-based treatment technology for atrazine removal and destruction: Sorbent reusability and chemical stability, and effect of water matrices, Journal of Hazardous Materials 299 (2015) 444-452.
<https://doi.org/https://doi.org/10.1016/j.jhazmat.2015.07.031>.

[193] H. Chen, E. Bramanti, I. Longo, M. Onor, C. Ferrari, Oxidative decomposition of atrazine in water in the presence of hydrogen peroxide using an innovative microwave photochemical reactor, Journal of Hazardous Materials 186(2) (2011) 1808-1815.
<https://doi.org/https://doi.org/10.1016/j.jhazmat.2010.12.065>.

[194] F.J. Beltrán, G. Ovejero, B. Acedo, Oxidation of atrazine in water by ultraviolet radiation combined with hydrogen peroxide, Water Research 27(6) (1993) 1013-1021.
[https://doi.org/https://doi.org/10.1016/0043-1354\(93\)90065-P](https://doi.org/https://doi.org/10.1016/0043-1354(93)90065-P).

[195] E. Hu, H. Cheng, Catalytic effect of transition metals on microwave-induced degradation of atrazine in mineral micropores, Water Research 57 (2014) 8-19.
<https://doi.org/https://doi.org/10.1016/j.watres.2014.03.015>.

[196] X. Wei, Z. Wu, C. Du, Z. Wu, B.-C. Ye, G. Cravotto, Enhanced adsorption of atrazine on a coal-based activated carbon modified with sodium dodecyl benzene sulfonate under microwave heating, Journal of the Taiwan Institute of Chemical Engineers 77 (2017) 257-262.
<https://doi.org/https://doi.org/10.1016/j.jtice.2017.04.004>.

- [197] F. Erdmann, A. Ghantous, J. Schüz, Environmental Agents and Childhood Cancer, in: J. Nriagu (Ed.), Encyclopedia of Environmental Health (Second Edition), Elsevier, Oxford, 2019, pp. 347-359. <https://doi.org/https://doi.org/10.1016/B978-0-12-409548-9.11725-7>.
- [198] J.A. Khan, N.S. Shah, H.M. Khan, Decomposition of atrazine by ionizing radiation: Kinetics, degradation pathways and influence of radical scavengers, Separation and Purification Technology 156 (2015) 140-147. <https://doi.org/https://doi.org/10.1016/j.seppur.2015.09.064>.
- [199] G. Xu, J.-z. Yao, L. Tang, X.-y. Yang, M. Zheng, H. Wang, M.-h. Wu, Electron beam induced degradation of atrazine in aqueous solution, Chemical Engineering Journal 275 (2015) 374-380. <https://doi.org/https://doi.org/10.1016/j.cej.2015.04.063>.
- [200] F. Govantes, O. Porrúa, V. García-González, E. Santero, Atrazine biodegradation in the lab and in the field: enzymatic activities and gene regulation, Microbial Biotechnology 2(2) (2009) 178-185. <https://doi.org/https://doi.org/10.1111/j.1751-7915.2008.00073.x>.
- [201] N. Shapir, E.F. Mongodin, M.J. Sadowsky, S.C. Daugherty, K.E. Nelson, L.P. Wackett, Evolution of Catabolic Pathways: Genomic Insights into Microbial s-Triazine Metabolism, Journal of Bacteriology 189(3) (2007) 674-682. <https://doi.org/10.1128/JB.01257-06>.
- [202] M.L. de Souza, M.J. Sadowsky, L.P. Wackett, Atrazine chlorohydrolase from *Pseudomonas* sp. strain ADP: gene sequence, enzyme purification, and protein characterization, Journal of Bacteriology 178(16) (1996) 4894-4900. <https://doi.org/10.1128/jb.178.16.4894-4900.1996>.
- [203] N. Shapir, C. Pedersen, O. Gil, L. Strong, J. Seffernick, J. Sadowsky Michael, P. Wackett Lawrence, *TrzN* from *Arthrobacter aurescens* TC1 Is a Zinc Amidohydrolase, Journal of Bacteriology 188(16) (2006) 5859-5864. <https://doi.org/https://doi.org/10.1128/JB.00517-06>.
- [204] L. Seffernick Jennifer, G. Johnson, J. Sadowsky Michael, P. Wackett Lawrence, Substrate Specificity of Atrazine Chlorohydrolase and Atrazine-Catabolizing Bacteria, Applied and Environmental Microbiology 66(10) (2000) 4247-4252. <https://doi.org/10.1128/AEM.66.10.4247-4252.2000>.
- [205] L. Seffernick Jennifer, A. Aleem, P. Osborne Jeffrey, G. Johnson, J. Sadowsky Michael, P. Wackett Lawrence, Hydroxyatrazine *N*-Ethylaminohydrolase (*AtzB*): an Amidohydrolase Superfamily Enzyme Catalyzing Deamination and Dechlorination, Journal of Bacteriology 189(19) (2007) 6989-6997. <https://doi.org/https://doi.org/10.1128/JB.00630-07>.
- [206] N. Shapir, P. Osborne Jeffrey, G. Johnson, J. Sadowsky Michael, P. Wackett Lawrence, Purification, Substrate Range, and Metal Center of *AtzC*: the *N*-Isopropylammelide Aminohydrolase Involved in Bacterial Atrazine Metabolism, Journal of Bacteriology 184(19) (2002) 5376-5384. <https://doi.org/https://doi.org/10.1128/JB.184.19.5376-5384.2002>.
- [207] S. Rousseaux, A. Hartmann, G. Soulas, Isolation and characterisation of new Gram-negative and Gram-positive atrazine degrading bacteria from different French soils, FEMS

Microbiology Ecology 36(2-3) (2001) 211-222. <https://doi.org/10.1111/j.1574-6941.2001.tb00842.x>.

[208] V. García-González, F. Govantes, O. Porrúa, E. Santero, Regulation of the *Pseudomonas* sp. Strain ADP Cyanuric Acid Degradation Operon, *Journal of Bacteriology* 187(1) (2005) 155-167. <https://doi.org/10.1128/JB.187.1.155-167.2005>.

[209] S. Karns Jeffrey, Gene Sequence and Properties of ans-Triazine Ring-Cleavage Enzyme from *Pseudomonas* sp. Strain NRRLB-12227, *Applied and Environmental Microbiology* 65(8) (1999) 3512-3517. <https://doi.org/10.1128/AEM.65.8.3512-3517.1999>.

[210] Z. Getenga, U. Dörfler, A. Iwobi, M. Schmid, R. Schroll, Atrazine and terbuthylazine mineralization by an *Arthrobacter* sp. isolated from a sugarcane-cultivated soil in Kenya, *Chemosphere* 77(4) (2009) 534-539. <https://doi.org/https://doi.org/10.1016/j.chemosphere.2009.07.031>.

[211] C.L. Bahena, S.S. Martínez, D.M. Guzmán, M. del Refugio Trejo Hernández, Sonophotocatalytic degradation of alazine and gesaprim commercial herbicides in TiO₂ slurry, *Chemosphere* 71(5) (2008) 982-989. <https://doi.org/https://doi.org/10.1016/j.chemosphere.2007.11.007>.

[212] D. Wen, B. Chen, B. Liu, An ultrasound/O₃ and UV/O₃ process for atrazine manufacturing wastewater treatment: a multiple scale experimental study, *Water Science and Technology* 85(1) (2021) 229-243. <https://doi.org/10.2166/wst.2021.633>.

[213] S.M. Sarmiento, J.T.G. Miranda, Kinetics of the atrazine degradation process using H₂O₂-UVC, *Water Science and Technology* 69(11) (2014) 2279-2286. <https://doi.org/10.2166/wst.2014.158>.

[214] S.A. Popova, G.G. Matafonova, V.B. Batoev, Removal of organic micropollutants from water by sonopholytic-activated persulfate process, *IOP Conference Series: Materials Science and Engineering* 687(6) (2019) 066051. <https://doi.org/10.1088/1757-899x/687/6/066051>.

[215] A.J. Moreira, A.C. Borges, L.F.C. Gouvea, T.C.O. MacLeod, G.P.G. Freschi, The process of atrazine degradation, its mechanism, and the formation of metabolites using UV and UV/MW photolysis, *Journal of Photochemistry and Photobiology A: Chemistry* 347 (2017) 160-167. <https://doi.org/https://doi.org/10.1016/j.jphotochem.2017.07.022>.

[216] A.J. Moreira, B.S. Pinheiro, A.F. Araújo, G.P.G. Freschi, Evaluation of atrazine degradation applied to different energy systems, *Environmental Science and Pollution Research* 23(18) (2016) 18502-18511. <https://doi.org/10.1007/s11356-016-6831-x>.

[217] A. Tauber, C. von Sonntag, Products and Kinetics of the OH-radical-induced Dealkylation of Atrazine, *Acta hydrochimica et hydrobiologica* 28(1) (2000) 15-23. [https://doi.org/https://doi.org/10.1002/\(SICI\)1521-401X\(200001\)28:1<15::AID-AHEH15>3.0.CO;2-2](https://doi.org/https://doi.org/10.1002/(SICI)1521-401X(200001)28:1<15::AID-AHEH15>3.0.CO;2-2).

- [218] W. Song, J. Li, C. Fu, Z. Wang, X. Zhang, J. Yang, W. Hogland, L. Gao, Kinetics and pathway of atrazine degradation by a novel method: Persulfate coupled with dithionite, *Chemical Engineering Journal* 373 (2019) 803-813. <https://doi.org/https://doi.org/10.1016/j.cej.2019.05.110>.
- [219] J.A. Khan, X. He, N.S. Shah, M. Sayed, H.M. Khan, D.D. Dionysiou, Degradation kinetics and mechanism of desethyl-atrazine and desisopropyl-atrazine in water with OH and SO₄-based-AOPs, *Chemical Engineering Journal* 325 (2017) 485-494. <https://doi.org/https://doi.org/10.1016/j.cej.2017.05.011>.
- [220] I. Yanagisawa, T. Oyama, N. Serpone, H. Hidaka, Successful Scission of a Recalcitrant Triazinic Ring. The Photoassisted Total Breakup of Cyanuric Acid in Ozonized TiO₂ Aqueous Dispersions in the Presence of an Electron Acceptor (H₂O₂), *The Journal of Physical Chemistry C* 112(46) (2008) 18125-18133. <https://doi.org/10.1021/jp8037285>.
- [221] X. Ding, S. Wang, W. Shen, Y. Mu, L. Wang, H. Chen, L. Zhang, Fe@Fe₂O₃ promoted electrochemical mineralization of atrazine via a triazinon ring opening mechanism, *Water Research* 112 (2017) 9-18. <https://doi.org/https://doi.org/10.1016/j.watres.2017.01.024>.
- [222] N. Borràs, R. Oliver, C. Arias, E. Brillas, Degradation of Atrazine by Electrochemical Advanced Oxidation Processes Using a Boron-Doped Diamond Anode, *The Journal of Physical Chemistry A* 114(24) (2010) 6613-6621. <https://doi.org/10.1021/jp1035647>.
- [223] WorldHealthOrganization, Pesticide residues in food: 2007, toxicological evaluations, sponsored jointly by FAO and WHO, with the support of the International Programme on Chemical Safety, joint meeting of the FAO Panel of Experts on Pesticide Residues in Food and the Environment and the WHO Core Assessment Group, World Health Organization, Geneva, Switzerland, 18-27 September 2007.
- [224] K. Ralston-Hooper, J. Hardy, L. Hahn, H. Ochoa-Acuña, L.S. Lee, R. Mollenhauer, M.S. Sepúlveda, Acute and chronic toxicity of atrazine and its metabolites deethylatrazine and deisopropylatrazine on aquatic organisms, *Ecotoxicology* 18(7) (2009) 899-905. <https://doi.org/10.1007/s10646-009-0351-0>.
- [225] G.W. Stratton, Effects of the herbicide atrazine and its degradation products, alone and in combination, on phototrophic microorganisms, *Archives of Environmental Contamination and Toxicology* 13(1) (1984) 35-42. <https://doi.org/https://doi.org/10.1007/BF01055644>.
- [226] E.P.o.C.i.t.F. Chain, E.F. Efsa Panel on Food Contact Materials, A. Processing, Scientific Opinion on Melamine in Food and Feed, *EFSA Journal* 8(4) (2010) 1573. <https://doi.org/https://doi.org/10.2903/j.efsa.2010.1573>.
- [227] S. Rousseaux, A. Hartmann, G. Soulas, Isolation and characterisation of new Gram-negative and Gram-positive atrazine degrading bacteria from different French soils, *FEMS Microbiology Ecology* 36(2-3) (2001) 211-222. <https://doi.org/10.1111/j.1574-6941.2001.tb00842.x>.

- [228] V. Sánchez, F.J. López-Bellido, P. Cañizares, L. Rodríguez, Assessing the phytoremediation potential of crop and grass plants for atrazine-spiked soils, *Chemosphere* 185 (2017) 119-126. <https://doi.org/https://doi.org/10.1016/j.chemosphere.2017.07.013>.
- [229] S.M. Arnold, W.J. Hickey, R.F. Harris, Degradation of Atrazine by Fenton's Reagent: Condition Optimization and Product Quantification, *Environmental Science & Technology* 29(8) (1995) 2083-2089. <https://doi.org/https://doi.org/10.1021/es00008a030>.
- [230] N. Yang, Y. Liu, J. Zhu, Z. Wang, J. Li, Study on the efficacy and mechanism of Fe-TiO₂ visible heterogeneous Fenton catalytic degradation of atrazine, *Chemosphere* 252 (2020) 126333. <https://doi.org/https://doi.org/10.1016/j.chemosphere.2020.126333>.
- [231] A. Ventura, G. Jacquet, A. Bermond, V. Camel, Electrochemical generation of the Fenton's reagent: application to atrazine degradation, *Water Research* 36(14) (2002) 3517-3522. [https://doi.org/https://doi.org/10.1016/S0043-1354\(02\)00064-7](https://doi.org/https://doi.org/10.1016/S0043-1354(02)00064-7).
- [232] J. Peng, X. Lu, X. Jiang, Y. Zhang, Q. Chen, B. Lai, G. Yao, Degradation of atrazine by persulfate activation with copper sulfide (CuS): Kinetics study, degradation pathways and mechanism, *Chemical Engineering Journal* 354 (2018) 740-752. <https://doi.org/https://doi.org/10.1016/j.cej.2018.08.038>.
- [233] X. Xu, W. Chen, S. Zong, X. Ren, D. Liu, Atrazine degradation using Fe₃O₄-sepiolite catalyzed persulfate: Reactivity, mechanism and stability, *Journal of Hazardous Materials* 377 (2019) 62-69. <https://doi.org/https://doi.org/10.1016/j.jhazmat.2019.05.029>.
- [234] X. Wang, Y. Wang, N. Chen, Y. Shi, L. Zhang, Pyrite enables persulfate activation for efficient atrazine degradation, *Chemosphere* 244 (2020) 125568. <https://doi.org/https://doi.org/10.1016/j.chemosphere.2019.125568>.
- [235] D. Zhu, L. Jiang, R.-l. Liu, P. Chen, L. Lang, J.-w. Feng, S.-j. Yuan, D.-y. Zhao, Wire-cylinder dielectric barrier discharge induced degradation of aqueous atrazine, *Chemosphere* 117 (2014) 506-514. <https://doi.org/https://doi.org/10.1016/j.chemosphere.2014.09.031>.
- [236] C. Petrier, B. David, S. Laguian, Ultrasonic degradation at 20 kHz and 500 kHz of atrazine and pentachlorophenol in aqueous solution: Preliminary results, *Chemosphere* 32(9) (1996) 1709-1718. [https://doi.org/https://doi.org/10.1016/0045-6535\(96\)00088-4](https://doi.org/https://doi.org/10.1016/0045-6535(96)00088-4).

Chapter II. Methods and protocols

II.1. Methodology

Atrazine (ATZ) with a triazine ring structure is chemically stable and refractory to degradation. The existing atrazine degradation technologies have limitations (slow degradation kinetics, low remediation efficiency, etc.), and the research on the degradation mechanism is still incomplete. So, this thesis aims to develop an innovative and highly efficient method for atrazine degradation and compare it comprehensively with conventional methods. The experiments described in this thesis cover three parts: atrazine degradation, metabolites analysis and toxicity analysis. The experimental design of this thesis is shown in the following schematic diagram (Figure II.1).

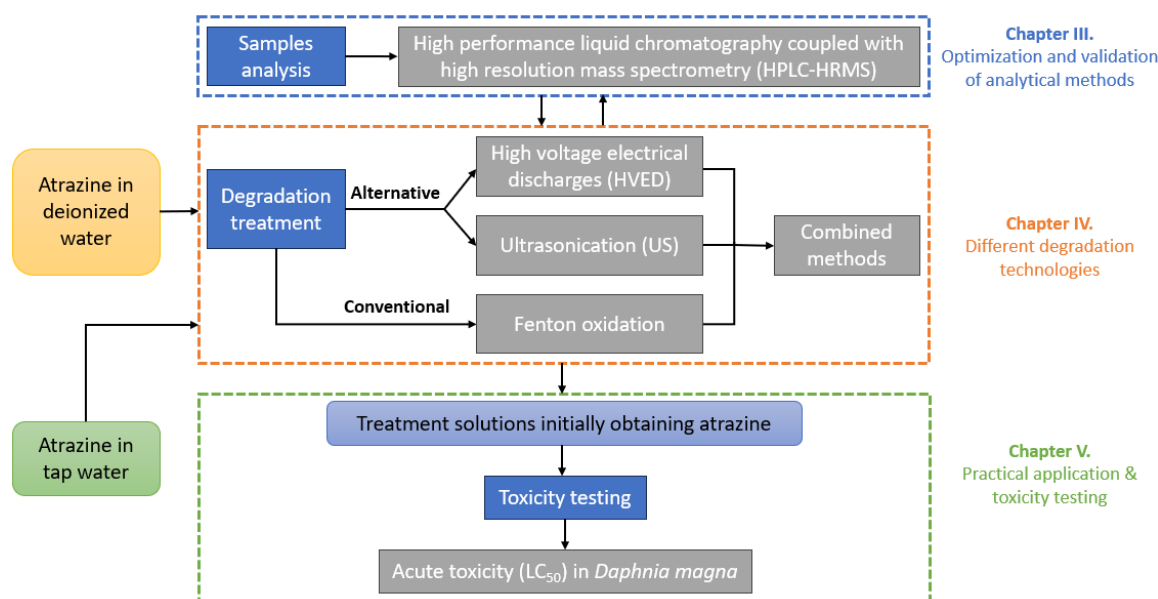


Figure II.1. Schematic diagram of the experimental design in this thesis.

II.2. Development and validation of analytical methods for real-time monitoring atrazine degradation process by HPLC-HRMS

In this part, the first task is to optimize and validate a new analytical method for atrazine degradation monitoring. Considering the low water solubility of atrazine (34.7 mg/L in water, 25 °C) and the detection limit in chromatography, an initial concentration of atrazine of 20 mg/L was adopted in atrazine degradation process. This concentration is prepared by adding 1 mg of atrazine, purchased from Sigma-

Aldrich (St. Quentin Fallavier, France) per 50 mL of deionized water (conductivity 0.055 $\mu\text{S}/\text{cm}$ at 25°C) acquired from a water purification device Rephile Direct-Pure® UP 10 (MA, USA).

Table II.1. Preparation of calibration solution.

Calibration point	ATZ	Preparation of ATZ solutions (L1-L8)		
	Target concentration (μM)	Mother solution	Volume of mother solution (mL)	Final solution (mL)
L8	90	90 μM ATZ stock solution		
L7	60	L8	1	1.5
L6	30	L7	0.5	1
L5	20	L7	0.5	1.5
L4	10	L5	0.5	1
L3	5	L4	0.5	1
L2	2.5	L3	0.5	1
L1	1	L2	0.5	2

In order to overcome the uncertainty of the measurements related to the sample preparation and mass spectrometry stages, the calibration curve will be produced by internal calibration. As shown in [Table II.1](#), atrazine stock solution with a concentration of 90 μM was used to prepare 8 different concentrations of atrazine solutions (L1-L8), that is, 8 calibration points. The internal standard (IS) was atrazine-D5 (atrazine labelled isotopically with 5 deuterium), purchased from Sigma-Aldrich (St. Quentin Fallavier, France). To prepare IS solution, 0.15 mg atrazine-D5 was dissolved to 6 mg/L with acetonitrile, LC-MS grade solvents and formic acid were bought from Biosolve Chimie (Dieuze, France). Each calibration point will contain the same quantity of IS solution, corresponding to a volume of 20 μL . The final dilution of the calibration points will be performed with a total volume of 200 μL (180 μL atrazine solution + 20 μL IS solution) in 1-ml vials, analysed by high performance liquid chromatography coupled with high resolution mass

spectrometry (HPLC-HRMS). [Figure II.2](#) shows a linear relationship between the response and the concentration.

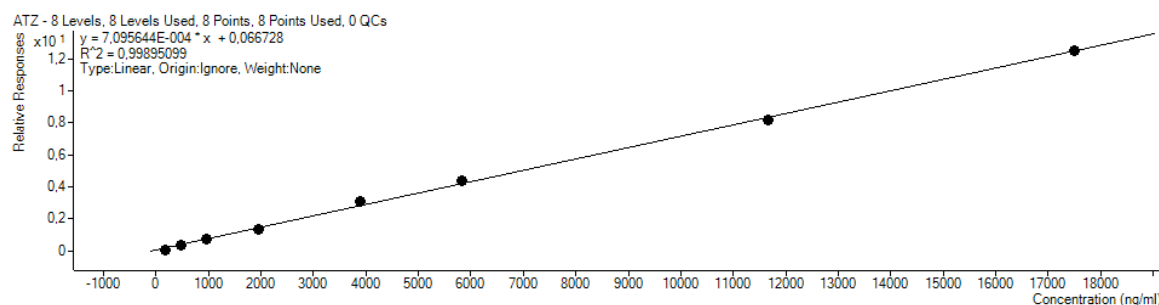


Figure II.2. Calibration curve of atrazine.

Atrazine and its metabolites detection and semi quantitative evaluation were performed by HPLC-HRMS. The HPLC system (Infinity 1290, Agilent Technologies, France) with DAD, was connected to a Q-TOF micro hybrid quadrupole time of flight mass spectrometer (Agilent 6538, Agilent Technologies, France) with electrospray ionization (ESI). HPLC was carried out on a Thermo Hypersyl Gold C18 (USP L1) column (100 × 2.1 mm, 1.9 μm, 175 Å), connected to an Agilent Infinity 1290 HPLC at 40 °C.

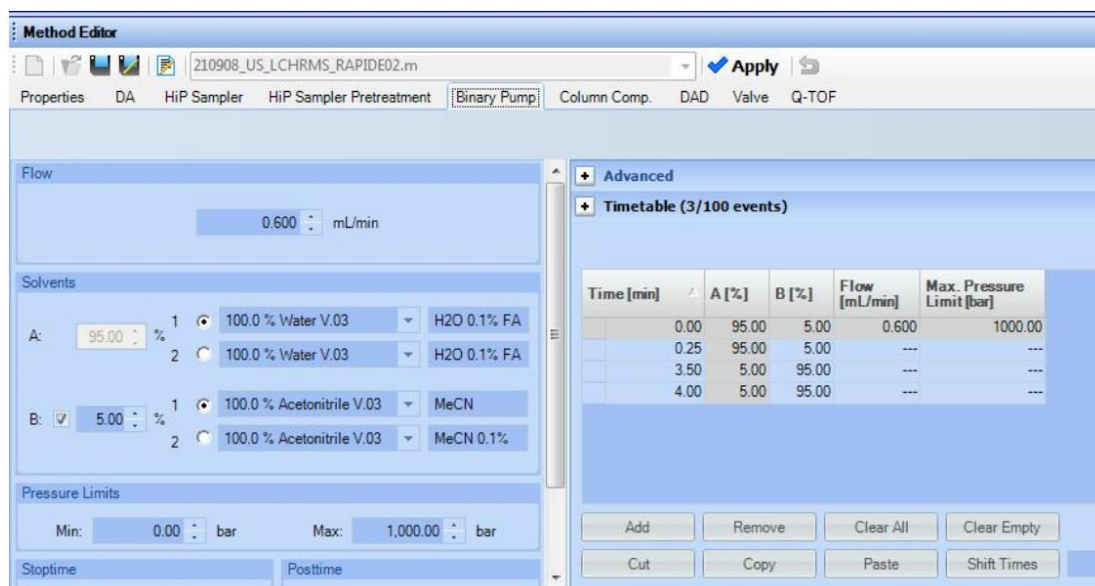


Figure II.3. The gradient program of HPLC-HRMS.

As [Figure II.3](#) shown, the solvent system was A: 0.1% formic acid in Milli-Q water and B: Acetonitrile. The gradient program began with 5% B, held at 5% for 0.25 min and ramped to 95% at 3.50 min, held at 95% for 0.5 min. The flow rate

was set at 0.600 mL/min. All compounds' responses were measured in ESI+ and were calibrated externally. The ESI Gas Temp was 350 °C, at electrospray voltage +3800 V. Drying Gas was set at 10 L/min and Nebuliser was at 30 psi. Fragment voltage was set at 110 V. HRMS spectrum was registered at 5 Hz in the mass range of 50 to 1200 m/z with internal calibration.

Because this new analytical method is fast, efficient, highly sensitive and accurate, it was used to monitor the degradation process of atrazine in real time. For more details see chapter III.

II.3. Effects of different technologies (HVED, US and Fenton oxidation) on atrazine degradation

After validating the analytical method, it was possible to study the effects of different technologies (HVED, US and Fenton oxidation) on atrazine degradation, including degradation efficiency, metabolite kinetics and reaction mechanism. This study focused on one single compound atrazine in deionized water, and the initial concentration was maintained at 20 mg/L. Initially, atrazine was separately degraded by three technologies (HVED, US and Fenton oxidation), and a horizontal comparison was conducted between them. This was to explore how technologies affect the degradation pathways of atrazine, such as dechlorination-hydroxylation, dealkylation and alkyl oxidation.

Considering that hydroxyl radicals $\bullet OH$ play an important role on atrazine degradation and can be more activated in the presence of Fenton's reagent, combined approaches, namely alternative techniques (HVED and US) coupled with Fenton oxidation were conducted. Theoretically, the combination method can stimulate the generation of hydroxyl radicals more and achieve a high degradation rate in a short time. For example, for "US+Fenton" combined treatment, the addition of Fenton reagent is beneficial to the release of hydroxyl radicals $\bullet OH$ from its self-combination product hydrogen peroxide.

In short, the advanced oxidation treatment (HVED) was compared with physical treatment (US) as well as traditional chemical treatment (Fenton oxidation) for atrazine degradation. By monitoring the degradation pathways of atrazine during these three treatments, a more reasonable proposal for the reaction

mechanism can be obtained. In addition, kinetic studies on the degradation metabolites were also performed, which helped to evaluate the toxicity before and after atrazine degradation. Attention was also focused on the energy consumption during treatment. For more details see chapter IV.

II.4. Practical application of atrazine degradation in tap water & toxicity test of experimental wastewater

This part considers the interaction between the degradation technology and the actual environment, including two aspects. The first aspect is a degradation application in a real environment, degrading atrazine in tap water. The second aspect is environmental assessment through toxicity testing of experimental wastewater.

For the first aspect, the HPLC-HRMS analysis method was used to determine and quantify atrazine and its metabolites. Besides, to explore the effect of a real matrix (tap water) compared to the model matrix (deionized water), four comparative experiments were carried out, one was the degradation of only tap water, the second was the degradation of atrazine's tap water solution, the third was the degradation of only deionized water, and the fourth was the degradation of atrazine's deionized water solution. Due to the abundance of impurities in tap water, the degradation process of atrazine is affected by other competing reactions.

In order to verify the metabolite differences between different treatments, normalized statistical analysis was performed on each HPLC-HRMS data. Some new untargeted metabolites appeared, but interference from other impurities will affect their resolution. Therefore, comprehensive untargeted molecular data acquisition is required, and the open-source software MS-DIAL can achieve this through mass spectrum deconvolution. The MS-DIAL program was used to normalize data imported from MS raw data and perform principal component analysis (PCA). PCA score plots help to clearly observe the distribution of sampling points for each treatment, so as to know the difference in degradation metabolites between treatments.

For the second aspect, the crustacean *D. magna* was used to test the potential toxicity of experimental wastewater after degradation treatment. This part

of the work was carried out in collaboration with Dr. Messika REVEL (associate professor in ecotoxicology, UniLaSalle, campus de Rennes, France) and Dr. Stéphane FIRMIN (deputy director research unit AGHYLE UP2018.C101, UniLaSalle, campus de Beauvais, France). *D. magna* was cultured artificially in the laboratory. The experimental wastewater needs to be diluted before conducting toxicity tests to prevent *D. magna* from being unable to survive due to ultra-high concentrations. All toxicity tests were conducted in a chamber under the same abiotic conditions as the culture and protocols and analyses were carried out in accordance with the Organisation for Economic Cooperation and Development (OECD) guidelines for immobilization test of *D. magna*. Lethal concentration 50 (LC₅₀) is used as a toxicity indicator, which represents the average concentration that induced death in 50% of the test organisms. According to the LC₅₀ value, the toxicity ranking of the experimental wastewater after degradation treatment can be evaluated. From this we can judge which degradation technology is more environmentally friendly. Additionally, this result can be compared with previous toxicity assessments based on metabolite kinetics. For more details see chapter V.

All in all, an ideal atrazine degradation technology should consider not only high degradation efficiency but also environmental friendliness. This is also the direction of our future work.

II.5. Organization of chapters III, IV, and V.

As mentioned above, the experimental and results part of this manuscript includes chapters III, IV, and V. For each chapter, it consists of chapter introduction, materials and methods, results and discussion, chapter conclusion and chapter references. The work of chapter III and IV have been published, and the work of chapter V was summarized and prepared for publication. These three publications are inserted into the chapter results and discussion.

Chapter III. Development and validation of analytical methods for real-time monitoring atrazine degradation process by HPLC-HRMS

III.1. Chapter introduction

The herbicide atrazine is a commonly used chlorinated s-triazine herbicide for the prevention of broadleaf and grassy weeds [1]. The triazine ring structure of atrazine makes it chemically stable and refractory [2]. Compared with the challenging triazine ring cleavage pathway, the degradation of atrazine is more prone to other pathways, such as dechlorination-hydroxylation [3], N-dealkylation [4], alkyl-oxidation [5], etc. In these diverse atrazine degradation pathways, its degradative metabolites are numerous and complex. For example, atrazine can be converted into hydroxyatrazine (HA) by dechlorination-hydroxylation, and can be converted into deethylatrazine (DEA) and deisopropylatrazine (DIA) by N-dealkylation, which are metabolites commonly detected in agricultural soils [6], surface, and groundwater [7]. But according to the known acute oral toxicity LD₅₀ value in male rats [8], the metabolites DEA (1890 mg/kg) and DIA (2290 mg/kg) are much more toxic than atrazine (3090 mg/kg). The formation of highly toxic metabolites should be avoided during the degradation process; however, this is not easy to achieve because it will be affected by the treatment process used.

Conventional degradation technologies include biodegradation [9,10] and chemical degradation [11], but the former generally require more treatment time and the latter uses chemical oxidants that maybe not environmentally friendly. Advanced oxidation processes (AOPs), such as ultrasound [12], microwave radiation [13], photocatalysis [14], etc., have received widespread attention. AOPs are broadly defined as a series of alternative treatment procedures that degrade organic contaminants in wastewater through reactive oxygen species, primarily hydroxy radicals $\bullet OH$ [15]. Most of these works use liquid chromatography–mass spectrometry (LC-MS) to study degradation kinetics of atrazine and formation mechanism of metabolites [5,16,17]. Problems with their analytical methods are low resolution and delayed detection of degradation kinetics after samples are transferred and stored. So, in order to solve these problems, it is necessary to create and validate a new analytical method for real-time monitoring during the

degradation process.

Therefore, this chapter will mainly focus on:

- 1) optimization and validation of high-performance liquid chromatography coupled with high-resolution mass spectrometry (HPLC-HRMS).
- 2) development of an online analytical method combining reaction system, automatic sampling and HPLC-HRMS;
- 3) comparison of online and offline analytical methods, whether there is a difference in sampling timeliness.;
- 4) exploration of the feasibility of atrazine degradation by Fenton oxidation and ultrasound;
- 5) mechanism study of atrazine degradation kinetics and metabolites formation kinetics.

More details can be found in the next section III.2 **“Real-time monitoring of the atrazine degradation by liquid chromatography and high-resolution mass spectrometry: effect of Fenton process and ultrasound treatment”**, which is published in the journal *“Molecules”*. It was conducted under the direction of Dr. Franck MERLIER, Prof. Nabil GRIMI, Dr. Nadia BOUSSETTA and Dr. Gérald ENDERLIN.

III.2. Real-time monitoring of the atrazine degradation by liquid chromatography and high-resolution mass spectrometry: effect of Fenton process and ultrasound treatment

Abstract

High resolution mass spectrometry (HRMS) was coupled with ultra-high-performance liquid chromatography (uHPLC) to monitor atrazine (ATZ) degradation process of Fenton/ultrasound (US) treatment in real time. Samples were automatically taken through a peristaltic pump, and then analysed by HPLC-HRMS. The injection in the mass spectrometer was performed every 4 min for 2 h. ATZ and its degradation metabolites were sampled and identified. Online Fenton experiments in different equivalents of Fenton reagents, online US experiments with/without Fe^{2+} and offline Fenton experiments were conducted. Higher equivalents of Fenton reagents promoted the degradation rate of ATZ and the

generation of the late-products such as Ammeline (AM). Besides, adding Fe^{2+} accelerated ATZ degradation in US treatment. In offline Fenton, the degradation rate of ATZ was higher than that of online Fenton, suggesting the offline samples were still reacting in the vial. The online analysis precisely controls the effect of reagents over time through automatic sampling and rapid detection, which greatly improves the measurement accuracy. The experimental set up proposed here both prevents the degradation of potentially unstable metabolites and provides a good way to track each metabolite.

Keywords: atrazine metabolite; online sampling-LC-HRMS; Fenton; ultrasound degradation

1. Introduction

Although the quantity of pesticides in water was significantly reduced in France between 2008 and 2018 [18], certain molecules, such as atrazine, banned in Europe since 2003, persist in the environment. Atrazine (2-chloro-4-ethylamino-6-isopropylamino-1,3,5-triazine) is a triazine herbicide with a wide range of application, for grassy and broadleaf weed control in corn, sugarcane, sorghum and other crops [19-22]. However, atrazine is also considered as one of the most toxic herbicides [23], because it can act as an endocrine disruptor that can produce damage to the endocrine system, causing a series of pathological changes and reproductive abnormalities [24,25]. In addition, atrazine is also a potential carcinogen due to negative impact on human health such as tumors, breast, ovarian, and uterine cancers as well as leukemia and lymphoma [26,27].

The literature reports numerous attempts aimed at degrading this water pesticide. The reported treatments are microwave-assisted photo reactions [28], high voltage electrical discharges [29], ultrasound [12,30], advanced oxidation processes (AOPs) [31,32] and bioremediation [33]. However, these treatments produce new molecules which are sometimes even more toxic to humans and the environment [31,34]. In Fenton oxidation, hydrogen peroxide (H_2O_2) is activated by ferrous (Fe^{2+}) ions to generate hydroxyl radicals ($HO\cdot$). In ultrasound treatment, high energy leads to water splitting, generating hydroxyl radicals ($HO\cdot$) and hydrogen radicals ($H\cdot$). Hydroxyl radicals ($HO\cdot$) dominate the degradation of atrazine in Fenton oxidation and in ultrasound treatment [12].

In order to evaluate the performance of these treatments on pesticides degradation in water, it is essential to use analytical techniques to follow the evolution of its metabolites during the treatments. Most of the studies use chromatographic techniques with UV (LC-UV) [29,31,35] detection with or without mass spectrometry coupling (LC-MS). Compared with low-resolution tandem mass spectrometry (LC-MS/MS) [36], high-resolution mass spectrometry (LC-HRMS) [37] has higher accuracy in terms of metabolite characterization and exact mass specificity. In most cases, the required sampling for the kinetic monitoring of the degradation is carried out by spot sampling prior to transfer or storage [30,31,38]. When monitoring the kinetics of Fenton reaction, the presence of reagents in the medium can lead to errors in the estimation of metabolite amounts due to potential evolution of the samples and incomplete cessation of the reaction. To ensure reliable observation of the kinetics of each metabolite, automatic sampling can be combined with the LC-MS system [39]. Fenton reactions or ultrasound (US) treatments were previously monitored online with detections by Fourier transform infrared spectroscopy (FTIR) [40], illumination-assisted droplet spray ionization mass spectrometry IA-DSI-MS [41] or fluorescence [42].

The aim of the present study is to demonstrate the feasibility of monitoring the kinetics of a Fenton reaction or US treatment by means of LC-HRMS. This coupling will thus make it possible to increase both the sampling frequency and to minimize the sample analysis time, allowing access to the most unstable metabolites [41].

2. Materials and Methods

2.1. Chemicals and Reagents

Solvents and formic acid were purchased from Biosolve Chimie with UPLC-MS grade (Dieuze, Moselle, France). Atrazine (ATZ), atrazine-D5 (ATZ-D5), deisopropylatrazine (DIA), deethylatrazine (DEA), deethyldeisopropylatrazine (DEDIA), hydroxyatrazine (HA) and ammeline (AM) were purchased from Sigma-Aldrich (St. Quentin Fallavier, France). Buffers were prepared with Milli-Q water, purified using a Milli-Q system (Millipore, Molsheim, France).

2.2. Internal Standard (IS) Preparation

Atrazine isotopically labelled with 5 deuterium (ATZ-D5) was used as an internal standard. To prepare a working IS solution, ATZ-D5 solution of 2 mg/L in acetonitrile was diluted to 15 ng/mL in distilled water.

2.3. Preparation of Calibration Standard and Quality Control (QC) Samples

Stock solutions of ATZ, DEA, DEDIA, AM, HA and DIA were prepared separately at 50 mg/L by dissolving accurately-weighed amounts of the compound in methanol. The working standard solutions of ATZ were prepared by serial dilution of the ATZ stock solutions with distilled water, to give final concentrations of 10, 5, 2, 1, 0.5 and 0.25 ng/mL. Calibration curve standard samples of ATZ were prepared by spiking 20 μ L of IS solution with 180 μ L of working standard solutions. QC samples were prepared in the same way.

2.4. Sample Preparation

An automatic sampling method was used for the online analysis. Online samples were taken every 4 min. The reaction solution (4 μ L) was automatically injected into the HPLC, while the IS solution (2 μ L) was added when switching the sampling valve by HPLC auto injector. For offline analysis, the reaction solution (50 μ L) was manually mixed with the IS solution (20 μ L). Then the 1 μ L mixed solution was injected into the LC-HRMS (see Section 3.5.5).

2.5. Instrumentation and Analytical Conditions

2.5.1. Offline HFUS Experiment with/without Fe²⁺

Two initial solutions of ATZ (20 mg/L, 50 mL, 4.64 μ mol) with/without 10 eq. Fe²⁺ (13 mg, 46.4 μ mol FeSO₄·7H₂O) were treated by ultrasound (525 kHz, 80 W) for 2 h. After these two experiments, 2 × 9 samples were taken (1 mL of final treatment solution was added to 1.5 mL of vial), 2 × 3 of which were used for 0-day analysis, and the rest were stored in different refrigerators (4 °C, -20 °C, and -80 °C). Absolute quantification was performed by LC-UV at 260 nm without addition of internal standard.

2.5.2. Online Fenton Experiment

The initial solution of ATZ (20 mg/L, 92.72 μ mol/L) was prepared by dissolving ATZ (5 mg, 23.18 μ mol, 215.68 g/mol) into 250 mL of distilled water.

Different equivalents of Fenton reagents 10 eq., 5 eq., 2 eq. and 1 eq. were added, respectively, to four initial solutions of ATZ (15 mL, 1.392 μmol): $\text{FeSO}_4 \cdot 7\text{H}_2\text{O}$ (10 eq., 3.9 mg, 13.92 μmol) and 30% H_2O_2 solution (10 eq., 1.422 mL, 13.92 μmol); $\text{FeSO}_4 \cdot 7\text{H}_2\text{O}$ (5 eq., 1.95 mg, 6.96 μmol) and 30% H_2O_2 solution (5 eq., 0.711 mL, 6.96 μmol); $\text{FeSO}_4 \cdot 7\text{H}_2\text{O}$ (2 eq., 1.56 mg, 2.784 μmol) and 30% H_2O_2 solution (2 eq., 0.284 mL, 2.784 μmol); $\text{FeSO}_4 \cdot 7\text{H}_2\text{O}$ (1 eq., 0.39 mg, 1.392 μmol) and 30% H_2O_2 solution (1 eq., 0.142 mL, 1.392 μmol). Those four reactions were incubated for 2 h with a magnetic stirrer at 500 rpm. The time $t = 0$ min corresponds to the first LCMS sample tested. Fenton reagents were added at $t = 4$ min.

2.5.3. Online LFUS Experiment with/without Fe^{2+}

The initial solution of ATZ (15 mL, 1.392 μmol) without Fe^{2+} was treated by ultrasound (50 kHz, 70 W) for 2 h. Then, in another controlled experiment with Fe^{2+} , the initial solution of ATZ (15 mL, 1.392 μmol) was treated by ultrasound (50 kHz, 70 W) in the same way, but after 4 min $\text{FeSO}_4 \cdot 7\text{H}_2\text{O}$ (10 eq., 3.9 mg, 13.92 μmol) was added. As the temperature rose during ultrasonic treatment, a water circulating cooling device was used on the outer wall of the reaction system.

2.5.4. Offline Fenton Experiment

Nine initial atrazine solutions (7.5 mL, 0.696 μmol) were divided into three groups, and then different equivalents of Fenton reagents 10 eq., 5 eq. and 2 eq. were added, respectively. The reactions were incubated on a magnetic stirrer at 500 rpm. Samples were taken at 0 h, 1 h, 2 h, 4 h, 8 h and 22 h. At time $t = 0$ min, Fenton reagents were not added. At time $t = 4$ min, Fenton reagents were added.

2.5.5. HPLC-HRMS

Atrazine and metabolites detection and semi quantitative evaluation were performed by LC-HRMS. The HPLC system (Infinity 1290, Agilent Technologies, France) with DAD, was connected to a Q-TOF micro hybrid quadrupole time of flight mass spectrometer (Agilent 6538, Agilent Technologies, France) with electrospray ionization (ESI). HPLC was carried out on a Thermo Hypersyl Gold C18 (USP L1) column (100 \times 2.1 mm, 1.9 μm , 175 A), connected to an Agilent Infinity 1290 HPLC at 40 $^\circ\text{C}$. The solvent system was A: 0.1% formic acid in Milli-Q water and B: Acetonitrile. The gradient program began with 5% B, held at 5% for

0.25 min and ramped to 95% at 3.50 min, held at 95% for 0.5 min. The flow rate was set at 0.600 mL/min. All compounds' responses were measured in ESI+ and were calibrated externally. The ESI Gas Temp was 350 °C, at electrospray voltage +3800 V. Drying Gas was set at 10 L/min and Nebuliser was at 30 psi. Fragment voltage was set at 110 V. HRMS spectrum was registered at 5 Hz in the mass range of 50 to 1200 m/z with internal calibration.

2.5.6. HPLC-HRMS Online Setup

The system consists of a 20 mL glass reactor with a double wall for temperature control and an ultrasound probe (Figure 1a). Sampling is carried out by suction using a peristaltic pump (Welco WMP1-F1.6FB-WP), equipped with a brushless motor. This pump was used with a voltage of 13 V DC corresponding to a flow rate of 1 mL/min. A glass tip was inserted into a flexible tube with 1.6 mm internal diameter connected to a 6-way high pressure valve (Agilent 1316C module). A sampling loop consists of a capillary tube type thermo viper SST "Black" (0.18 mm ID × 150 mm). In the initial position, the mixture is recycled to the reactor. At the time of analysis, the content of the loop is sent to the automatic injector which simultaneously injects 1 μL of an ATZ-D5 (IS) solution before being separated and analysed on the LC-ESI-HRMS system. After 50 s, the valve switches back to its initial state in order to prepare the next sample. The sampling and analysis cycle have a 4 min duration.

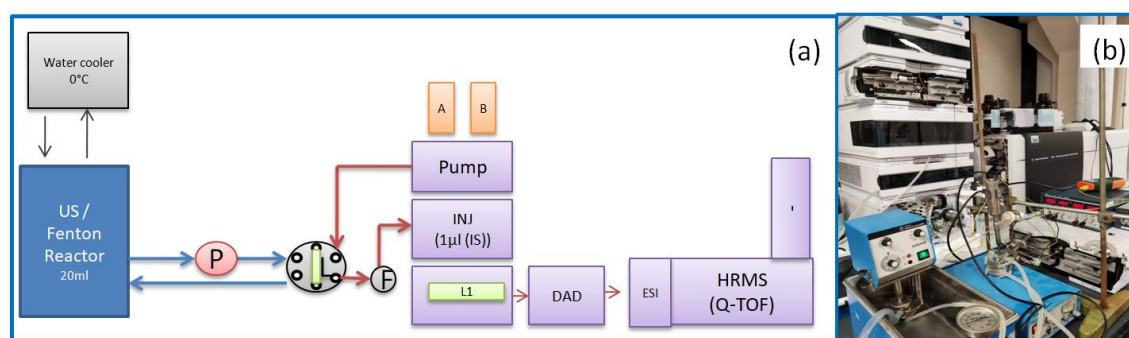


Figure 1. (a) Scheme of online sampling setup where, P is the peristaltic pump, F is the 0.2 μm filter, A and B is HPLC eluant, L1 is the C18 column. (b) Photo of actual system.

2.6. Data Analysis

Software MassHunter (Version B.07.00, Agilent Technologies, Santa Clara,

CA 95051, United States), was used for data processing. For Mass Profiler Pro workflow, an untargeted compound was generated by MFE algorithm

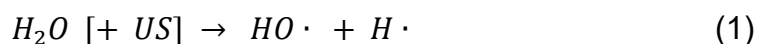
2.7. Compound Identification

The main metabolites of atrazine were validated by the conjunction of exact mass, MS/MS fragmentations, and retention time from standards [43]. A complementary list of metabolites was established from the literature and sought from the exact mass of the mono-isotope ion, if necessary, verified by MS/MS and compared in relative retention time compared to data from the literature.

3. Results and Discussion

3.1. Influence of Sample Storage after High Frequency Ultrasound (HFUS) Treatment

Figure 2 shows the effect of storage time on the concentration of residual ATZ. At 0-day, the initial ATZ solutions were treated by US experiments with and without Fe^{2+} respectively (US+ Fe^{2+} and US) at room temperature. Samples were taken after 2 h for LC-HRMS analysis, and then transferred to different temperatures refrigerators (4 °C, -20 °C, -80 °C) for analysis after 7 and 30 days.



High frequency ultrasound (HFUS) used at 525 kHz generates high temperature and a high-pressure region of bubbles in which hydroxyl radicals ($HO\cdot$) and hydrogen radicals ($H\cdot$) are produced by water splitting, and then the self-combination of radicals $HO\cdot$ gives hydrogen peroxides (Equations (1) and (2)) [44]. Fe^{2+} promotes the regeneration of radical ($HO\cdot$) from hydrogen peroxide (Equation (3)) [45]. The combination of Fe^{2+} and HFUS acts in concert towards the production of hydroxyl radicals ($HO\cdot$), which promotes the degradation of ATZ. As shown in Figure 2, at 0-day, the concentration of residual ATZ of US+ Fe^{2+} treatment for 2 h was much lower than that of US treatment for 2 h.

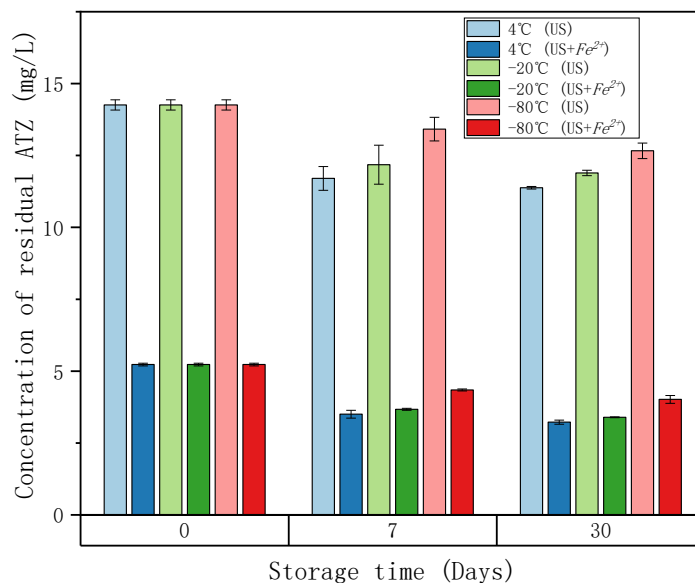


Figure 2. The effect of storage time on the concentration of residual ATZ. At 0-day, the initial ATZ solutions were treated by HFUS without or with Fe^{2+} , US or US+ Fe^{2+} . Conditions: $[ATZ]_0 = 0.093$ mmol/L; $[FeSO_4 \cdot 7H_2O]_0 = 0.93$ mmol/L for treatment US+ Fe^{2+} ; volume = 50 mL; ultrasound frequency = 525 kHz; reaction time = 2 h (see Section 2.5.1). Samples were taken and then stored at different temperatures (4 °C, -20 °C, and -80 °C).

In addition, with the increase of storage time, the concentration of residual ATZ decreased. Lower storage temperature prevented the reduction of residual ATZ to some extent, but still could not stop the further reactions during storage. This observation shows the interest of minimizing the interval time between treatment and its characterization in order to be able to monitor the least stable metabolites as well as possible.

3.2. Sonolysis and Fenton Reaction Reactor Coupled to LC-HRMS

To minimize degradation caused by the presence of ions or reactive molecules, automatic sampling was performed directly from the reactor containing the atrazine solution. Samples were then chromatographically separated. Conventional sampling followed by LC-MS or LC-MS/MS [12,46] analysis requires incompressible time of minutes or even days when the instruments are unavailable for analysis. Our experimental set up (see Section 2.5.6) makes it possible to take samples in real time and to analyze samples with a cycle of 4 min. A liquid circulation system was set up through flexible tubes, replaced regularly to limit

adsorption and release phenomena, and a glass tip in suction was equipped for sampling. A specially designed peristaltic pump was used, so as to ensure flow rates on the order of 1 mL/min and limit the dead volume of the sampling loop. A high-pressure six-way valve ensured a 4 min cycle of sampling and injection into the HPLC system. This valve was switched to the analysis position, while an internal standard consisting of ATZ-D5 was injected via the HPLC syringe, and switched back to sampling mode 50 s after initial analysis time (T_0), thus allowing a sampling cycle of 3.10 min before the next chromatographic separation.

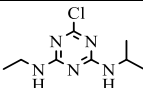
Since the treatments last for several hours, it is important to add a constant quantity of internal standard to the sample, which normalizes the areas of metabolites' peaks. Any degradation of the chromatographic separation was monitored for possible contamination of the ionization source by electrospray and mass drift of the analyzer, especially when Fe^{2+} ions are present in Fenton treatments as well as in $US+Fe^{2+}$ treatments. Here, the more portable low-frequency ultrasound (LFUS) device at 50 kHz was used instead of the unportable high-frequency ultrasound (HFUS) device at 525 kHz.

Acquisition without prior selection of precursors is possible using the high-resolution mass spectrometer. This enables non-targeted analysis and helps to understand the reaction mechanism.

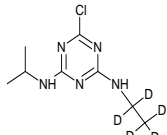
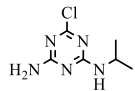
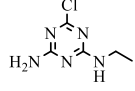
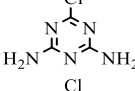
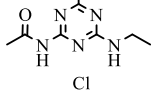
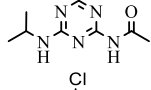
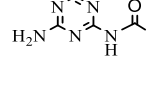
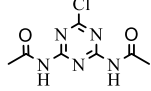
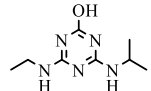
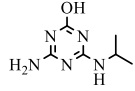
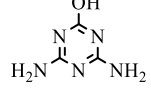
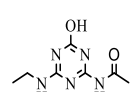
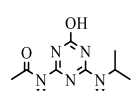
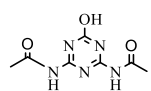
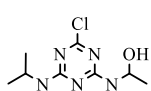
3.3. Related Compounds

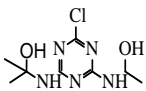
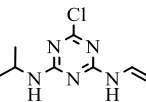
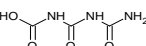
The initial substrate ATZ, internal standard ATZ-D5, and other detected metabolites are shown in [Table 1](#). The “metabolite level” corresponds to the potential level of transformations from ATZ to metabolite according to the degradation pathways (see Supplementary Materials [Figure S2](#). Proposed atrazine degradation pathways scheme).

Table 1. Information of related compounds.

Entries	Chemical Structure	Molecular Formula	Abbreviation	Name	m/z	Retention Time (min)		Metabolite Level
						Online	Offline	
1		$C_8H_{14}ClN_5$	ATZ	Atrazine	216.1010	2.558	2.178	0

Chapter III. Development and validation of analytical methods for real-time monitoring atrazine degradation process by HPLC-HRMS

2		C ₈ H ₉ D ₅ ClN ₅	ATZ-D5	Atrazine-D5	221.1324	2.579	2.168	\
3		C ₆ H ₁₀ ClN ₅	DEA	Deethylatrazine	188.0698	1.910	1.751	1
4		C ₅ H ₈ ClN ₅	DIA	Deisopropylatrazine	174.0541	1.620	1.463	1
5		C ₃ H ₄ ClN ₅	DDA	Didealkylatrazine	146.0228	1.023	0.905	2
6		C ₇ H ₁₀ ClN ₅ O	CDET	Simazine amide	216.0647	1.820	1.691	1
7		C ₈ H ₁₂ ClN ₅ O	CDIT	Atrazine amide	230.0804	2.091	1.875	1
8		C ₅ H ₆ ClN ₅ O	CDAT	Deisopropylatrazine amide	188.0334	1.264	1.257	2
9		C ₇ H ₈ ClN ₅ O ₂	CDDT	N,N'-(6-Chloro-1,3,5-triazine-2,4-diyl)diacetamide	230.0440	1.451	1.407	3
10		C ₈ H ₁₅ N ₅ O	HA	Hydroxyatrazine	198.1350	1.233		1
11		C ₆ H ₁₁ N ₅ O	DEHA	Deethylhydroxyatrazine	170.1037	0.810		2
12		C ₃ H ₅ N ₅ O	AM	Ammeline	128.0567	0.490	0.475	3
13		C ₇ H ₁₁ N ₅ O ₂	ODET	N-[6-(ethylamino)-4-oxo-1,4-dihydro-1,3,5-triazin-2-yl]acetamide	198.0986	1.082	1.048	2
14		C ₈ H ₁₃ N ₅ O ₂	ODIT	Hydroxyatrazine amide	212.1142	1.213	1.067	2
15		C ₇ H ₉ N ₅ O ₃	ODDT	N,N'-(6-hydroxy-1,3,5-triazine-2,4-diyl)diacetamide	212.0778	1.141	1.013	3
16		C ₈ H ₁₄ ClN ₅ O	CNIT	N,N'-(6-((4-chloro-6-[(propan-2-yl)amino]-1,3,5-triazin-2-yl)amino)ethan-1-ol	232.0960	1.868	1.732	1

17		$C_8H_{14}ClN_5O_2$	HAHT	2-((4-chloro-6-((1-hydroxyethyl)amino)-1,3,5-triazin-2-yl)amino)propan-2-ol	248.0909	2.212	1.933	2
18		$C_8H_{12}ClN_5$	CVIT	6-chloro-N2-ethenyl-N4-(propan-2-yl)-1,3,5-triazine-2,4-diamine	214.0854	2.070		2
19		$C_3H_5N_3O_4$	CBOI	1-carboxybiuret	148.0353	0.416		4

3.4. Degradation Rate of Atrazine

3.4.1. Effect of Fenton Reagents Equivalents

Since the Fenton reagents play an important role in Fenton oxidation, experiments in different Fenton reagent equivalents were conducted. Here, the equivalent of Fenton reagents is the ratio of $[H_2O_2]$ or $[Fe^{2+}]$ to ATZ, where the molar concentrations of H_2O_2 or Fe^{2+} are kept the same.

As shown in [Figure 3](#), under low equivalents of Fenton reagents at 1 eq. and 2 eq. (The abbreviation “eq.” means equivalent.), the degradation rates were very slow. Only 25.7% and 37.2% of ATZ were degraded after two hours. However, increasing the equivalent of Fenton reagents effectively promoted the degradation of ATZ. It was found that ATZ was rapidly degraded within 20 min under high equivalents of Fenton reagents at 5 eq. and 10 eq. Then, the degradation rates slowed down to 89.8% and 92.7%, respectively, in 2 h.

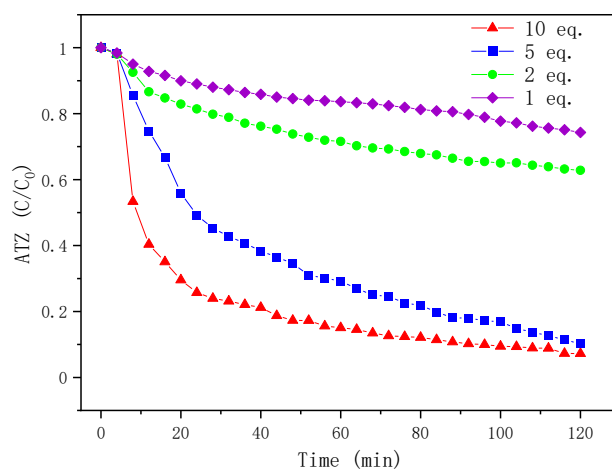
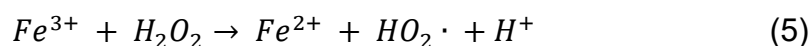
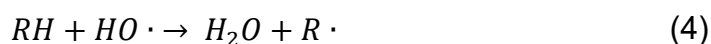
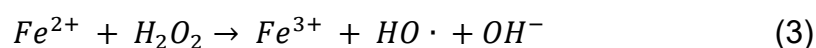


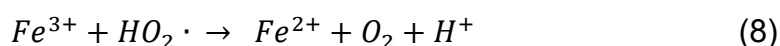
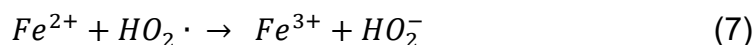
Figure 3. Time profiles of ATZ degradation for different Fenton reagent equivalents. Conditions: $[ATZ]_0 = 0.093$ mmol/L; $[FeSO_4 \cdot 7H_2O]_0 = [H_2O_2]_0 = 0.93$ mmol/L, 0.465 mmol/L, 0.186 mmol/L and 0.093 mmol/L for 10 eq., 5 eq., 2 eq. and 1 eq. Fenton reagents; volume = 15 mL; reaction time = 2 h (see Section 2.5.2).

The promotion effect of Fenton reagents could result from the production of hydroxyl radicals ($HO\cdot$). Hydrogen peroxide (H_2O_2) was activated by ferrous ion (Fe^{2+}) to generate hydroxyl radicals ($HO\cdot$). Radicals $HO\cdot$ were strong oxidants to degrade organic compounds RH (Equations (3) and (4)). In addition, Fe^{2+} can be regenerated by the reduction of Fe^{3+} with H_2O_2 according to Equation (5). The need to use a large amount of hydrogen peroxide argues for the exclusion of a radical chain mechanism. High equivalents of Fenton reagents were more favorable.



3.4.2. Effect of LFUS Treatment with/without Fe^{2+}

For online low-frequency ultrasound (LFUS) treatment at 50 kHz (70 W), adding or not adding Fe^{2+} showed an obvious difference in ATZ degradation. As shown in [Figure 4](#), at the first 20 min, the presence or absence of Fe^{2+} had little effect on ATZ degradation, but after 30 min, the degradation rate of ATZ was significantly increased by the activation of Fe^{2+} . A large number of transformations are in competition [47], according to the following admitted Equations (1)-(9). However, experimentally we can observe a beneficial effect on the generation of radicals both by ultrasound and the presence of ferrous ions.



Indeed, the mechanism of ultrasound is the implosion of the bubble with

high energy, followed by the generation of hydroxyl radicals ($HO\cdot$) and hydrogen radicals ($H\cdot$) from water and hydrogen peroxide dissociation (Equations (1) and (9)). At the same time, $HO\cdot$ could be consumed by the in-situ H_2O_2 formation occurring in the bulk solution due to the radicals' recombination (Equation (2)), which is not conducive to ATZ degradation. Fe^{2+} promotes ATZ degradation, possibly because it reacts with H_2O_2 and re-releases $HO\cdot$ (Equation (3)). Other transformations and recombination involving the radicals are possible and are not exhaustively reported.

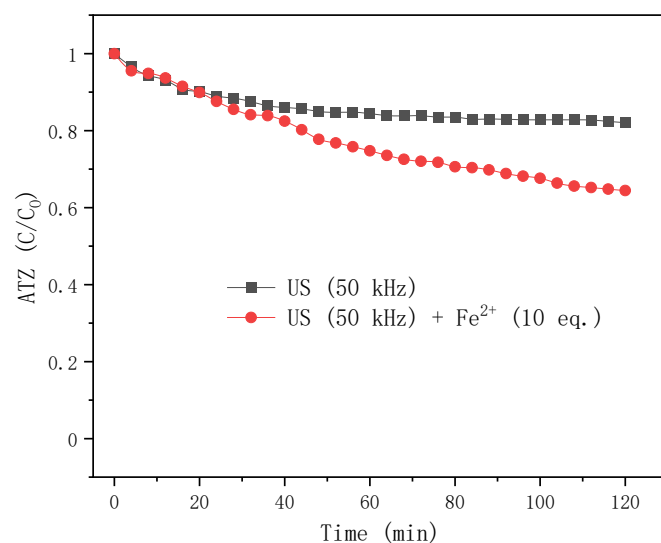


Figure 4. Time profiles of ATZ degradation during LFUS treatment with or without Fe^{2+} (US or US+ Fe^{2+}). Conditions: $[ATZ]_0 = 0.093$ mmol/L; $[FeSO_4 \cdot 7H_2O]_0 = 0.93$ mmol/L for treatment US+ Fe^{2+} ; volume = 15 mL; ultrasound frequency = 50 kHz; reaction time = 2 h (see Section 2.5.3).

3.4.3. Atrazine Degradation of Offline Fenton Experiments

In order to study the effect of the Fenton oxidation reaction time on ATZ degradation, offline Fenton experiments were conducted. As shown in [Figure 5](#), the reaction time had a great influence on the ATZ degradation. Regardless of the equivalents of Fenton reagents, the degradation rate of ATZ increased with time, and it was almost completely degraded after 8 h. In addition, comparing with [Figure 3](#), at 2 h, for the same equivalent of Fenton reagents, the ATZ degradation rates of offline Fenton seem to be greater than that of online Fenton. For example, after 2 h, the ATZ degradation rates of online Fenton at 2 eq., 5 eq. and 10 eq. are 37%,

90% and 93%, respectively (Figure 3), while that of offline Fenton at 2 eq., 5 eq. and 10 eq. are 47%, 90% and 94% (Figure 5). This is probably because the solution in the vial was still reacting after sampling, as we were able to observe during the stability tests (Figure 2). So, in order to improve accuracy, online HPLC-HRMS analysis is necessary, which can monitor the reaction process in real time.

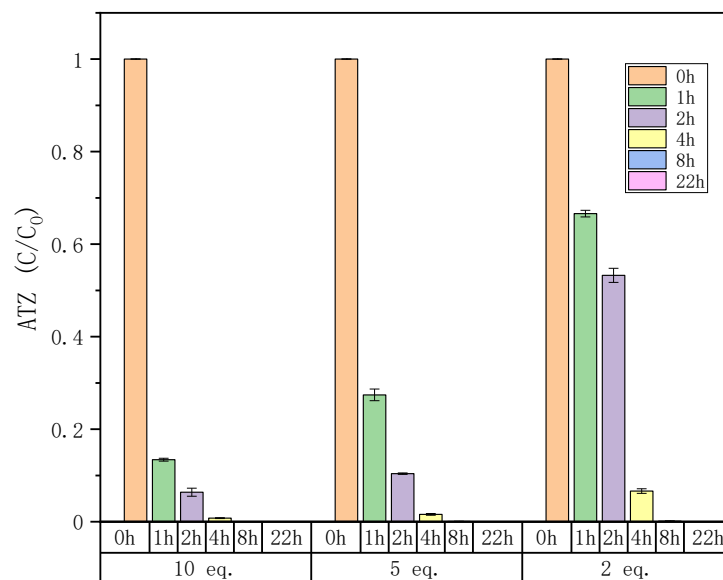


Figure 5. Time profiles of ATZ degradation during offline Fenton treatment for different equivalents of Fenton reagents. Conditions: $[ATZ]_0 = 0.093$ mmol/L; $[FeSO_4 \cdot 7H_2O]_0 = [H_2O_2]_0 = 0.93$ mmol/L, 0.465 mmol/L and 0.186 mmol/L for 10 eq., 5 eq. and 2 eq.; volume = 15 mL (see Section 2.5.4).

3.5. Kinetics of Metabolites

The equivalents of Fenton reagents affect the production of metabolites during the reaction. As shown in Figure 6, the kinetics of metabolites varies from the different equivalents of Fenton reagents. Generally, the kinetics of metabolites in high equivalents of the Fenton reagents system are more complicated, with more products, especially late degradation products such as AM [12]. With 1 and 2 eq. of oxidants, corresponding to the Fenton process (Figure 6a,b), 8 metabolites (DEA, DIA, CDET, CDIT, ODIT, CNIT, HAHT, and CVIT) were detected, but their changing trends were different. With 1 eq. Fenton reagents (Figure 6a), CDIT increased rapidly in the first 30 min until it reached about 4% and tended to balance; HAHT was more than CDIT in the first 20 min, but then its growth rate slowed down until the final 3.4%; other main products were DIA, CVIT and ODIT. With 2 eq. Fenton

reagents (Figure 6b), CDIT reached balance earlier and was greater than 4%; HAHT increased faster and eventually surpassed CDIT; other main products were DIA, CVIT and CNIT.

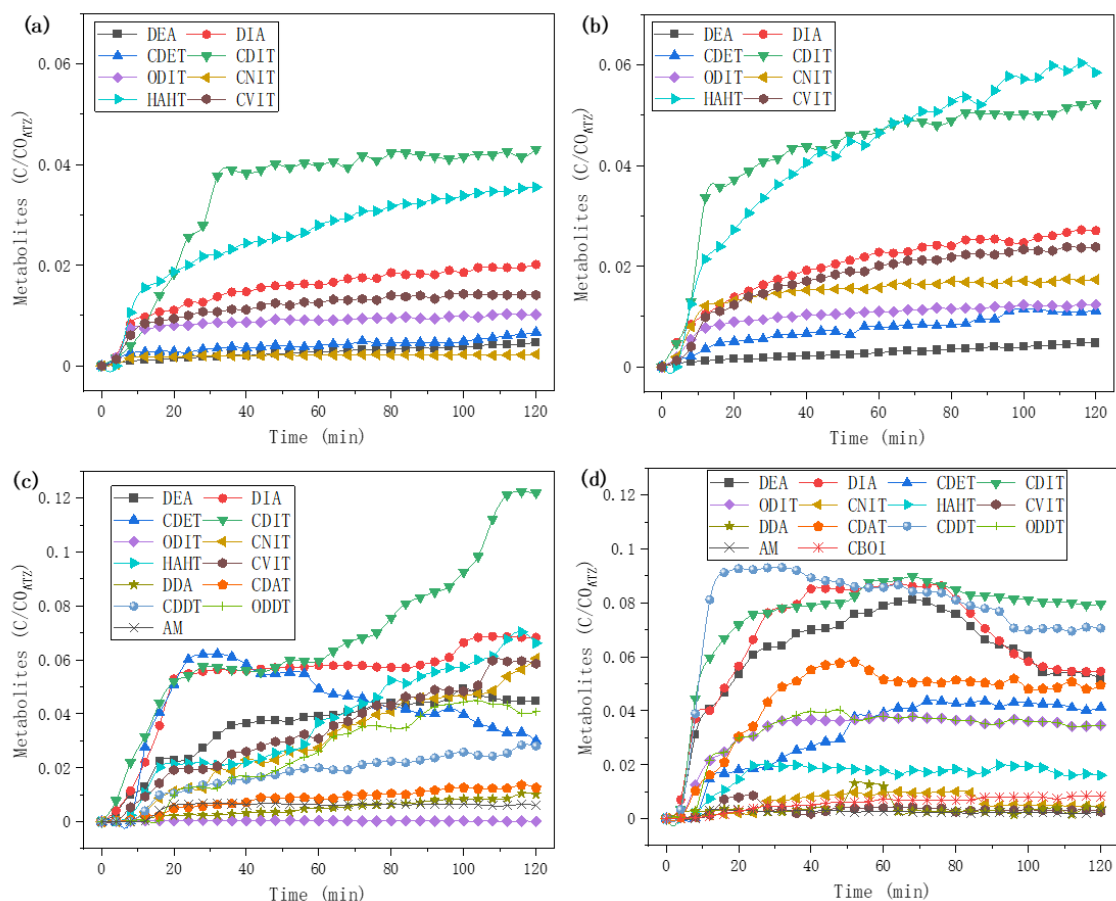


Figure 6. Kinetics of metabolites in online Fenton process. (a) Fenton reagents 1 eq.; (b) Fenton reagents 2 eq.; (c) Fenton reagents 5 eq.; (d) Fenton reagents 10 eq. (see Section 2.5.2).

With 5 eq. and 10 eq. Fenton reagents (Figure 6c,d), except the above 8 metabolites (DEA, DIA, CDET, CDIT, ODIT, CNIT, HAHT, and CVIT), another 5 metabolites (DDA, CDAT, CDDT, ODDT, and AM) were detected. In addition, a ring-broken compound CBOI was found in the 10 eq. Fenton process. In general, for a high equivalents Fenton process, the metabolites increased rapidly in the first 20 min due to the quick activation of H_2O_2 by Fe^{2+} , and also more late degradation products were generated due to a higher concentration of hydroxyl radicals ($HO\cdot$). With 5 eq. Fenton reagents (Figure 6c), CDIT, HAHT, DIA, CVIT, and CNIT were still the main products; CDET increased in the first 30 min and then decreased;

other main products were DEA, ODDT, and CDDT, which increased slowly; smaller molecules DDA and AM appeared. In the 10 eq. Fenton process (Figure 6d), the main products CDDT, CDIT, DIA, and DEA were all firstly increased and then decreased; other main products CDAT, CDET, ODIT, ODDT, and HAHT were all increased until they reached balance; DDA had a small peak around 55 min, while AM was still a small amount as well as the ring-broken compound CBOI.

As shown in Figure 7, ferrous ion Fe^{2+} has an effect on the kinetics of metabolites during the US process. Six metabolites (DEA, DIA, CDIT, ODIT, and HA) were detected in US treatment without Fe^{2+} (Figure 7a), while 3 more metabolites (DEHA, CDET, and ODET) were detected in US treatment with Fe^{2+} (Figure 7b). When using ultrasound without Fe^{2+} , the metabolites increased very slowly in the first 20 min. This is probably because the initial US cavitation had not produced enough hydroxyl radicals ($HO\cdot$). The main product DIA increased to the maximum at 40 min and then decreased, while the second main product CDIT increased in the first 60 min and then reached balance. DEA increased slowly all the time; ODIT increased suddenly at 40 min and then approached DEA. When using ultrasound with Fe^{2+} , DIA and DEA increased to the maximum at 30 min and 76 min, respectively, and then decreased. ODIT linearly increased. In comparison, adding Fe^{2+} promoted the generation of dealkylation products (DIA and DEA), and the dichlorination products (ODIT, ODET, HA and DEHA), but inhibited the generation of acylation products CDIT.

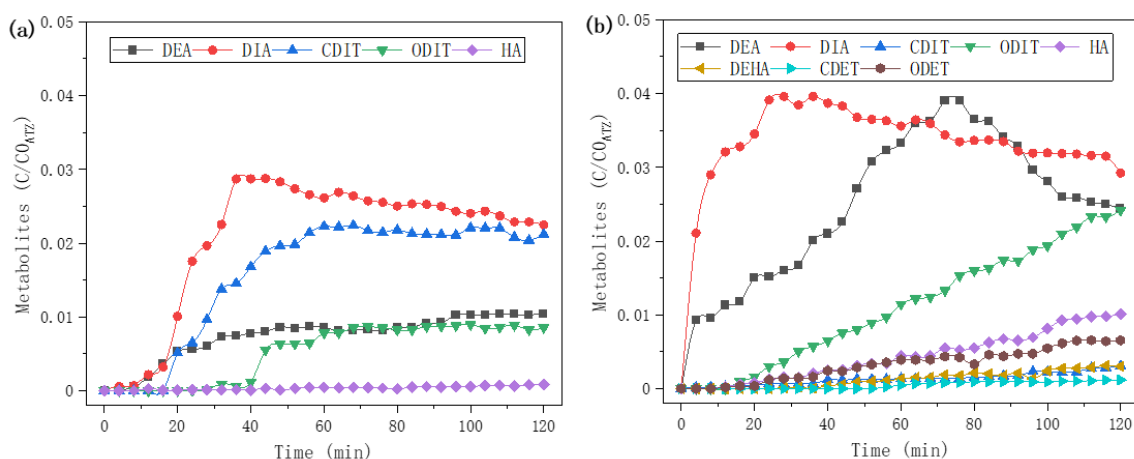


Figure 7. Kinetics of metabolites in online LFUS 50 kHz process. (a) Without 10 eq. Fe^{2+} ; (b) With 10 eq. Fe^{2+} (see Section 2.5.3).

In Fenton oxidation, the substitution of chlorine by hydroxyl is favored by the increase of Fenton reagents' amount (Table 2). However, the ratio of metabolites without chlorine to metabolites with chlorine is relatively stable over time in the case of the Fenton reaction, regardless of the amount of Fenton reagents once the threshold of 50 min has been reached. This result is consistent with the previous work [48] which proposed a practical model for predicting ATZ decay performance based on the Fenton reagents. In this model, Fenton's process can be characterized as a process with two stages (i.e., a rapid stage I followed by a retarded stage II). In rapid stage I, the rapidly generated $HO\cdot$ radicals prioritized the allylic-oxidation and the dealkylation of ATZ, competing with the dechlorination of ATZ. In retarded stage II, $HO\cdot$ radicals were deficient, but some less reactive radicals ($HOO\cdot$ and $O_2\cdot$) presented. These less reactive radicals were not active enough to oxidize ATZ, but were still useful in oxidizing selective intermediates. Therefore, although dechlorinated products were slowly increasing, chlorinated products remained at a high level throughout the Fenton process due to the rapid initial production and consumption of $HO\cdot$ radicals.

As proposed in previous works [12,49], in the US system, ATZ molecules mainly congregate and decay at the gas bubble interfaces, and only a small proportion decayed in the bulk solution because $HO\cdot$ radicals concentrate and react at the surface of bubbles. Radicals $HO\cdot$ tend to degrade ATZ through allylic oxidation and dealkylation. So, at the bubble interfaces, ATZ is rapidly converted to chlorinated products. These chlorinated products and ATZ re-diffused to the bubble interface will be continuously degraded by newly generated $HO\cdot$ radicals, followed by the gradual increase of dechlorinated products. Furthermore, Fe^{2+} can release C radicals through the Fenton reaction with H_2O_2 generated from the self-combination of $HO\cdot$ radicals. Therefore, in the US+ Fe^{2+} system, there are more $HO\cdot$ radicals than in the US-only system, which contributes to the increased ratio of dechlorinated products to chlorinated products (Table 2). This ratio increases obviously over time, in contrast to Fenton's, because $HO\cdot$ radicals are continuously generated in the US system but rapidly generated and depleted in the Fenton system.

Table 2. Distribution of metabolites by ring substituent during treatments after 50 and 100 min, respectively. *

Treatment	50 min				100 min			
	Cl	OH	Ring Opening	C/C ₀ (ATZ)	Cl	OH	Ring Opening	C/C ₀ (ATZ)
^a Fenton_1 eq.	92.56%	7.44%		84.08%	93.32%	6.68%		77.75%
^a Fenton_2 eq.	94.20%	5.80%		72.84%	94.45%	5.55%		65.00%
^a Fenton_5 eq.	91.23%	8.77%		31.02%	89.30%	10.70%		16.90%
^a Fenton_10 eq.	85.70%	13.19%	1.10%	17.27%	83.37%	14.92%	1.71%	9.46%
US_50 kHz	89.86%	10.14%		84.73%	86.44%	13.56%		82.81%
^b US_50 kHz + Fe ²⁺	81.01%	18.99%		76.80%	64.54%	35.46%		67.62%

* The sum of the percentages containing chlorine, hydroxyl groups, and ring-opening products was 100%. ^a Keeping the same molar concentrations of FeSO₄·7H₂O and H₂O₂, different equivalents of Fenton reagents were used on the degradation of atrazine by Fenton oxidation. ^b 10 eq. FeSO₄·7H₂O was added to the degradation of atrazine by ultrasound at 50 kHz.

For Fenton oxidation, whatever the amount of iron, amidation is the most observed process followed by dealkylation after 50 min (Table 3), which is in agreement with the most recent work [46]. In the context of the use of ultrasound, a simple transformation of ATZ to HA is observed, as also observed by Shi when using a catalyst [50]. Fenton reactions mainly produce metabolites by amidation. Petrier [30] proposed a mechanism suited to the operating conditions. Ultrasonic reactions produce more abundant dealkylated compounds, to the detriment of amides, hydroxy and dehydrogenated.

Preferential oxidation paths are observed depending on the quantity of hydroxyl radicals produced and available. The greater this quantity of radicals, the deeper the oxidation, up to an opening of the aromatic ring. In the light of these first results, it would be interesting to follow some degradation products such as CNIT to identify their evolution either towards CDIT or towards imines that can serve as intermediaries for the creation of dealkylated metabolites.

Table 3. Distributions of metabolites by type of transformation during treatments after 50 and 100 min, respectively. *

Treatment	Amidation	Dealkylation	Dehydrogenation	Hydroxylation	Substitution (Conversion of ATZ to HA)
50 min					
Fenton_1 eq.	47.65%	16.58%	10.81%	24.96%	
Fenton_2 eq.	38.33%	14.15%	11.37%	36.15%	
Fenton_5 eq.	47.46%	29.32%	8.45%	14.77%	
Fenton_10 eq.	61.77%	32.39%	0.70%	5.14%	
US_50 kHz	41.94%	57.51%			0.55%
US_50 kHz + Fe^{2+}	15.82%	80.14%			4.04%
100 min					
Fenton_1 eq.	43.96%	17.23%	11.01%	27.80%	
Fenton_2 eq.	37.40%	14.21%	11.56%	36.83%	
Fenton_5 eq.	43.58%	26.04%	9.64%	20.75%	
Fenton_10 eq.	67.20%	26.82%	0.71%	5.27%	
US_50 kHz	47.09%	52.04%			0.88%
US_50 kHz + Fe^{2+}	28.44%	63.32%			8.25%

* The sum of the percentages of each transformation was 100%.

4. Conclusion

In this work, the atrazine degradation process of Fenton/US treatment was monitored in real-time by an online HPLC-HRMS analysis system. Compared with offline analysis, online analysis can avoid additional reactions after sampling, which greatly improved measurement accuracy. In addition, this online method is effective because of automatic sampling and it only takes 4 min analysis time. During analysis, ATZ, ATZ-D5, and seventeen metabolites were identified by accurate mass measurement, which provided abundant information on the atrazine degradation process. The results showed that high equivalents of Fenton reagents promoted the degradation rate of ATZ and the generation of late degradation products such as AM. In addition, adding Fe^{2+} accelerated ATZ degradation in US treatment. The kinetics of metabolites in different conditions was useful for mechanisms research. However, because of the complexity of the reaction process,

there are still compounds that are difficult to detect, especially the small and trace molecules. Therefore, for follow-up work, set-up improvement and conditions optimization will be conducted, so as to expand the upper and lower detection limits and improve detection accuracy.

Supplementary Materials: Table S1: Metabolite identification of Fenton oxidation (2 eq. Fenton reagents) and ultrasound treatment (US 50 kHz + Fe^{2+}) after 50 min; Figure S1: Extracted ion chromatogram (LC-ESI+) during the degradation of atrazine in automatic sampling during the experiment of 2 eq. Fenton reagents ($m/z \pm 20$ ppm); Figure S2: Proposed atrazine degradation pathways scheme. The red and blue boxes, respectively, indicate the main products of Fenton oxidation (2 eq. Fenton reagents) and ultrasound treatment (US 50 kHz + Fe^{2+}) after 50 min.

Table S1. Metabolite identification of Fenton oxidation (2 eq. Fenton reagents) and ultrasound treatment (US 50 kHz + Fe^{2+}) after 50 min.

Molecular formula	Abbreviation	Name	m/z	rt (min)	C/C0(ATZ)_ Color marking: greater than 0.5 %	
					2 eq. Fenton reagents	US 50 kHz + Fe^{2+}
$C_8H_9D_5ClN_5$	ATZ-D5	Atrazine-D5	221.1324	2.58	IS	
$C_8H_{14}ClN_5$	ATZ	Atrazine	216.1010	2.56	72.842 %	76.801 %
$C_8H_{12}ClN_5O$	CDIT	Atrazine amide	230.0804	2.09	4.608 %	0.127 %
$C_8H_{14}ClN_5O_2$	HAHT	2-((4-chloro-6-[(1-hydroxyethyl)amino]-1,3,5-triazin-2-yl)amino)propan-2-ol	248.0909	2.21	4.479 %	
$C_5H_8ClN_5$	DIA	Deisopropylatrazine	174.0541	1.62	2.117 %	3.649 %
$C_8H_{12}ClN_5$	CVIT	6-chloro-N2-ethenyl-N4-(propan-2-yl)-1,3,5-triazine-2,4-diamine	214.0854	2.07	1.899 %	
$C_8H_{14}ClN_5O$	CNIT	1-((4-chloro-6-[(propan-2-yl)amino]-1,3,5-triazin-2-yl)amino)ethan-1-ol	232.0960	1.87	1.562 %	
$C_8H_{13}N_5O_2$	ODIT	Hydroxyatrazine amide	212.1142	1.21	1.072 %	0.892 %
$C_7H_{10}ClN_5O$	CDET	Simazine amide	216.0647	1.82	0.641 %	
$C_6H_{10}ClN_5$	DEA	Deethylatrazine	188.0698	1.91	0.247 %	3.073 %
$C_5H_6ClN_5O$	CDAT	Deisopropylatrazine amide	188.0334	1.26	0.047 %	
$C_7H_{11}N_5O_2$	ODET	N-[6-(Ethylamino)-4-oxo-1,4-dihydro-1,3,5-triazin-2-yl]acetamide	198.0986	1.08	0.037 %	0.327 %
$C_3H_5N_5O$	AM	Ammeline	128.0567	0.49		
$C_3H_4ClN_5$	DDA	Didealkylatrazine	146.0228	1.02		
$C_3H_5N_3O_4$	CBOI	1-carboxybiuret	148.0353	0.42		
$C_6H_{11}N_5O$	DEHA	Deethylhydroxyatrazine	170.1037	0.81		0.097 %
$C_8H_{15}N_5O$	HA	Hydroxyatrazine	198.1350	1.23		0.343 %
$C_7H_9N_5O_3$	ODDT	N,N'-(6-hydroxy-1,3,5-triazine-2,4-diyl)diacetamide	212.0778	1.14		
$C_7H_8ClN_5O_2$	CDDT	N,N'-(6-Chloro-1,3,5-triazine-2,4-diyl)diacetamide	230.0440	1.45		

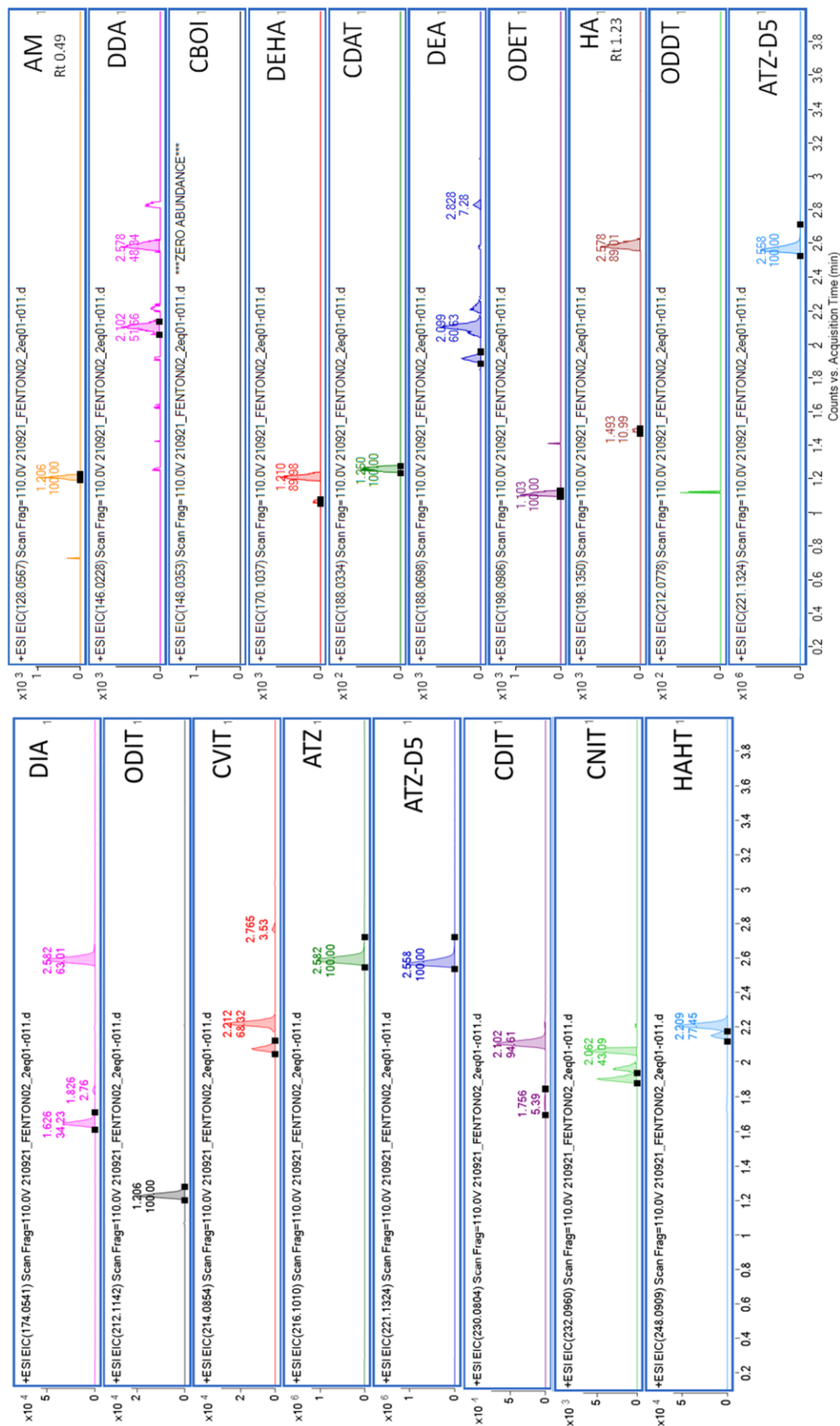


Figure S1. Extracted ion chromatogram LC-ESI+ - HRMS during the degradation of atrazine in automatic sampling during the experiment of 2 eq. Fenton reagents ($m/z \pm 20$ ppm).

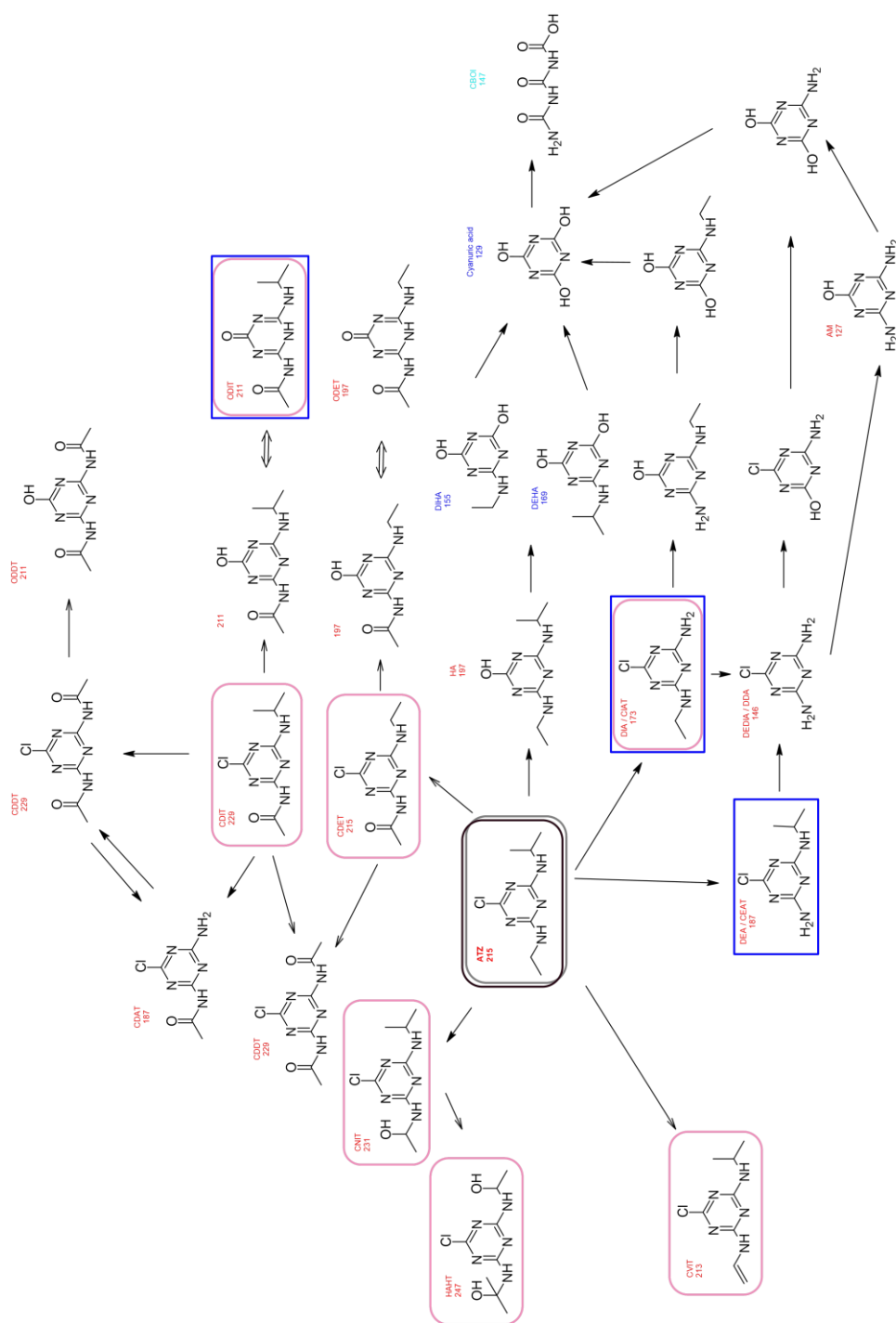


Figure S2. Proposed atrazine degradation pathways scheme. The red and blue boxes respectively indicate the main products of Fenton oxidation (2 eq. Fenton reagents) and ultrasound treatment (US 50 kHz + Fe^{2+}) after 50 min, according to the data from table SI.1.

III.3. Chapter conclusion

The main point of Chapter III is to establish an online analytical method for monitoring the degradation process of atrazine in real time. That is, sample was automatically abstracted from the reaction device through a peristaltic pump, and injected into the high-performance liquid chromatography coupled with high resolution mass spectrometry (HPLC-HRMS) analysis system, with a cycle of every four minutes. Considering the portability of the reaction device, Fenton oxidation and ultrasound were chosen to explore the feasibility of monitoring the degradation process. The results showed that offline monitoring suffered from large data deviations due to sample storage and transfer, while real-time monitoring avoided this problem, captured potentially unstable compounds and accurately obtained the metabolic kinetics. In addition to atrazine and atrazine-D5, 17 degradation metabolites were detected and identified. The distribution of these metabolites during different degradation processes indicated that US treatment was more prone to hydroxyl substitution of chlorine than Fenton oxidation, and the less toxic product hydroxyatrazine (HA) was only detected in US treatment.

Fenton oxidation and US treatment showed different degradation behaviours in atrazine degradation. In Fenton oxidation, atrazine was rapidly degraded within the first few minutes, and higher equivalent amounts of Fenton's reagent are more effective. This is related to the rapid consumption of hydroxyl radicals $\bullet OH$ activated through the Fenton reaction at the beginning. Conversely, atrazine degradation remained slow in US treatment and was improved by the addition of ferrous ions Fe^{2+} . This is because the cavitation effect of low-frequency ultrasound is not strong enough, resulting in limited hydroxyl radicals $\bullet OH$ obtained from water splitting, and the hydroxyl radicals $\bullet OH$ will be consumed by self-combination into hydrogen peroxide H_2O_2 . The additive ferrous ions Fe^{2+} may react with H_2O_2 via Fenton oxidation and release $\bullet OH$, which contributes to degrade more atrazine.

It is very useful to study the degradation kinetics of atrazine and the formation kinetics of metabolites by this online analytical method. This lays the foundation for studying the degradation kinetics of more treatment processes, such as HVED, and further exploring the reaction mechanism of atrazine degradation.

III.4. References

- [1] R.A. Bachetti, N. Urseler, V. Morgante, G. Damilano, C. Porporatto, E. Agostini, C. Morgante, Monitoring of Atrazine Pollution and its Spatial-Seasonal Variation on Surface Water Sources of an Agricultural River Basin, *Bull Environ Contam Toxicol* 106 (2021) 929–935. <https://doi.org/10.1007/s00128-021-03264-x>.
- [2] Y. Tian, W. Shen, F. Jia, Z. Ai, L. Zhang, Sulfite promoted photochemical cleavage of s-triazine ring: The case study of atrazine, *Chemical Engineering Journal* 330 (2017) 1075–1081. <https://doi.org/https://doi.org/10.1016/j.cej.2017.08.048>.
- [3] Y. Mu, G. Zhan, C. Huang, X. Wang, Z. Ai, J. Zou, S. Luo, L. Zhang, Dechlorination-Hydroxylation of Atrazine to Hydroxyatrazine with Thiosulfate: A Detoxification Strategy in Seconds, *Environ Sci Technol* 53 (2019) 3208–3216. <https://doi.org/10.1021/acs.est.8b06351>.
- [4] J.Y. Shin, M.A. Cheney, Abiotic dealkylation and hydrolysis of atrazine by birnessite, *Environ Toxicol Chem* 24 (2005) 1353–1360. <https://doi.org/https://doi.org/10.1897/04-248R.1>.
- [5] Z. Jiang, J. Li, D. Jiang, Y. Gao, Y. Chen, W. Wang, B. Cao, Y. Tao, L. Wang, Y. Zhang, Removal of atrazine by biochar-supported zero-valent iron catalyzed persulfate oxidation: Reactivity, radical production and transformation pathway, *Environ Res* 184 (2020) 109260. <https://doi.org/https://doi.org/10.1016/j.envres.2020.109260>.
- [6] J. Mahía, A. Martín, M. Díaz-Raviña, Extractable atrazine and its metabolites in agricultural soils from the temperate humid zone, *Environ Geochem Health* 30 (2008) 147–152. <https://doi.org/10.1007/s10653-008-9149-x>.
- [7] P. Bhatti, A. Duhan, A. Pal, Monika, R.K. Beniwal, P. Kumawat, D.B. Yadav, Ultimate fate and possible ecological risks associated with atrazine and its principal metabolites (DIA and DEA) in soil and water environment, *Ecotoxicol Environ Saf* 248 (2022) 114299. <https://doi.org/https://doi.org/10.1016/j.ecoenv.2022.114299>.
- [8] World Health Organization., Food and Agriculture Organization of the United Nations., International Program on Chemical Safety., Pesticide residues in food--2007 : toxicological evaluations, World Health Organization, 2009.
- [9] P. Jakinala, N. Lingampally, A. Kyama, B. Hameeda, Enhancement of atrazine biodegradation by marine isolate *Bacillus velezensis* MHNK1 in presence of surfactin lipopeptide, *Ecotoxicol Environ Saf* 182 (2019) 109372. <https://doi.org/https://doi.org/10.1016/j.ecoenv.2019.109372>.
- [10] B.E. Herrera-Gallardo, R. Guzmán-Gil, J.A. Colín-Luna, J.C. García-Martínez, H.H. León-Santiesteban, O.M. González-Brambila, M.M. González-Brambila, Atrazine biodegradation in soil by *Aspergillus niger*, *Can J Chem Eng* 99 (2021) 932–946. <https://doi.org/https://doi.org/10.1002/cjce.23924>.
- [11] X. Xia, F. Zhu, J. Li, H. Yang, L. Wei, Q. Li, J. Jiang, G. Zhang, Q. Zhao, A Review Study on Sulfate-Radical-Based Advanced Oxidation Processes for Domestic/Industrial Wastewater Treatment: Degradation, Efficiency, and Mechanism, *Front Chem* 8 (2020).

<https://doi.org/10.3389/fchem.2020.592056>.

- [12] L.J. Xu, W. Chu, N. Graham, Atrazine degradation using chemical-free process of USUV: Analysis of the micro-heterogeneous environments and the degradation mechanisms, *J Hazard Mater* 275 (2014) 166–174. <https://doi.org/https://doi.org/10.1016/j.jhazmat.2014.05.007>.
- [13] E. Hu, H. Cheng, Y. Hu, Microwave-Induced Degradation of Atrazine Sorbed in Mineral Micropores, *Environ Sci Technol* 46 (2012) 5067–5076. <https://doi.org/10.1021/es204519d>.
- [14] M. Dehvari, A.A. Babaei, S. Esmaeili, Amplification of oxidative elimination of atrazine by Ultrasound/Ultraviolet-assisted Sono/Photocatalyst using a spinel cobalt ferrite-anchored MWCNT as peroxymonosulfate activator, *J Photochem Photobiol A Chem* 437 (2023) 114452. <https://doi.org/https://doi.org/10.1016/j.jphotochem.2022.114452>.
- [15] N. Wardenier, Z. Liu, A. Nikiforov, S.W.H. Van Hulle, C. Leys, Micropollutant elimination by O₃, UV and plasma-based AOPs: An evaluation of treatment and energy costs, *Chemosphere* 234 (2019) 715–724. <https://doi.org/https://doi.org/10.1016/j.chemosphere.2019.06.033>.
- [16] J.L. Acero, K. Stemmler, U. von Gunten, Degradation Kinetics of Atrazine and Its Degradation Products with Ozone and OH Radicals: A Predictive Tool for Drinking Water Treatment, *Environ Sci Technol* 34 (2000) 591–597. <https://doi.org/10.1021/es990724e>.
- [17] H. Blanchoud, F. Alliot, N. Chen, D. Valdes, Rapid SPE – LC MS/MS analysis for atrazine, its by-products, simazine and S metolachlor in groundwater samples, *MethodsX* 7 (2020) 100824. <https://doi.org/https://doi.org/10.1016/j.mex.2020.100824>.
- [18] N. Munz, C. Leu, I. Wittmer, Pesticides dans les cours d'eau suisses, *Aqua & Gas* 7–8 (2013) 78–87.
- [19] N. Udiković-Kolić, C. Scott, F. Martin-Laurent, Evolution of atrazine-degrading capabilities in the environment, *Appl Microbiol Biotechnol* 96 (2012) 1175–1189. <https://doi.org/10.1007/s00253-012-4495-0>.
- [20] X. Fan, F. Song, Bioremediation of atrazine: recent advances and promises, *J Soils Sediments* 14 (2014) 1727–1737. <https://doi.org/10.1007/s11368-014-0921-5>.
- [21] H. He, Y. Liu, S. You, J. Liu, H. Xiao, Z. Tu, A review on recent treatment technology for herbicide atrazine in contaminated environment, *Int J Environ Res Public Health* 16 (2019). <https://doi.org/10.3390/ijerph16245129>.
- [22] T. Komang Ralebitso, E. Senior, H.W. Van Verseveld, Microbial aspects of atrazine degradation in natural environments, *Biodegradation* 13 (2002) 11–19. <https://doi.org/10.1023/A:1016329628618>.
- [23] J. Hong, N. Boussetta, G. Enderlin, F. Merlier, N. Grimi, Degradation of Residual Herbicide Atrazine in Agri-Food and Washing Water, *Foods* 11 (2022). <https://doi.org/10.3390/foods11162416>.

- [24] T.B. Hayes, V. Khoury, A. Narayan, M. Nazir, A. Parka, T. Brown, L. Adame, E. Chan, D. Buchholz, T. Stueve, S. Gallipeau, Atrazine induces complete feminization and chemical castration in male African clawed frogs (*Xenopus laevis*), *Proc Natl Acad Sci U S A* 107 (2010) 4612–4617. <https://doi.org/10.1073/pnas.0909519107>.
- [25] S.E. Wirbisky, J.L. Freeman, Atrazine Exposure and Reproductive Dysfunction through the Hypothalamus-Pituitary-Gonadal (HPG) Axis, *Toxics* 3 (2015) 414–450. <https://doi.org/10.3390/toxics3040414>.
- [26] N. Yang, Y. Liu, J. Zhu, Z. Wang, J. Li, Study on the efficacy and mechanism of Fe-TiO₂ visible heterogeneous Fenton catalytic degradation of atrazine, *Chemosphere* 252 (2020) 126333. <https://doi.org/10.1016/j.chemosphere.2020.126333>.
- [27] J. Sass, P.A. MacLennan, E. Delzell, N. Sathiakumar, S.L. Myers, H. Cheng, W. Grizzle, V.W. Chen, X.C. Wu, Cancer incidence among triazine herbicide manufacturing workers [1] (multiple letters), *J Occup Environ Med* 45 (2003) 343–344. <https://doi.org/10.1097/01.jom.0000063624.37065.7a>.
- [28] G. Xiong, J. Liang, S. Zou, Z. Zhang, Microwave-assisted extraction of atrazine from soil followed by rapid detection using commercial ELISA kit, *Anal Chim Acta* 371 (1998) 97–103. [https://doi.org/https://doi.org/10.1016/S0003-2670\(98\)00266-9](https://doi.org/https://doi.org/10.1016/S0003-2670(98)00266-9).
- [29] C.A. Aggelopoulos, D. Tataraki, G. Rassias, Degradation of atrazine in soil by dielectric barrier discharge plasma – Potential singlet oxygen mediation, *Chemical Engineering Journal* 347 (2018) 682–694. <https://doi.org/10.1016/j.cej.2018.04.111>.
- [30] C. Petrier, B. David, S. Laguian, Ultrasonic degradation at 20 kHz and 500 kHz of atrazine and pentachlorophenol in aqueous solution : Preliminary results, *Chemosphere* 32 (1996) 1709–1718. [https://doi.org/10.1016/0045-6535\(96\)00088-4](https://doi.org/10.1016/0045-6535(96)00088-4).
- [31] J.L. Acero, K. Stemmler, U. von Gunten, Degradation Kinetics of Atrazine and Its Degradation Products with Ozone and OH Radicals: A Predictive Tool for Drinking Water Treatment, *Environ Sci Technol* 34 (2000) 591–597. <https://doi.org/10.1021/es990724e>.
- [32] A. Ventura, G. Jacquet, A. Bermond, V. Camel, Electrochemical generation of the Fenton's reagent: application to atrazine degradation, *Water Res* 36 (2002) 3517–3522. [https://doi.org/https://doi.org/10.1016/S0043-1354\(02\)00064-7](https://doi.org/https://doi.org/10.1016/S0043-1354(02)00064-7).
- [33] Y. Zhang, Z. Jiang, B. Cao, M. Hu, Z. Wang, X. Dong, Metabolic ability and gene characteristics of *Arthrobacter* sp. strain DNS10, the sole atrazine-degrading strain in a consortium isolated from black soil, *Int Biodeterior Biodegradation* 65 (2011) 1140–1144. <https://doi.org/https://doi.org/10.1016/j.ibiod.2011.08.010>.
- [34] M. Mortureux, Avis de l' Agence nationale de sécurité sanitaire de l' alimentation, de l' environnement et du travail, 2012.
- [35] H. Chen, E. Bramanti, I. Longo, M. Onor, C. Ferrari, Oxidative decomposition of atrazine in water in the presence of hydrogen peroxide using an innovative microwave photochemical

- reactor, J Hazard Mater 186 (2011) 1808–1815. <https://doi.org/10.1016/j.jhazmat.2010.12.065>.
- [36] Z. Kuklenyik, P. Panuwet, N.K. Jayatilaka, J.L. Pirkle, A.M. Calafat, Two-dimensional high performance liquid chromatography separation and tandem mass spectrometry detection of atrazine and its metabolic and hydrolysis products in urine, J Chromatogr B Analyt Technol Biomed Life Sci 901 (2012) 1–8. <https://doi.org/10.1016/j.jchromb.2012.05.028>.
- [37] R. López-Ruiz, R. Romero-González, S. Martín-Torres, A.M. Jimenez-Carvelo, L. Cuadros-Rodríguez, A.G. Frenich, Applying an instrument-agnostic methodology for the standardization of pesticide quantitation using different liquid chromatography-mass spectrometry platforms: a case study, Elsevier B.V., 2021. <https://doi.org/10.1016/j.chroma.2021.462791>.
- [38] B. Liu, W. Guo, H. Wang, Q. Si, Q. Zhao, H. Luo, N. Ren, Activation of peroxymonosulfate by cobalt-impregnated biochar for atrazine degradation: The pivotal roles of persistent free radicals and ecotoxicity assessment, J Hazard Mater 398 (2020) 122768. <https://doi.org/10.1016/j.jhazmat.2020.122768>.
- [39] F. Merlier, R. Jellali, E. Leclerc, Online monitoring of hepatic rat metabolism by coupling a liver biochip and a mass spectrometer, Analyst 142 (2017) 3747–3757. <https://doi.org/10.1039/c7an00973a>.
- [40] N. Merayo, D. Hermosilla, C. Negro, Á. Blanco, On-line FTIR as a novel tool to monitor Fenton process behavior, Chemical Engineering Journal 232 (2013) 519–526. <https://doi.org/10.1016/j.cej.2013.07.119>.
- [41] J. Jiang, D. Zhang, H. Zhang, K. Yu, N. Li, G. Zheng, Degradation mechanism study of fluoroquinolones in UV/Fe²⁺/peroxydisulfate by on-line mass spectrometry, Chemosphere 239 (2020). <https://doi.org/10.1016/j.chemosphere.2019.124737>.
- [42] Y. Fu, W. Li, H. Li, M. Huang, High-precision and on-line measurement of dissolved organic matter in Electro-Fenton process based on dual wavelength analysis with combination of fluorescence emission and ultraviolet absorption spectroscopy, Anal Chim Acta 1181 (2021) 338904. <https://doi.org/10.1016/j.aca.2021.338904>.
- [43] A.C. Schrimpe-Rutledge, S.G. Codreanu, S.D. Sherrod, J.A. McLean, Untargeted Metabolomics Strategies—Challenges and Emerging Directions, J Am Soc Mass Spectrom 27 (2016) 1897–1905. <https://doi.org/10.1007/s13361-016-1469-y>.
- [44] J. Wang, Z. Wang, C.L.Z. Vieira, J.M. Wolfson, G. Pingtian, S. Huang, Review on the treatment of organic pollutants in water by ultrasonic technology, Ultrason Sonochem 55 (2019) 273–278. <https://doi.org/https://doi.org/10.1016/j.ultsonch.2019.01.017>.
- [45] E. Neyens, J. Baeyens, A review of classic Fenton's peroxidation as an advanced oxidation technique, J Hazard Mater 98 (2003) 33–50. [https://doi.org/https://doi.org/10.1016/S0304-3894\(02\)00282-0](https://doi.org/https://doi.org/10.1016/S0304-3894(02)00282-0).

- [46] Q. Guo, C. Guan, L. Luo, Z. Wang, H. Pan, J. Jiang, New insights into atrazine degradation by the novel manganese dioxide/bisulfite system: Product formation and Mn reuse, *J Clean Prod* 368 (2022) 133106. <https://doi.org/10.1016/j.jclepro.2022.133106>.
- [47] A.D. Bokare, W. Choi, Review of iron-free Fenton-like systems for activating H₂O₂ in advanced oxidation processes, *J Hazard Mater* 275 (2014) 121–135. <https://doi.org/https://doi.org/10.1016/j.jhazmat.2014.04.054>.
- [48] K.H. Chan, W. Chu, Model applications and mechanism study on the degradation of atrazine by Fenton's system, *J Hazard Mater* 118 (2005) 227–237. <https://doi.org/https://doi.org/10.1016/j.jhazmat.2004.11.008>.
- [49] Y.L. Pang, A.Z. Abdullah, S. Bhatia, Review on sonochemical methods in the presence of catalysts and chemical additives for treatment of organic pollutants in wastewater, *Desalination* 277 (2011) 1–14. <https://doi.org/https://doi.org/10.1016/j.desal.2011.04.049>.
- [50] H. Shi, Y. Wang, C. Tang, W. Wang, M. Liu, G. Zhao, Mechanism investigation on the enhanced and selective photoelectrochemical oxidation of atrazine on molecular imprinted mesoporous TiO₂, *Appl Catal B* 246 (2019) 50–60. <https://doi.org/10.1016/j.apcatb.2019.01.018>.

Chapter IV. Effects of different technologies (HVED, US and Fenton oxidation) on atrazine degradation

IV.1. Chapter introduction

The above Chapter III demonstrated the feasibility of using Fenton oxidation and 50 kHz ultrasound for the degradation of atrazine, but neither method was good enough. Although atrazine was degraded by Fenton oxidation with high efficiency (>90%, after 2 h), it was not environmentally friendly and produced more toxic degradation metabolites such as deethylatrazine (DEA), deisopropylatrazine (DIA) and ammeline (AM). In addition, the degradation efficiency of atrazine by low-frequency ultrasound at 50 kHz was very low (<50%, after 2 h). The chemical structure of atrazine is stable and its degradation metabolites are diverse and toxic, so it is necessary to find a new efficient and low-toxic degradation method for atrazine degradation. In recent years, high-voltage electrical discharges (HVED) have received more and more attention in wastewater treatment [1]. It is considered as a promising wastewater treatment technology due to its high efficiency and environmental compatibility [2]. Therefore, HVED was used in atrazine degradation in this chapter.

Although HVED technology has been used to degrade atrazine, there is currently no complete analysis of the kinetics and mechanism of metabolite formation [3, 4]. So, in this chapter, HVED technology was applied to the rapid and deep degradation of atrazine, in comparison with chemical method Fenton oxidation and physical method ultrasound at 525 kHz. Besides, a combined approach was attempted, whereby additional Fenton's reagent was added to the HVED treatment and ultrasound treatment to pursue higher atrazine degradation efficiency. Metabolite formation kinetics during atrazine degradation processes monitored by the HPLC-HRMS analysis system (introduced in Chapter III) helped understand the degradation pathways of different treatments and contributed to proposing detailed degradation mechanisms. Moreover, the degradation efficiency and energy consumption of different treatments are discussed at the end.

More details can be found in the next section IV.2 **“Degradation of herbicide atrazine in water by high voltage electrical discharge in**

comparison with Fenton oxidation and ultrasound treatments", which is published in the journal "*RSC Sustainability*". It was conducted under the direction of Prof. Nabil GRIMI, Dr. Franck MERLIER, Dr. Nadia BOUSSETTA and Dr. Gérald ENDERLIN.

IV.2. Degradation of herbicide atrazine in water by high voltage electrical discharge in comparison with Fenton oxidation and ultrasound treatments

Abstract

Atrazine, the most commonly used herbicide, has been reported to pollute the water environment and do harms to humans health. It is thus urgent to find an efficient way to degrade atrazine. Although various advanced oxidation processes including high voltage electrical discharge (HVED) have been applied to degrade atrazine, the formation kinetics of its metabolites are still incomplete, and the detoxification of the degradation process remains to be clarified. Here, the degradation of atrazine by HVED was investigated, in comparison with traditional Fenton oxidation and ultrasound treatment. Nineteen metabolites of atrazine degradation were identified and quantified by high performance liquid chromatography coupled with high resolution mass spectrometry (HPLC-HRMS) techniques. Results show that, HVED is more advantageous because of its high degradation rate of atrazine (89%), short processing time (1000 s, corresponding to 10 ms effective time), and the presence of less toxic main metabolites Hydroxyatrazine. Hydroxyl radicals ($\cdot OH$) play an important role on atrazine degradation. Adding ferrous ions (Fe^{2+}) during HVED and ultrasound processes, benefits to degradation of atrazine, because of $\cdot OH$ radicals released from hydrogen peroxide (H_2O_2). Based on the formation kinetics of atrazine degradation metabolites, detailed mechanisms of atrazine degradation pathways were proposed.

Keywords: atrazine; degradation techniques; electrical discharge; ultrasound; Fenton oxidation; mechanism

Sustainability spotlight

The growing harvests have been increased by using pesticides extensively in response to the global food crisis. The health effects of excessive pesticide residues in drinking water may be severe. The widely used herbicide atrazine and its metabolites can remain in the environment for decades due to their stability and refractory degradation, becoming a major source of pollution. There is thus a strong need to efficiently degrade these persistent organic pollutants. Herein high voltage electrical discharges were applied to achieve rapid and deep degradation of recalcitrant pesticides. At the same time, we supplemented the data of pesticide degradation metabolites. Our work aligns with UN SDG 6 (water and sanitation) and SDG 12 (chemicals and waste management).

1. Introduction

As the production of agriculture has developed, pesticides have become increasingly important for controlling pests and weeds. However, the overuse of pesticides has been a source of concern for environmental pollution issues[5] and inherent impacts on human health[6]. Among these pesticides, atrazine is the most commonly used chlorotriazine herbicide to control weeds.[7] Atrazine's low biodegradability and high soil mobility make it persistent in non-agricultural soils[8], ground - and surface water[9]. Atrazine was reported as endocrine disrupting chemicals (EDCs) causing a threat to the reproductive system of mammals[10], amphibians[11], and fishes[12]. Although European Union announced a ban of atrazine in 2003,[13] it is still extensively used in the United States[14], Brazil[15], and other countries[16]. The degradation of residual atrazine is thus becoming an urgent issue for environmental protection, especially for water security which is listed as a priority by the "European Green Deal" proposed by the European Commission. The degradation of chemically stable atrazine is challenging, and common water treatment technologies are limited by trace organic concentrations[17] and strictive fouling control[18], so there is increasing effort to develop efficient advanced oxidation processes[7], such as Fenton/Fenton like oxidation[19-21], ultrasounds[22-24] and so on. Among them, high voltage electrical discharge (HVED) has attracted more attention because of its advantages, high degradation efficiency and environmental friendliness.

During the HVED process, the electrical discharge plasma (a partially or fully ionized gas consisting of electrons, free radicals, ions and neutrals) is generated in a high voltage reactor[1]. This process is simultaneously affected by physical and chemical effects, generating various oxidizing species. The generated oxidizing species, such as hydroxy radicals ($\cdot OH$), greatly promote the degradation of pollutants. Previous works[25, 26] demonstrated the viability of plasma for waste water treatment. To date, the application of HVED technology for atrazine degradation is still under development. Based on the plasma-phase distribution, the existing examples of atrazine degradation by HVED can be divided into two cases: one is direct discharge in water (electrohydraulic discharge)[27, 28], and the other is discharge in the gas phase[3, 29-34]. However, these reported works are incomplete on the formation kinetics of atrazine degradation metabolites.

Here, the energy was directly injected into the atrazine aqueous solution through a plasma channel formed by HVED between two submerged electrodes. It was aimed at investigating the ability of HVED system to degrade atrazine in aqueous solution; comparing the results with other chemical degradation technique (Fenton oxidation) and physical degradation technique (ultrasound); studying the effect of Fe^{2+} on atrazine degradation; identifying atrazine degradation metabolites by high performance liquid chromatography coupled with high resolution mass spectrometry (HPLC-HRMS) analysis system[35]; proposing detailed mechanisms of atrazine degradation pathways based on the formation kinetics of atrazine degradation metabolites.

2. Materials and Methods

2.1 Materials

LC-MS grade solvents and formic acid were bought from Biosolve Chimie (Dieuze, France). Atrazine and the internal standard Atrazine-D5 were bought from Sigma-Aldrich (St. Quentin Fallavier, France). In the preparation of the buffer solution, Milli-Q water purified with the Milli-Q system of Millipore (Millsheim, France) was used. Iron (II) sulfate heptahydrate ($FeSO_4 \cdot 7H_2O$) was purchased from Acros Organics with a purity of 99.5%. Hydrogen peroxide (H_2O_2) was purchased from Alfa Aesar with a purity of 35%.

2.2 Methods

Figure 1 shows the experimental set up. The initial atrazine aqueous solutions of 20 mg/L were treated by three degradation methods including HVED, ultrasounds and Fenton oxidation. After degradation, the treated fluid containing a mixture of atrazine and its metabolites was analyzed by HPLC-HRMS. The qualitative and quantitative analysis was conducted by Agilent MassHunter Workstation software (Version B.07.00, Agilent Technologies, Santa Clara, CA 95051, United States).

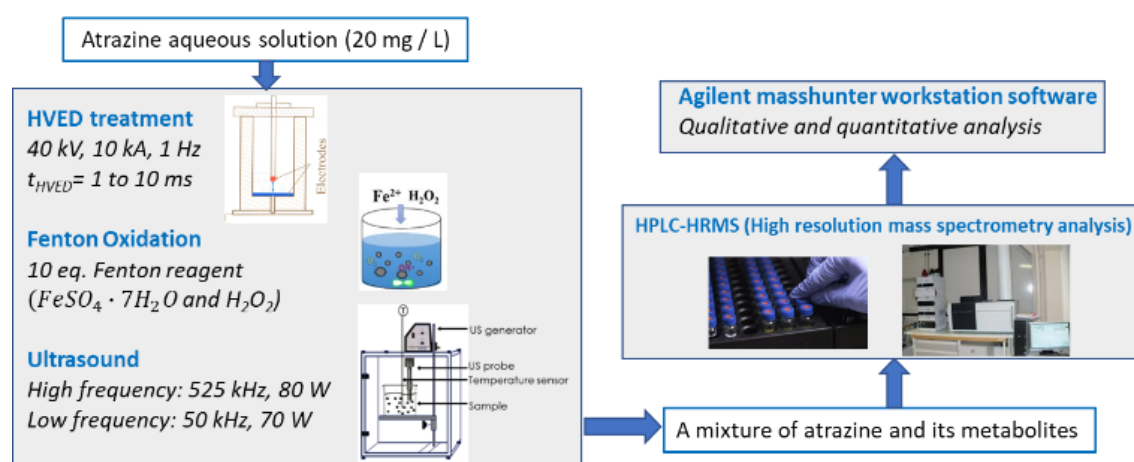


Figure 1. Schema of the experimental procedures.

2.3 HVED treatment

Figure 2 shows the schematic of the treatment chamber and pulse protocols for HVED. The high voltage electrical discharges were applied in a treatment chamber with a capacity of 1 L, using an electrical generator (Basis, Saint-Quentin, France) supplying a voltage of 40 kV, a current of 10 kA, and a frequency of 1 Hz. The generated pulses have a duration of approximately 10 μ s. The average energy of an electric pulse supplied by the generator, is $W_{1 Pulse} = 200$ J/Pulse. The atrazine solution was introduced between two stainless steel electrodes. The first point electrode is connected to the generator; the second, a plane electrode is connected to the ground. The electrical treatment consisted in applying n pulses (or n electrical discharges) in liquid. The total processing time was 1000 s (the total effective time was 10 ms).

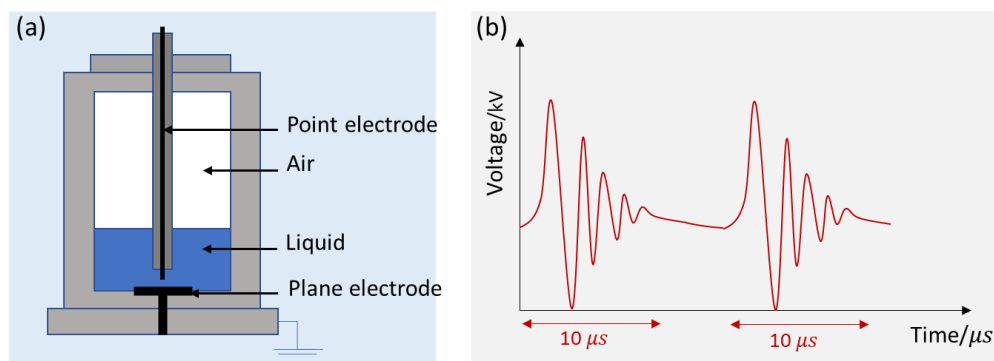


Figure 2. Schematic representation of HVED (a) treatment chamber and (b) pulsed protocols.

A volume (250 or 500 mL) of the initial atrazine aqueous solutions (20 mg/L, 0.093 mmol/L) was added in the treatment chamber, which then treated by HVED. The initial concentration of ferrous sulfate $FeSO_4 \cdot 7H_2O$ was 0.93 mmol/L in HVED experiments adding Fe^{2+} . In addition, to study the effect of dissolved oxygen in discharge system, the degradation of atrazine under argon atmosphere was studied. A volume (500 mL) of the initial atrazine aqueous solutions (20 mg/L, 0.093 mmol/L) was degassed, and poured into the treatment chamber filled with an argon atmosphere, which then treated by HVED. Samples were taken at 0, 100, 200, 400, 700 and 1000 s, and the corresponding effective time was 0, 1, 2, 4, 7, 10 ms. With a frequency of 1 Hz, the corresponding number of pulses was 0, 100, 200, 400, 700 and 1000. The specific energy consumption of HVED, W_{HVED} (J/L) was calculated as follow:

$$W_{HVED} = (W_{1 Pulse} \times n) / V \quad (1)$$

Where $W_{1 Pulse}$ is the average energy of one pulse (J/Pulse); n is the number of pulses; V is the treated volume (L).

2.4 Ultrasound treatment

For high frequency ultrasound, the atrazine solution (50 mL, 20 mg/L, 0.093 mmol/L) was poured into a 250-mL cup-shaped horn-type ultrasonic reactor purchased from SinapTec (Lezennes, France), and passed through a constant frequency of 525 kHz with 80 W power. The air flow was passed through the interlayer of the inner and outer walls to stabilize the temperature at 50 °C.

For low frequency ultrasound, an ultrasonic processor (Vibra-Cell 72434,

Fisher Scientific, Illkirch, France) at 50 kHz frequency with 70 W power was applied. The atrazine solution (50 mL, 20 mg/L, 0.093 mmol/L) was poured into a 100-mL flat-bottom flask. The probe tip was placed at the center of the liquid. Temperature was kept at 50 °C by water bath. The total treatment time was 8 h. Sampling at 0, 1, 2, 4 and 8 h. The initial concentration of ferrous sulfate $FeSO_4 \cdot 7H_2O$ was 0.93 mmol/L in ultrasound experiments adding Fe^{2+} . The specific energy consumption of ultrasound, W_{US} (J/L), was calculated as follow:

$$W_{US} = (P_{US} \times t)/V \quad (2)$$

Where P_{US} is the power (W); t is the treatment time (s); V is the treatment volume of the liquid (L).

2.5 Fenton oxidation treatment

Three initial atrazine solutions (50 mL, 20 mg/L, 0.093 mmol/L) were poured into three 100-mL flat-bottom flasks with magnets, and 10 eq., 5 eq. and 2 eq. equivalents of Fenton reagents (The ratio of initial $FeSO_4 \cdot 7H_2O$ or H_2O_2 molar concentration to initial atrazine molar concentration was 10, 5 and 2, where $[FeSO_4 \cdot 7H_2O]_0 = [H_2O_2]_0 = 0.93$ mmol/L, 0.465 mmol/L and 0.186 mmol/L.) were added, respectively. The reaction lasted for 8 h. Sampling at 0, 1, 2, 4 and 8 h.

2.6 Analysis by HPLC-HRMS

Atrazine and its metabolites detected and quantified by HPLC-HRMS. A diode array detector (DAD) type HPLC system (Infinity 1290, Agilent Technologies, France), was connected with a micro hybrid quadrupole time of flight (Q-TOF) and electrospray ionization (ESI) type mass spectrometer (Agilent 6538, Agilent Technologies, France). HPLC analyses were performed using a Thermo Hypersil Gold C18 (USP L1) column (100 × 2.1 mm, 1.9 μm, 175 Å) at 40 °C. Eluents A and B consisted of 0.1% (v/v) formic acid in deionized water and 100% acetonitrile, respectively. The elution profile was 0-0.3 min 5% B, 0.3-1.7 min 5-30% B (linear gradient), 1.7-3.5 min 95% B (linear gradient), 3.5-4 min 95% B. The flow rate was 0.600 mL/min. The responses of compounds were measured in positive ESI mode with external calibration. By using the electrospray scan mode with a frequency of 5 Hz in the mass range of 50 to 1200 m/z and an electrospray voltage of 3800 V, fragment voltage of 110 V, positive ion electrospray mass spectra were obtained.

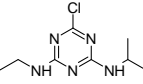
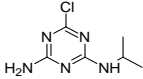
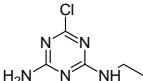
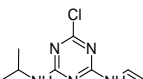
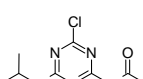
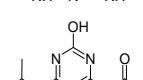
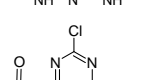
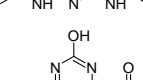
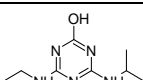
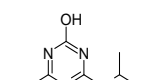
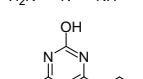
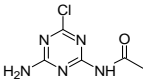
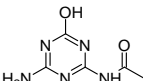
The atomizing nitrogen temperature was 350°C, the pressure was 30 psi, and the flow rate was 10 L/min.

3. Results and discussion

3.1 Atrazine and its detected metabolites

The abbreviations of atrazine and its detected metabolites are shown in Table 1.

Table 1. Atrazine and its detected metabolites.

Abbreviation	Structure	Formula	Name	m/z	Retention Time (min)	Detected process
ATZ		C ₈ H ₁₄ ClN ₅	Atrazine	216.1010	2.558	
DEA		C ₆ H ₁₀ ClN ₅	Deethylatrazine	188.0698	1.910	
DIA		C ₅ H ₈ ClN ₅	Deisopropylatrazine	174.0541	1.620	
CVIT		C ₈ H ₁₂ ClN ₅	6-chloro-N2-ethenyl-N4-(propan-2-yl)-1,3,5-triazine-2,4-diamine	214.0854	2.070	All treatments (HFUS, LFUS, Fenton, HVED)
CDIT		C ₈ H ₁₂ ClN ₅ O	N-[4-Chloro-6-(isopropylamino)-1,3,5-triazin-2-yl]acetamide	230.0804	2.091	
ODIT		C ₈ H ₁₃ N ₅ O ₂	N-[4-Hydroxy-6-(isopropylamino)-1,3,5-triazin-2-yl]acetamide	212.1142	1.213	
CDET		C ₇ H ₁₀ ClN ₅ O	N-[4-Chloro-6-(ethylamino)-1,3,5-triazin-2-yl]acetamide	216.0647	1.820	
ODET		C ₇ H ₁₁ N ₅ O ₂	N-[6-(Ethylamino)-4-oxo-1,4-dihydro-1,3,5-triazin-2-yl]acetamide	198.0986	1.082	
HA		C ₈ H ₁₅ N ₅ O	Hydroxyatrazine	198.1350	1.233	All treatments except Fenton
DEHA		C ₆ H ₁₁ N ₅ O	Deethylhydroxyatrazine	170.1037	0.810	
DIHA		C ₅ H ₉ N ₅ O	Deisopropylhydroxyatrazine	156.0880	0.560	
CDAT		C ₅ H ₆ ClN ₅ O	N-(4-Amino-6-chloro-1,3,5-triazin-2-yl)acetamide	188.0334	1.264	All treatments except HVED
OEAT		C ₅ H ₇ N ₅ O ₂	N-(4-Amino-6-hydroxy-1,3,5-triazin-2-yl)acetamide	170.0673	0.727	

Abbreviation	Structure	Formula	Name	m/z	Retention Time	Detected process
CDDT		C ₇ H ₈ ClN ₅ O ₂	N,N'-(6-Chloro-1,3,5-triazine-2,4-diyl)diacetamide	230.0440	1.451	
ODDT		C ₇ H ₉ N ₅ O ₃	N,N'-(6-hydroxy-1,3,5-triazine-2,4-diyl)diacetamide	212.0778	1.141	
DDA		C ₃ H ₄ ClN ₅	Didealkylatrazine	146.0228	1.023	All treatments except LFUS
AM		C ₃ H ₅ N ₅ O	Ammeline	128.0567	0.490	All treatments except LFUS
CBOI		C ₃ H ₅ N ₃ O ₄	1-carboxybiuret	148.0353	0.416	HVED (very trace)
CNIT		C ₈ H ₁₄ ClN ₅ O	1-((4-chloro-6-((propan-2-yl)amino)-1,3,5-triazin-2-yl)amino)ethan-1-ol	232.0960	1.868	Fenton
HAHT		C ₈ H ₁₄ ClN ₅ O ₂	2-((4-chloro-6-((1-hydroxyethyl)amino)-1,3,5-triazin-2-yl)amino)propan-2-ol	248.0909	2.212	Fenton

3.2 Atrazine degradation by HVED

In [Figure 3](#), atrazine degradation rates by HVED as a function of the effective time are given for different experimental conditions. As the results shown, for the atrazine solution of 500 mL, within 2 ms of discharge, the degradation rate of atrazine in argon atmosphere was lower than that in air atmosphere, indicating that dissolved oxygen might enhance the degradation of atrazine in discharge process. According to the references[36, 37], dissolved oxygen can react with the high-energy electrons and produce superoxide radical anions $O_2^{\cdot-}$ (Equation (3)) that can degrade atrazine. So, it would be better to conduct the discharge experiments directly under the air.

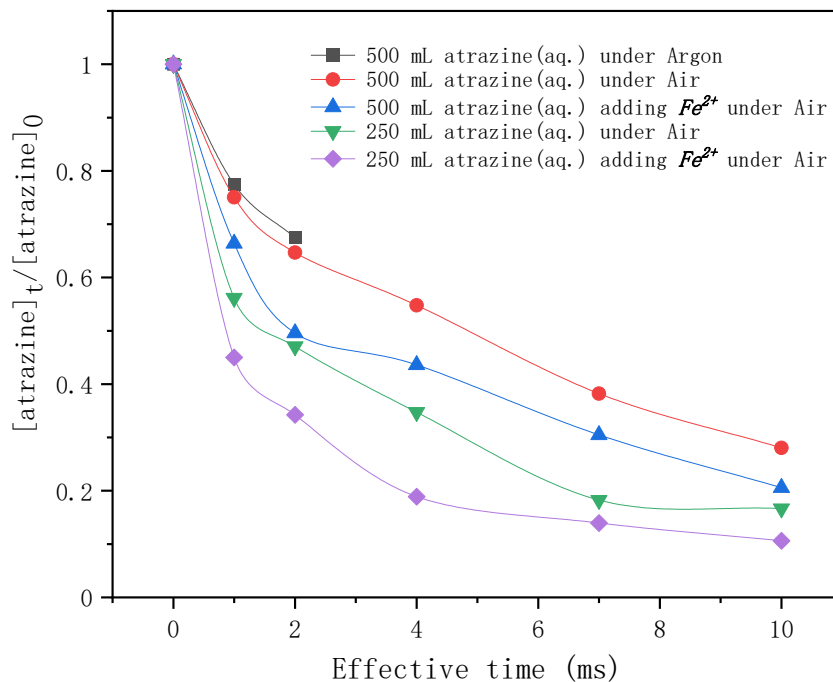
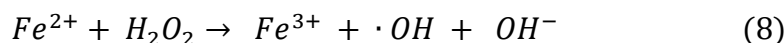
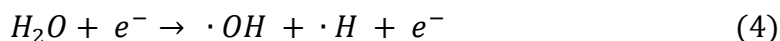


Figure 3. Time profiles of atrazine degradation by HVED in different treatment volumes adding Fe^{2+} or not.

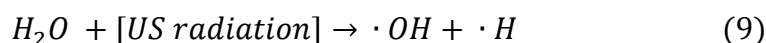
In addition, four comparative HVED experiments were conducted in different treatment volumes with or without Fe^{2+} addition. In the same treatment volume, adding Fe^{2+} enhanced the degradation rate of atrazine. This result is consistent with results from the literature[27], ferrous sulfate $FeSO_4 \cdot 7H_2O$ added in the pulsed electrical discharge reactor improved the degradation of atrazine due to the classical Fenton reaction. During electrical discharge process, the electron impact of H_2O molecules is the main way to produce hydroxy radicals $\cdot OH$ (Equation (4))[38]. Reactions between radicals can produce hydrogen, hydrogen peroxide, or reformatted water (Equation (5)-(7)). These self-quenching reactions lead to the consumption of radicals $\cdot OH$, which inhibit atrazine degradation. However, adding ferrous ions Fe^{2+} reduced this $\cdot OH$ radicals' consumption via Fenton reaction (Equation (8)). The results also show that higher degradation rate of atrazine was observed for lower treatment volume. The specific energy consumption per unit pulse (J/L/Pulse) is 400 J/L/Pulse for 500 mL, and 800 J/L/Pulse for 250 mL. At the same treatment time, the pulse number is the same; the specific energy consumption is higher for the lowest treated volume thus enhancing the degradation rate of atrazine.



3.3 Atrazine degradation by ultrasound

Figure 4 shows the effect of frequency and Fe^{2+} on atrazine degradation by ultrasound. The degradation rates of atrazine by HFUS (525 kHz) were much higher than those with LFUS (50 kHz). The frequency and power of irradiation determine the physical characteristics of ultrasonication, such as bubble sizes and collapse temperatures. A higher frequency causes higher turbulence because the bubbles are more likely to implose, enhancing mass transfers. The results also showed that adding Fe^{2+} greatly improved atrazine degradation regardless of the frequency.

In atrazine aqueous solution, the main sono-chemical dissociation processes are homolytic cleavages of water to release radicals $\cdot OH$ and $\cdot H$ (Equation (9)).



But the self-combination of produced radicals $\cdot OH$ (Equation (6)) with a second-order rate constant of $5 \times 10^9 \text{ M}^{-1} \cdot \text{s}^{-1}$, [39] is faster than the degradation of atrazine with a rate constant of $2.4 \times 10^9 \text{ M}^{-1} \cdot \text{s}^{-1}$. [27] The addition of Fe^{2+} is beneficial to the degradation of atrazine by releasing radical $\cdot OH$ from its self-combination product hydrogen peroxide by classical Fenton reaction (Equation (8)).

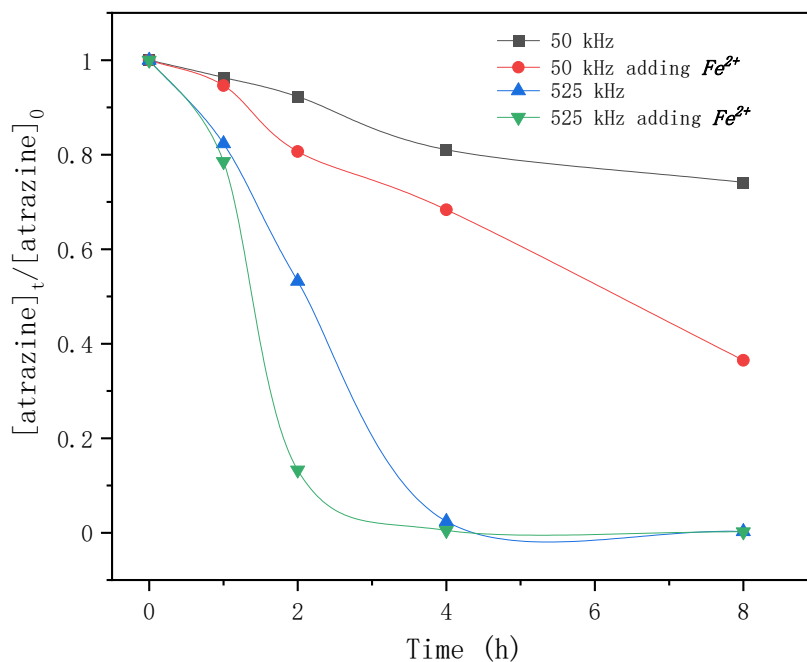


Figure 4. Time profiles of atrazine degradation by ultrasound in different frequency adding Fe^{2+} or not.

3.4 Atrazine degradation by Fenton oxidation

In [Figure 5](#), the equivalents of the Fenton reagents were studied on the degradation of atrazine by Fenton oxidation. Within the first 5 hours, atrazine was degraded more rapidly by adding 5 eq. and 10 eq. Fenton reagents. After 5 h, atrazine was nearly completely degraded regardless of the equivalents of Fe^{2+} . For 5 eq. and 10 eq. Fenton reagents, the elimination of atrazine was rapid within the first hour, and tended to slow down until reaching equilibrium. For 2 eq. Fenton reagents, the degradation rate of atrazine was rapid in the first hour, but flattened in the second hour, and later it became rapid again until it reached equilibrium. The reason may be due to the consumption of Fe^{2+} and the generation of $\cdot OH$ radicals.

As mentioned above, in classical Fenton reaction, ferrous ions Fe^{2+} react with hydrogen peroxide to form radicals $\cdot OH$ which are the reactive oxygen species for atrazine degradation. When most of the ferrous ions Fe^{2+} are converted to ferric ions Fe^{3+} , the generated ferric ions Fe^{3+} tend to react with hydrogen peroxides to release ferrous ions Fe^{2+} (Equation (10)). According to the reference[40], the reaction rate constants of Equation (8) and Equation (10) are $76 \text{ M}^{-1}\cdot\text{s}^{-1}$ and $0.01 \text{ M}^{-1}\cdot\text{s}^{-1}$ respectively. The reaction between radicals $\cdot OH$ and atrazine is

instantaneous (Equation (11)), and its reaction rate constant is $2.4 \times 10^9 \text{ M}^{-1} \cdot \text{s}^{-1}$. [27] Therefore, for 2 eq. Fe^{2+} , at the beginning, radicals $\cdot\text{OH}$ formed by Fenton reaction quickly degraded atrazine.

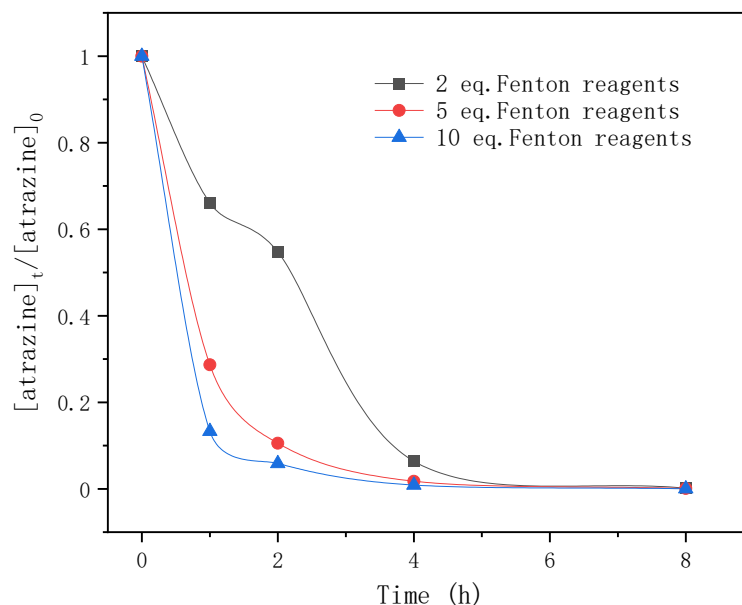
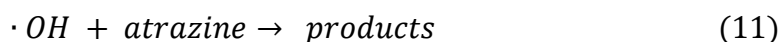


Figure 5. Time profiles of atrazine degradation for different Fenton reagent equivalents.

As Fe^{2+} was consumed, the formation of radicals $\cdot\text{OH}$ was inhibited and the degradation rate of atrazine was flattened. Then the release of Fe^{2+} from Fe^{3+} restarted Fenton reaction and re-provided radicals $\cdot\text{OH}$ for atrazine degradation. For 5 eq. and 10 eq. Fe^{2+} , sufficient Fe^{2+} ensured the continuous generation of radicals $\cdot\text{OH}$ from hydrogen peroxides, so the degradation rate of atrazine was very fast until it reached equilibrium. In this study, high equivalents of Fe^{2+} were found to favor atrazine degradation.



3.5 Formation kinetics of metabolites

Figure 6 shows the formation kinetics of metabolites during atrazine degradation by different treatments. The chemical structures of these metabolites represented by abbreviation are shown in Table 1. In 525 kHz ultrasound treatment (Figures 6(a) and 6(b)), dealkylation and carbonylation products such as DIA, CDIT and CDAT, are the major metabolites while the dechlorination products are less

present, and adding Fe^{2+} improved the production of dealkylation products DEA and DIA. In low frequency ultrasound treatment (Figure 6(c)), dealkylation and carbonylation products CDIT and CDET as well as the dechlorination product ODIT are the main metabolites. In Fenton oxidation (Figure 6(d)), the formation kinetics of metabolites were more variable over time, and it produced final main product Ammeline (AM).

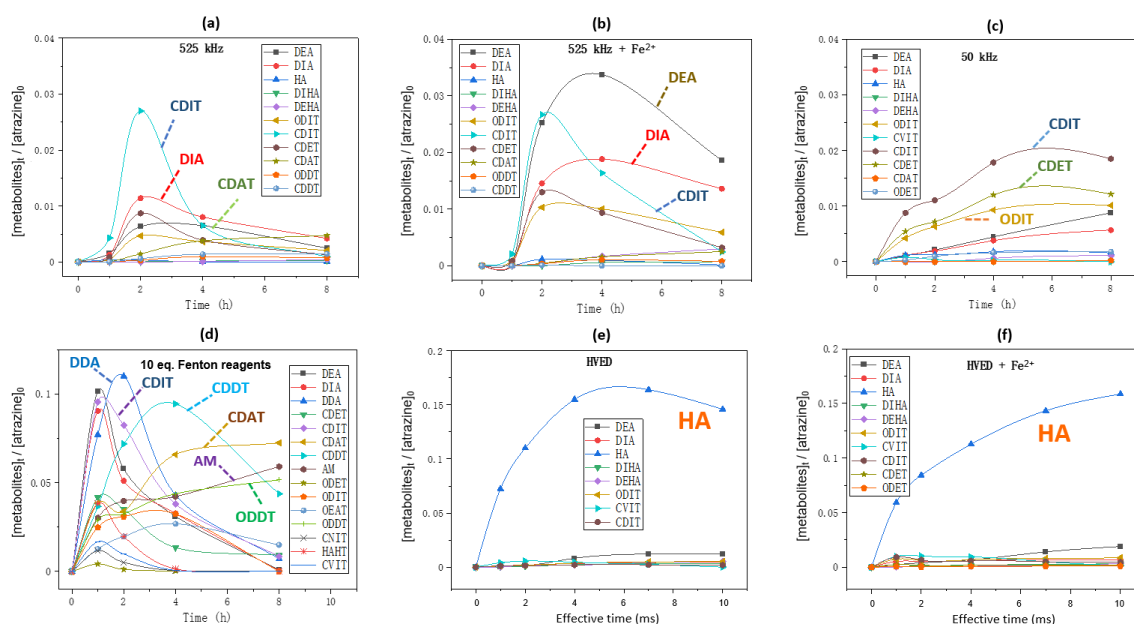


Figure 6. Formation kinetics of metabolites during atrazine degradation (a) and (b) 50 mL of atrazine solution was treated by ultrasound 525 kHz with or without 10 eq. $FeSO_4 \cdot 7H_2O$ addition; (c) 50 mL of atrazine solution was treated by ultrasound 50 kHz with or without 10eq. $FeSO_4 \cdot 7H_2O$ addition; (d) 50 mL of atrazine solution was added by 10 eq. H_2O_2 and 10 eq. $FeSO_4 \cdot 7H_2O$; (e) and (f) 250 mL of atrazine solution was treated by HVED with or without 10 eq. $FeSO_4 \cdot 7H_2O$ addition. Initial atrazine concentration is always 0.093 mmol/L.

In HVED treatment (Figures 6(e) and 6(f)), the dechlorination product Hydroxyatrazine (HA) was the main product no matter adding Fe^{2+} or not. Notably, the ring cleavage product Carboxybiuret (CBOI) was detected in the HVED treatment, which is not shown below (Figures 6(e) and 6(f)) due to its trace amounts. This implies that HVED treatment is a potential degradation pathway for s-triazine ring-cleavage. In the future, we will make more effort to promote this s-triazine ring-cleavage so as to pursue mineralization.

3.6 Proposed mechanism

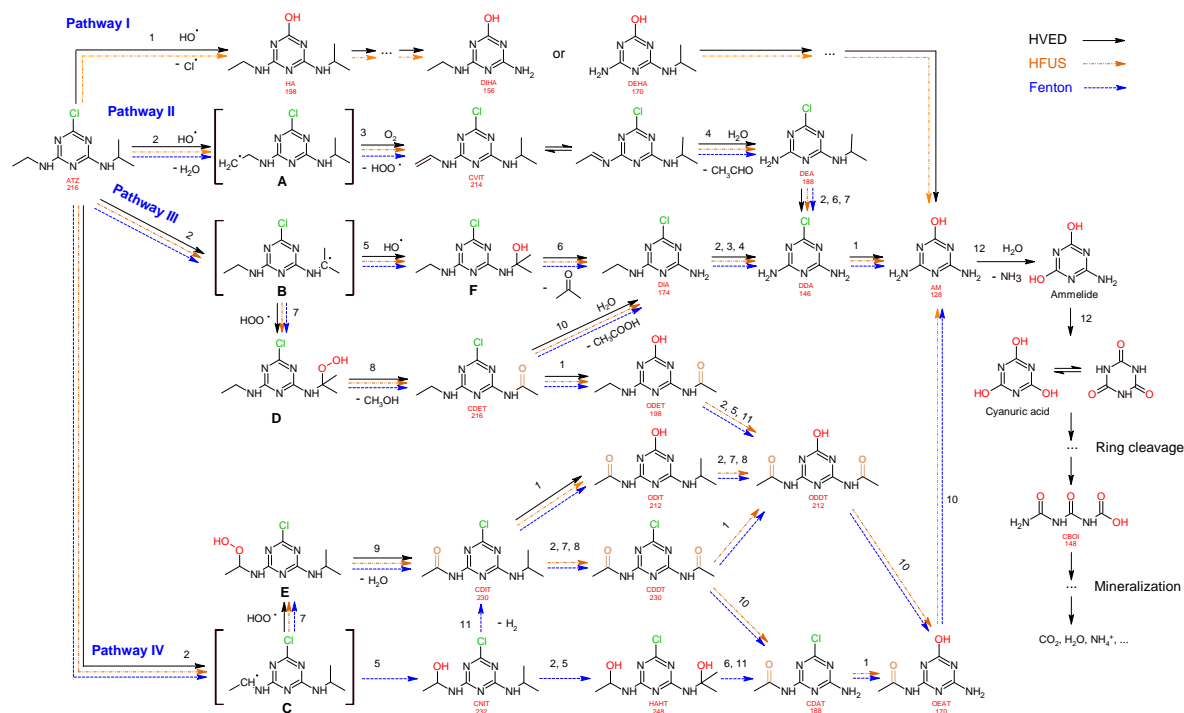


Figure 7. Proposed degradation pathways of atrazine.

Based on the formation kinetics of metabolites, the mechanism of atrazine degradation was proposed in [Figure 7](#). Radicals $\cdot OH$ may attack atrazine molecule in different positions, including attack to the alkylamino side chains[41], or attack to the *ipso*-position of chlorine substituent[42]. So, we proposed four pathways I, II, III and IV on atrazine degradation according to different positions of $\cdot OH$ attack.

Pathway I

An attack of radical $\cdot OH$ at the *ipso*-position of chlorine substituent might lead to a geminal chlorohydrine, yielding HO-adduct by elimination of an HCl molecule.[41, 43] The dechlorination-hydroxylated product HA was detected in HVED and HFUS processes, and it could be further degraded into DEHA and DIHA, followed by the generation of deeper oxidation products. It is noteworthy that hydroxylated atrazine degradation products were found to be less toxic.[44] So, HVED process appears to be more desirable for atrazine detoxification, since it mainly produced hydroxylated product HA ([Figures 6\(e\)](#) and [6\(f\)](#)).

Pathway II

Radical $\bullet OH$ attacks β -C adjacent to N atom on ethylamino side chain, generating carbon-center radical **A** through H-atom abstraction. The carbon-centered radical **A** could be attacked by dissolved O_2 to form per-hydroxyl radical ($HOO\bullet$) and olefination products CVIT. Further oxidation of CVIT might lead to the formation of acetaldehyde and dealkylated product DEA.[45] CVIT and DEA were both detected in HVED, HFUS and Fenton processes.

Pathway III

Radical $\bullet OH$ attacks α -C adjacent to N atom on iso-propylamino side chain, generating carbon-center radical **B** through H-atom abstraction. The carbon-center radical **B** could be further attacked by $\bullet OH$ to form alkylic-hydroxylation intermediates **F**, leading to the generation of acetone and dealkylated product DIA. Another way, per-hydroxyl radical ($HOO\bullet$) might attack the carbon-center radical **B**, inducing the generation of atrazine-peroxide intermediate **D** which might produce methanol and alkylic-oxidation product CDET.[42] CDET might produce dechlorination-hydroxylated product ODET or dealkylated product DIA through the hydrolysis of the amide group.[43] Both DIA and DEA mentioned in Pathway II could be further oxidized into the fully dealkylated DDA and its dechlorination-hydroxylated product ammeline (AM). CDET, ODET, DIA, DDA and AM were detected in HVED, HFUS and Fenton processes. But DDA and AM were not found in LFUS process, indicating that low frequency ultrasound is not conducive to deeper oxidation.

Pathway IV

Radical $\bullet OH$ attacks α -C adjacent to N atom on ethylamino side chain, generating carbon-center radical **C** through H-atom abstraction. The carbon-center radical **C** could be attacked by $\bullet OH$ to form alkylic-hydroxylation intermediate CNIT. Then, intermediate CNIT might produce alkylic-oxidation product CDIT through H-abstraction[46], or produce another alkylic-hydroxylation intermediate HAHT[22]. CNIT and HAHT were detected in Fenton process. HAHT might further oxidized into dealkylated product CDAT and its dechlorination-hydroxylated product OEAT. Another way, the carbon-center radical **C** could be attacked by $HOO\bullet$ and form atrazine-peroxide intermediate **E**, followed by the generation of CDIT. CDIT could produce its dechlorination-hydroxylated product ODIT, or be further oxidized into

CDDT, followed by the generation of ODDT and CDAT. Previous studies[47, 48] have shown that carboxybiuret (CBOI) formed from ring cleavage of cyanuric acid, might undergo spontaneous decarboxylation to biuret, which could be further mineralized into small molecules such as CO₂, H₂O, NH₃, etc. However, the specific mechanism of ring cleavage is still uncertain, which will be the content of future research. In HVED process, CDDT, ODDT, CDAT and OEAT were not detected, but AM and the ring cleavage product CBOI were detected, indicating that HVED treatment is more favorable for mineralization.

In the final degradation stage of these four pathways, dechlorination-hydroxylated product AM is generated, and its deeper oxidations may lead to the formation of the ring cleavage product CBOI, which could be further mineralized into small molecules such as CO₂, H₂O, NH₃, etc. However, the specific mechanism of ring cleavage is still unclear and needs further study.

3.7 Comparison of different degradation techniques

Table 2. Comparison of high frequency ultrasound, Fenton oxidation and HVED treatment.

Technologies	Degradation rate of atrazine	Main formed metabolites	Specific energy consumption (kJ/L)
Ultrasound (525 kHz)	47% (treatment time 2 h)	DIA	11520 kJ/L
Ultrasound (525 kHz) + Fe ²⁺	87% (treatment time 2 h)	DEA	
Fenton oxidation (10 eq. Fenton reagents)	>95% (treatment time 2 h)	AM	
HVED (250 mL ATZ solution)	83% (effective time 10 ms)		
HVED + Fe ²⁺ (250 mL atrazine solution)	89% (effective time 10 ms)	HA	800 kJ/L

In table 2, high frequency ultrasound, Fenton oxidation and HVED treatment were compared in terms of degradation rate of atrazine, main formed metabolites and specific energy consumption. The toxicity ranking of atrazine and its

metabolites is ATZ>DEA>DIA>AM>DDA>HA.[7] For high frequency ultrasound treatment, after 2 h, atrazine degradation was unfavorable with only 47 %, and adding ferrous ions doubled the degradation rate to 87%, but the disadvantages still exist with the presence of toxic main metabolites and a high energy consumption. For Fenton oxidation, although it reached the highest atrazine degradation rate of 95%, it produced toxic main metabolite AM. For HVED, adding ferrous ions enhanced the degradation rate of atrazine from 83% to 89%, due to the Fenton reaction, in which ferrous ions reacted with hydrogen peroxide produced by the discharge[27]. By comparison, HVED is more advantageous because of the high degradation efficiency in short treatment time, the presence of less toxic main metabolite HA and the lower energy consumption.

4. Conclusion

An innovative atrazine degradation method was reported using high voltage electrical discharge (HVED). The HVED method was compared with the traditional atrazine degradation method, Fenton oxidation and ultrasounds at high or low frequency. HVED treatment was more advantageous, since atrazine can be mostly degraded (89 %) with the addition of ferrous ions, in short effective time (10 ms), while the treatment time of Fenton oxidation and ultrasounds lasted for 2 h. Besides, the main generated metabolite hydroxyatrazine (HA) in HVED process, was less toxic than deethylatrazine (DEA) and deisopropylatrazine (DIA) generated in ultrasounds process, and ammeline (AM) generated in Fenton process. Also, when the degradation rates of atrazine were around 87%, the specific energy requirement of HVED (800 kJ/L) was much lower than that of ultrasounds at high frequency (11520 kJ/L). In addition, ferrous ions Fe^{2+} promoted the degradation of atrazine in those three treatments via Fenton reaction with hydrogen peroxide H_2O_2 , releasing the important reactive oxygen species, hydroxyl radicals $\cdot OH$. Finally, the formation kinetics of metabolites and the proposed pathways may provide a reference for future research on atrazine degradation.

IV.3. Chapter conclusion

In this chapter, high voltage electrical discharge was applied for atrazine degradation, which was compared with Fenton oxidation and ultrasound treatment. In comparison, HVED was more advantageous. On one hand, the effective time of HVED was on the millisecond level, which means that a high degradation rate of atrazine can be obtained in a very short time (10 ms) through HVED treatment, while Fenton oxidation and ultrasound generally required 2 hours. On the other hand, from the perspective of the main metabolites produced, hydroxyatrazine (HA) remained the main one during the degradation process of HVED, its toxicity is much lower than that of atrazine, and it is also less toxic than most other products, such as deethylatrazine (DEA), deisopropylatrazine (DIA) and ammeline (AM) generated from Fenton oxidation and ultrasound treatment.

Considering energy saving and environmental protection, when reaching the same atrazine degradation rate (>80%), the specific energy consumption of 800 kJ/L of HVED is more friendly than the 11520 kJ/L of 525 kHz high-frequency ultrasound. In addition, the HVED technology was combined with the catalyst Fe^{2+} and achieved a higher degradation efficiency. The primary oxide H_2O_2 generated in the HVED system underwent Fenton reaction with the action of the catalyst Fe^{2+} to obtain reactive oxygen species hydroxyl radicals $\cdot OH$, which made the degradation of atrazine more rapid.

Moreover, a series of atrazine degradation metabolites were detected and identified by HPLC-HRMS analytical system. Among them, there was a triazine ring cleavage product 1-Carboxybiuret (CBOI), which appeared in trace amounts during the atrazine degradation process by HVED. This means that HVED has the potential to achieve atrazine mineralization. However, atrazine degraded by HVED mainly produced primary degradation product HA. Perhaps future work can increase input voltage and the frequency of electric shocks to see if it promotes deeper degradation.

Based on the formation kinetics of metabolites during different degradation processes of atrazine by HVED, ultrasound and Fenton oxidation, a possible reaction mechanism was proposed, which provides a reference for future work.

IV.4. References

- [1] B. Jiang, J. Zheng, S. Qiu, M. Wu, Q. Zhang, Z. Yan, Q. Xue, Review on electrical discharge plasma technology for wastewater remediation, *Chemical Engineering Journal* 236 (2014) 348-368.
- [2] Ö.S. Kuşçu, E. Eke, Oxidation of olive mill wastewater by a pulsed high-voltage discharge using oxygen or air, *Journal of Environmental Chemical Engineering* 9 (2021) 104701.
- [3] T. Shen, X. Wang, P. Xu, C. Yang, J. Li, P. Wang, G. Zhang, Effect of dielectric barrier discharge plasma on persulfate activation for rapid degradation of atrazine: Optimization, mechanism and energy consumption, *Environmental Research* 212 (2022) 113287.
- [4] S. Mededovic, B.R. Locke, Side-Chain Degradation of Atrazine by Pulsed Electrical Discharge in Water, *Industrial & Engineering Chemistry Research* 46 (2007) 2702-2709.
- [5] D. Munaron, B. Mérigot, V. Derolez, N. Tapie, H. Budzinski, A. Fiandrino, Evaluating pesticide mixture risks in French Mediterranean coastal lagoons waters, *Sci. Total Environ.* 867(2023) (2022) 161303. <https://doi.org/https://doi.org/10.1016/j.scitotenv.2022.161303>.
- [6] B.G. Silva Pinto, T.K. Marques Soares, M. Azevedo Linhares, N. Castilhos Ghisi, Occupational exposure to pesticides: Genetic danger to farmworkers and manufacturing workers – A meta-analytical review, *Science of The Total Environment* 748 (2020) 141382. <https://doi.org/https://doi.org/10.1016/j.scitotenv.2020.141382>.
- [7] J. Hong, N. Boussetta, G. Enderlin, F. Merlier, N. Grimi, Degradation of Residual Herbicide Atrazine in Agri-Food and Washing Water, *Foods* 11(16) (2022) 2416. <https://doi.org/https://doi.org/10.3390/foods11162416>.
- [8] F. Giannini-Kurina, J. Borello, I. Cañas, S. Hang, M. Balzarini, Mapping atrazine persistence in soils of central Argentina using INLA, *Soil and Tillage Research* 219 (2022) 105320. <https://doi.org/https://doi.org/10.1016/j.still.2022.105320>.
- [9] T. Bohn, E. Cocco, L. Gourdol, C. Guignard, L. Hoffmann, Determination of atrazine and degradation products in Luxembourgish drinking water: origin and fate of potential endocrine-disrupting pesticides, *Food Additives & Contaminants: Part A* 28(8) (2011) 1041-1054. <https://doi.org/10.1080/19440049.2011.580012>.
- [10] Y. Yun, S. Lee, C. So, R. Manhas, C. Kim, T. Wibowo, M. Hori, N. Hunter, Oocyte Development and Quality in Young and Old Mice following Exposure to Atrazine, *Environmental Health Perspectives* 130(11) (2022) 117007. <https://doi.org/10.1289/EHP11343>.
- [11] T.B. Hayes, V. Khoury, A. Narayan, M. Nazir, A. Park, T. Brown, L. Adame, E. Chan, D. Buchholz, T. Stueve, S. Gallipeau, Atrazine induces complete feminization and chemical castration in male African clawed frogs (*Xenopus laevis*), *Proceedings of the National Academy of Sciences* 107(10) (2010) 4612-4617. <https://doi.org/10.1073/pnas.0909519107>.

- [12] S.E. Wirbisky, J.L. Freeman, Atrazine Exposure and Reproductive Dysfunction through the Hypothalamus-Pituitary-Gonadal (HPG) Axis, *Toxics* 3(4) (2015) 414-450. <https://doi.org/10.3390/toxics3040414>.
- [13] J. Bethsass, A. Colangelo, European Union Bans Atrazine, While the United States Negotiates Continued Use, *International Journal of Occupational and Environmental Health* 12(3) (2006) 260-267. <https://doi.org/10.1179/oeh.2006.12.3.260>.
- [14] J.A. Rusiecki, A. De Roos, W.J. Lee, M. Dosemeci, J.H. Lubin, J.A. Hoppin, A. Blair, M.C.R. Alavanja, Cancer Incidence Among Pesticide Applicators Exposed to Atrazine in the Agricultural Health Study, *JNCI: Journal of the National Cancer Institute* 96(18) (2004) 1375-1382. <https://doi.org/10.1093/jnci/djh264>.
- [15] E.M. Brovini, B.C.T. de Deus, J.A. Vilas-Boas, G.R. Quadra, L. Carvalho, R.F. Mendonça, R.d.O. Pereira, S.J. Cardoso, Three-bestseller pesticides in Brazil: Freshwater concentrations and potential environmental risks, *Science of The Total Environment* 771 (2021) 144754. <https://doi.org/https://doi.org/10.1016/j.scitotenv.2020.144754>.
- [16] J.T. Sun, L.L. Pan, Y. Zhan, D.C.W. Tsang, L.Z. Zhu, X.D. Li, Atrazine contamination in agricultural soils from the Yangtze River Delta of China and associated health risks, *Environmental Geochemistry and Health* 39(2) (2017) 369-378. <https://doi.org/10.1007/s10653-016-9853-x>.
- [17] X. Cheng, H. Liang, A. Ding, X. Tang, B. Liu, X. Zhu, Z. Gan, D. Wu, G. Li, Ferrous iron/peroxymonosulfate oxidation as a pretreatment for ceramic ultrafiltration membrane: Control of natural organic matter fouling and degradation of atrazine, *Water Research* 113 (2017) 32-41. <https://doi.org/https://doi.org/10.1016/j.watres.2017.01.055>.
- [18] P. Wang, Y. Yin, Y. Guo, C. Wang, Preponderant adsorption for chlorpyrifos over atrazine by wheat straw-derived biochar: experimental and theoretical studies, *RSC Advances* 6(13) (2016) 10615-10624. <https://doi.org/10.1039/C5RA24248G>.
- [19] Y. Liu, J. Wang, Multivalent metal catalysts in Fenton/Fenton-like oxidation system: A critical review, *Chemical Engineering Journal* 466 (2023) 143147. <https://doi.org/https://doi.org/10.1016/j.cej.2023.143147>.
- [20] S. Wang, J. Wang, Electron Beam Technology Coupled to Fenton Oxidation for Advanced Treatment of Dyeing Wastewater: from Laboratory to Full Application, *ACS ES&T Water* 2(5) (2022) 852-862. <https://doi.org/10.1021/acsestwater.2c00040>.
- [21] S. Wang, G. Yu, J. Wang, Treatment of tributyl phosphate by fenton oxidation: Optimization of parameter, degradation kinetics and pathway, *Chemosphere* 317 (2023) 137889. <https://doi.org/https://doi.org/10.1016/j.chemosphere.2023.137889>.
- [22] L.J. Xu, W. Chu, N. Graham, Atrazine degradation using chemical-free process of USUV: Analysis of the micro-heterogeneous environments and the degradation mechanisms, *Journal of Hazardous Materials* 275 (2014) 166-174. <https://doi.org/https://doi.org/10.1016/j.jhazmat.2014.05.007>.

- [23] X. Lu, W. Qiu, J. Peng, H. Xu, D. Wang, Y. Cao, W. Zhang, J. Ma, A Review on Additives-assisted Ultrasound for Organic Pollutants Degradation, *Journal of Hazardous Materials* 403 (2021) 123915. <https://doi.org/https://doi.org/10.1016/j.jhazmat.2020.123915>.
- [24] S.M.R. Azam, H. Ma, B. Xu, S. Devi, M.A.B. Siddique, S.L. Stanley, B. Bhandari, J. Zhu, Efficacy of ultrasound treatment in the removal of pesticide residues from fresh vegetables: A review, *Trends in Food Science & Technology* 97 (2020) 417-432. <https://doi.org/https://doi.org/10.1016/j.tifs.2020.01.028>.
- [25] M.R. Ghezzar, F. Abdelmalek, M. Belhadj, N. Benderdouche, A. Addou, Enhancement of the bleaching and degradation of textile wastewaters by Gliding arc discharge plasma in the presence of TiO₂ catalyst, *Journal of Hazardous Materials* 164(2) (2009) 1266-1274. <https://doi.org/https://doi.org/10.1016/j.jhazmat.2008.09.060>.
- [26] V.I. Grinevich, E.Y. Kvitkova, N.A. Plastinina, V.V. Rybkin, Application of Dielectric Barrier Discharge for Waste Water Purification, *Plasma Chemistry and Plasma Processing* 31(4) (2011) 573-583. <https://doi.org/10.1007/s11090-010-9256-1>.
- [27] S. Mededovic, B.R. Locke, Side-Chain Degradation of Atrazine by Pulsed Electrical Discharge in Water, *Industrial & Engineering Chemistry Research* 46(9) (2007) 2702-2709. <https://doi.org/10.1021/ie070020a>.
- [28] Y. Shang, N. Jiang, Z. Liu, C. Li, H. Sun, H. Guo, B. Peng, J. Li, Pulsed discharge plasma assisted with Z-scheme graphene-TiO₂-MnFe₂O₄ for simultaneous removal of atrazine and Cr (VI): Performance and mechanism, *Chemical Engineering Journal* 452 (2023) 139342. <https://doi.org/https://doi.org/10.1016/j.cej.2022.139342>.
- [29] J. Feng, L. Jiang, D. Zhu, K. Su, D. Zhao, J. Zhang, Z. Zheng, Dielectric barrier discharge plasma induced degradation of aqueous atrazine, *Environmental Science and Pollution Research* 23(9) (2016) 9204-9214. <https://doi.org/10.1007/s11356-016-6148-9>.
- [30] M. Hijosa-Valsero, R. Molina, H. Schikora, M. Müller, J.M. Bayona, Removal of priority pollutants from water by means of dielectric barrier discharge atmospheric plasma, *Journal of Hazardous Materials* 262 (2013) 664-673. <https://doi.org/https://doi.org/10.1016/j.jhazmat.2013.09.022>.
- [31] P. Vanraes, G. Willems, A. Nikiforov, P. Surmont, F. Lynen, J. Vandamme, J. Van Durme, Y.P. Verheust, S.W.H. Van Hulle, A. Dumoulin, C. Leys, Removal of atrazine in water by combination of activated carbon and dielectric barrier discharge, *Journal of Hazardous Materials* 299 (2015) 647-655. <https://doi.org/https://doi.org/10.1016/j.jhazmat.2015.07.075>.
- [32] Q. Wang, A. Zhang, P. Li, P. Héroux, H. Zhang, X. Yu, Y. Liu, Degradation of aqueous atrazine using persulfate activated by electrochemical plasma coupling with microbubbles: removal mechanisms and potential applications, *J. Hazard. Mater.* 403(2021) (2021) 124087. <https://doi.org/https://doi.org/10.1016/j.jhazmat.2020.124087>.
- [33] N. Wardenier, Z. Liu, A. Nikiforov, S.W.H. Van Hulle, C. Leys, Micropollutant elimination by O₃, UV and plasma-based AOPs: An evaluation of treatment and energy costs,

- Chemosphere 234 (2019) 715-724.
<https://doi.org/https://doi.org/10.1016/j.chemosphere.2019.06.033>.
- [34] D. Zhu, L. Jiang, R.-l. Liu, P. Chen, L. Lang, J.-w. Feng, S.-j. Yuan, D.-y. Zhao, Wire-cylinder dielectric barrier discharge induced degradation of aqueous atrazine, *Chemosphere* 117 (2014) 506-514. <https://doi.org/https://doi.org/10.1016/j.chemosphere.2014.09.031>.
- [35] J. Hong, N. Boussetta, G. Enderlin, N. Grimi, F. Merlier, Real-Time Monitoring of the Atrazine Degradation by Liquid Chromatography and High-Resolution Mass Spectrometry: Effect of Fenton Process and Ultrasound Treatment, *Molecules* 27(24) (2022). <https://doi.org/10.3390/molecules27249021>.
- [36] G. Nie, L. Xiao, J. Bi, S. Wang, X. Duan, New insight to piezocatalytic peroxymonosulfate activation: The critical role of dissolved oxygen in mediating radical and nonradical pathways, *Applied Catalysis B: Environmental* 315 (2022) 121584. <https://doi.org/https://doi.org/10.1016/j.apcatb.2022.121584>.
- [37] X. Wang, Y. Wang, N. Chen, Y. Shi, L. Zhang, Pyrite enables persulfate activation for efficient atrazine degradation, *Chemosphere* 244 (2020) 125568. <https://doi.org/https://doi.org/10.1016/j.chemosphere.2019.125568>.
- [38] P. Lukes, B.R. Locke, Plasmachemical oxidation processes in a hybrid gas-liquid electrical discharge reactor, *Journal of Physics D: Applied Physics* 38(22) (2005) 4074. <https://doi.org/10.1088/0022-3727/38/22/010>.
- [39] Y. Hu, Z. Zhang, C. Yang, Measurement of hydroxyl radical production in ultrasonic aqueous solutions by a novel chemiluminescence method, *Ultrasonics Sonochemistry* 15(5) (2008) 665-672. <https://doi.org/https://doi.org/10.1016/j.ultsonch.2008.01.001>.
- [40] D.R. Grymonpré, A.K. Sharma, W.C. Finney, B.R. Locke, The role of Fenton's reaction in aqueous phase pulsed streamer corona reactors, *Chemical Engineering Journal* 82(1) (2001) 189-207. [https://doi.org/https://doi.org/10.1016/S1385-8947\(00\)00345-4](https://doi.org/https://doi.org/10.1016/S1385-8947(00)00345-4).
- [41] A. Tauber, C. von Sonntag, Products and Kinetics of the OH-radical-induced Dealkylation of Atrazine, *Acta hydrochimica et hydrobiologica* 28(1) (2000) 15-23. [https://doi.org/https://doi.org/10.1002/\(SICI\)1521-401X\(200001\)28:1<15::AID-AHEH15>3.0.CO;2-2](https://doi.org/https://doi.org/10.1002/(SICI)1521-401X(200001)28:1<15::AID-AHEH15>3.0.CO;2-2).
- [42] C.A. Aggelopoulos, D. Tataraki, G. Rassias, Degradation of atrazine in soil by dielectric barrier discharge plasma – Potential singlet oxygen mediation, *Chemical Engineering Journal* 347 (2018) 682-694. <https://doi.org/https://doi.org/10.1016/j.cej.2018.04.111>.
- [43] Y. Ji, C. Dong, D. Kong, J. Lu, Q. Zhou, Heat-activated persulfate oxidation of atrazine: Implications for remediation of groundwater contaminated by herbicides, *Chemical Engineering Journal* 263 (2015) 45-54. <https://doi.org/https://doi.org/10.1016/j.cej.2014.10.097>.

[44] R.N. Lerch, W.W. Donald, Y.-X. Li, E.E. Alberts, Hydroxylated Atrazine Degradation Products in a Small Missouri Stream, *Environmental Science & Technology* 29(11) (1995) 2759-2768. <https://doi.org/10.1021/es00011a010>.

[45] J.A. Khan, X. He, N.S. Shah, H.M. Khan, E. Hapeshi, D. Fatta-Kassinos, D.D. Dionysiou, Kinetic and mechanism investigation on the photochemical degradation of atrazine with activated H₂O₂, S₂O₈²⁻ and HSO₅⁻, *Chemical Engineering Journal* 252 (2014) 393-403. <https://doi.org/https://doi.org/10.1016/j.cej.2014.04.104>.

[46] X. Kong, L. Wang, Z. Wu, F. Zeng, H. Sun, K. Guo, Z. Hua, J. Fang, Solar irradiation combined with chlorine can detoxify herbicides, *Water Research* 177 (2020) 115784. <https://doi.org/https://doi.org/10.1016/j.watres.2020.115784>.

[47] A.K. Bera, K.G. Aukema, M. Elias, L.P. Wackett, Structure of the Cyanuric Acid Hydrolase TrzD Reveals Product Exit Channel, *Scientific Reports* 7(1) (2017) 45277. <https://doi.org/10.1038/srep45277>.

[48] J.L. Murphy, M.J. Arrowood, X. Lu, M.C. Hlavsa, M.J. Beach, V.R. Hill, Effect of Cyanuric Acid on the Inactivation of *Cryptosporidium parvum* under Hyperchlorination Conditions, *Environmental Science & Technology* 49(12) (2015) 7348-7355. <https://doi.org/10.1021/acs.est.5b00962>.

Chapter V. Practical application of atrazine degradation in tap water & toxicity test of experimental wastewater

V.1. Chapter introduction

From 2013 to 2019, the European Environment Agency conducted a water quality survey in 27 EU countries, which showed that pesticides were found to exceed legal limits at between 3% and 7% of groundwater monitoring sites[1]. Data on the water quality of French cities released by the French government “Ministry of Solidarity and Health” [2] show that the concentration of atrazine and its metabolites in some areas exceeds the prescribed standard of 0.1 µg/L. There are obviously hidden dangers in French drinking water.

The toxicity of atrazine cannot be ignored. Its well-known hazards include frog hermaphroditism[3], zebrafish embryo abnormal development[4], interference with the human endocrine system[5], and the potential for breast cancer[6]. Therefore, it is very necessary to evaluate the toxicity of experimental wastewater from atrazine degradation systems. Ideally, the degraded atrazine solution should be less toxic than the initial atrazine solution.

The main purpose of this chapter is to evaluate the effect of a real matrix (tap water) compared to the model matrix (deionized water) on atrazine degradation, which involves two experimental works: study the effect of tap water and deionized water on atrazine degradation; distinguish the difference in metabolites between different treatments by normalized statistical analysis.

In addition, the toxicity of different degradation systems (HVED, US and Fenton oxidation) was evaluated by the lethal concentration LC₅₀ of *Daphnia magna* in experimental wastewater after the degradation of atrazine. This part of the work is a supplement to Chapter IV, in order to better evaluate the three technologies HVED, US and Fenton oxidation.

More details can be found in the next section V.2 “**Degradation of atrazine in French tap water by high voltage electrical discharge (HVED) and high frequency ultrasound (HFUS), with normalized statistical analysis and acute *Daphnia magna* toxicity test**”, which was summarized and prepared for

publication". This work was conducted under the direction of Prof. Nabil GRIMI, Dr. Franck MERLIER, Dr. Nadia BOUSSETTA and Dr. Gérald ENDERLIN, and in collaboration with Dr. Messika REVEL and Dr. Stéphane FIRMIN.

V.2. Degradation of atrazine in French tap water by high voltage electrical discharge (HVED) and high frequency ultrasound (HFUS), with normalized statistical analysis and acute *Daphnia magna* toxicity test

Abstract

Although atrazine has been banned, residues of it and its metabolites are still found in French groundwater in some areas. In response to the European Green Deal, this work focuses on the degradation of atrazine in the background of tap water. The degradation efficiency of atrazine in deionized water by HVED/HFUS treatment was higher than that in tap water with the same initial atrazine concentration, possibly due to competition from impurities in tap water such as ions and other organic compounds. The principal component score plot and the major metabolites heatmap of different treatments were obtained by normalized statistical analysis. In addition, the acute *Daphnia magna* toxicity testing of the degradation process was conducted. The acute toxicity (LC_{50}) in *Daphnia magna* was used to evaluate the toxicity of different treatment solutions initially containing atrazine. The atrazine solution treated by Fenton oxidation ($LC_{50} < 0.1$ mg/L) was much more toxic than that treated by HFUS ($LC_{50} > 5$ mg/L) and HVED ($1.5 < LC_{50} < 2.5$ mg/L). Therefore, the degradation of atrazine by HVED and HFUS is more efficient.

Keywords Pesticide, Atrazine, French tap water, Degradation, Acute toxicity, *Daphnia magna*

1. Introduction

In order to meet the increasingly strong global food demand in recent years, pesticides have been widely used in the development of agriculture. But this also brings pesticide pollution, especially when pesticides applied in farmland leak into lakes, rivers and groundwater, which will pose a serious threat to global human freshwater supplies [7]. One-third of fresh water for human consumption comes from groundwater, and for some countries such as Denmark and Malta it is the only source of water supply [8]. Groundwater quality monitoring has attracted attention and water legislation has been introduced. For example, in Europe, the Water Framework Directive was proposed and requires EU member states to achieve good chemical and quantitative status of groundwater, although this goal was not fully achieved due to the presence of persistent pollutants, especially pesticides [9]. According to water quality surveys conducted by the European Environment Agency in 27 EU countries between 2013 and 2019, pesticide levels in groundwater were found to exceed legal limits, especially in France [10]. Atrazine is a commonly used herbicide in agriculture [5]. A report [11] on French groundwater quality data over more than 20 years shows that atrazine can still be detected, although it was withdrawn from the market in 2003, and its concentration exceeded 0.1 µg/L in some areas. However, the Groundwater Directive [12] stipulates that the quality standard for pesticides is set at 0.1 µg/L, and there are obviously hidden dangers in French groundwater. The maximum concentrations of atrazine and its metabolites detected in tap water in the region of Hauts-de-France are shown in [Figure 1](#), according to the data of health control of water distributed commune by commune, obtained by the French government “Ministry of Solidarity and Health” on September 2023 [13]. It can be seen that the atrazine and its metabolites detected in some areas of Hauts-de-France still exceed the quality standards 0.1 µg/L. In addition to atrazine, other pesticides such as chloridazon are also present in French tap water [7]. To compare and complement our previous work [14, 15], atrazine was chosen as a model molecule to study in this work.

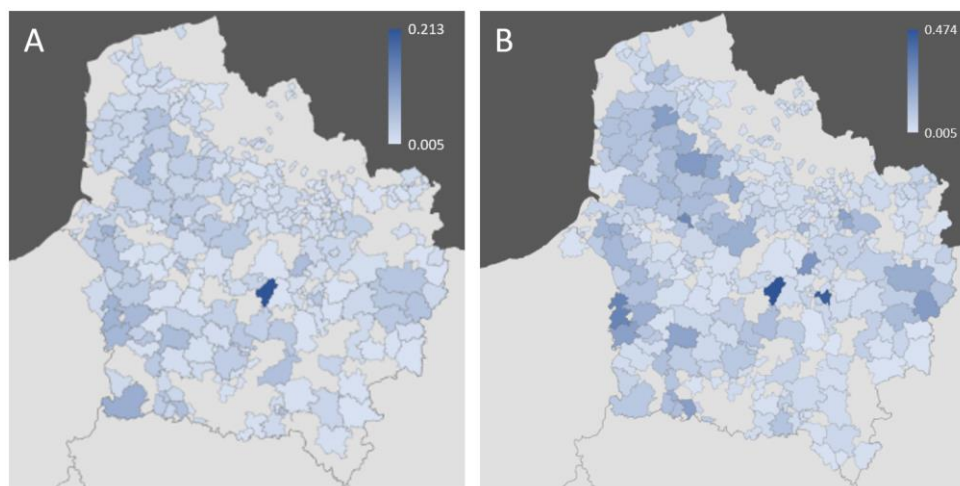


Figure 1. The maximum concentrations of atrazine (A) and its metabolites (B) detected in tap water in the region of Hauts-de-France. Data were from the health control of water distributed commune by commune by the French government “Ministry of Solidarity and Health” on September 2023 [13]. MySQL server was used to comply the data.

Potential health problems may occur if people absorb drinking water obtained from groundwater sources that contain excessive levels of atrazine [16]. It is reported that atrazine is one of the most harmful herbicides, with adverse effects on humans, fish, invertebrates and wildlife [17, 18]. The dangers of atrazine to human health include: As an endocrine disruptor, atrazine can disrupt the hormone balance in the human body [19] and may cause altered nervous system function and reproductive dysfunction [20]; Exposure to atrazine in drinking water is associated with an increased risk of adverse pregnancy outcomes [21, 22]; Atrazine is potentially carcinogenic and increases the incidence of cancers such as breast and ovarian cancer [23]. Exposure to atrazine during embryonic development in zebrafish caused reproductive problems [24], and low concentrations of atrazine (≥ 0.1 ppb) caused hermaphroditism in frogs [25]. Additionally, the endangered species biological assessment [26], published by United States Environmental Protection Agency (USEPA), shows that atrazine may cause harm to some endangered species. Considering the above-mentioned hazards caused by atrazine, more and more efforts are made to degrade atrazine into other low-toxic metabolites or non-toxic small molecules such as water and carbon dioxide. In these existing degradation works, most of them measured the toxicity of atrazine and its metabolites [27, 28], and few made toxicity assessment

of the degradation system [29, 30]. However, there has been no toxicity assessment of different degradation systems.

The purpose of this work is to evaluate the effect of a real matrix (tap water) compared to the model matrix (deionized water) for different techniques. The first part was the degradation of atrazine in tap water and deionized water by HVED and HFUS, and the quantification of atrazine concentration over time. The second part was the normalized statistical analysis of the differences in metabolites between different treatments. The third part was the toxicity test of experimental wastewater from three degradation systems: HVED, HFUS and Fenton oxidation, so as to select more environmentally friendly degradation methods for future work.

2. Materials and methods

2.1. Chemicals and materials

The used tap water was from the laboratory TIMR (Integrated Transformations of Renewable Matter), *Centre de Recherche Royallieu*, Université de Technologie de Compiègne, *CEDEX CS 60319, 60203 Compiègne, France*. The used deionized water (conductivity 0.055 $\mu\text{S}/\text{cm}$ at 25°C) was acquired from a water purification device Rephile Direct-Pure® UP 10 (MA, USA), which was bought from the distributeur Franceeau. LC-MS grade solvents and formic acid were bought from Biosolve Chimie (Dieuze, France). Atrazine (ATZ) and the internal standard ATZ-D5 were bought from Sigma-Aldrich (St. Quentin Fallavier, France).

The high frequency ultrasound (HFUS) was a 250-mL cup-shaped horn-type ultrasonic reactor purchased from SinapTec (Lezennes, France), and passed through a constant frequency of 525 kHz with 80 W power. The air flow was passed through the interlayer of the inner and outer walls to stabilize the temperature at 50 °C.

The high voltage electrical discharge (HVED) was applied in a treatment chamber with a capacity of 1 L, using an electrical generator (Basis, Saint-Quentin, France) supplying a voltage of 40 kV, a current of 10 kA, and a frequency of 1 Hz. The generated pulses have a duration of approximately 10 μs . The total processing

time was 16 min 40 s, that is 1000 s (the total effective time was 10 ms).

MS-DIAL software was a universal program for untargeted metabolomics, developed by Prof. Masanori Arita team (RIKEN) and Prof. Oliver Fiehn team (UC Davis) [31]. In this work, the version '4.9.221218 Windows x64' was used.

2.2. Four solutions with/without the addition of ATZ treated by HVED and HFUS

The four solutions included (1) 20 mg/L ATZ in deionized water; (2) 20 mg/L atrazine in tap water; (3) only deionized water; (4) only tap water. They were treated by HVED and HFUS, and the experiments were shown in [Table 1](#).

Table 1. Experiments of four solutions with/without the addition of ATZ treated by HVED and HFUS

Experiment	Solution	Treatment	Operation
HVED ATZ DW	20 mg/L ATZ in deionized water	HVED	The solution (250 mL) was treated for 16 min 40 s (effective time 10 ms). Samples were taken at 0, 1, 2, 4, 7, 10 ms of effective time, corresponding to T ₀ , T ₁ , T ₂ , T ₃ , T ₄ , T ₅ .
HVED ATZ TW	20 mg/L atrazine in tap water		
HVED DW	Only deionized water		
HVED TW	Only tap water		
HFUS ATZ DW	20 mg/L ATZ in deionized water	HFUS	The solution (100 mL) was treated for 2 h. Samples were taken at 0, 30, 60, 90, 120 min, corresponding to T ₀ , T ₁ , T ₂ , T ₃ , T ₄ .
HFUS ATZ TW	20 mg/L atrazine in tap water		
HFUS DW	Only deionized water		
HFUS TW	Only tap water		

2.3. Normalization and statistical analysis of the above four solutions after HVED/HFUS treatment

After HVED/HFUS treatment, samples were analyzed by high performance liquid chromatography coupled with high resolution mass spectrometry (HPLC-HRMS) to obtain MS raw data which were converted into ABF (analysis base file) format by the software "AnalysisBaseFileConverter.exe".

Normalization and statistical analysis in MS-DIAL version 4.9 software: The obtained ABF files were imported in MS-DIAL. LOWESS normalization was performed using the internal standard compound information. All quality control (QC) samples were recognized as 'quality control' and the injection order was set. All metabolite peaks were divided by the ion abundance of alignment spot ID (Internal standard ID). Output the alignment result and export peak intensity files containing the sample name, metabolite name, m/z and retention time in .csv format. Use MetaboAnalyst 6.0 to [27] perform visual and statistical analysis on these .csv files and produce principal component analysis (PCA) plots for estimating differences between sample groups.

2.4. HPLC-HRMS

ATZ and its metabolites detected and quantified by HPLC-HRMS [14]. A diode array detector (DAD) type HPLC system (Infinity 1290, Agilent Technologies, France), was connected to a hybrid quadrupole time of flight (Q-TOF) mass spectrometer with electrospray ionization (ESI) (Agilent 6538, Agilent Technologies, France). HPLC analyses were performed using a Thermo Hypersil Gold C18 (USP L1) column (100 × 2.1 mm, 1.9 μm, 175 Å) at 40 °C. Eluents A and B consisted of 0.1% (v/v) formic acid in deionized water and 100% acetonitrile, respectively. The elution profile was 0-0.3 min 5% B, 0.3-1.7 min 5-30% B (linear gradient), 1.7-3.5 min 95% B (linear gradient), 3.5-4 min 95% B. The flow rate was 0.600 mL/min. The responses of compounds were measured in positive ESI mode with external calibration. By using the electrospray scan mode with a frequency of 5 Hz in the mass range of 50 to 1200 m/z and an electrospray voltage of 3800 V, fragment voltage of 110 V, positive ion electrospray mass spectra were obtained. The atomizing nitrogen temperature was 350°C, the pressure was 30 psi, and the flow rate was 10 L/min.

2.5. Calibration curve of ATZ

In order to determine the concentration of atrazine in the experimental samples, a calibration curve of atrazine was prepared. The internal standard ATZ-D5 was added to the ATZ standard solutions with certain concentrations to reduce the error. Please see chapter II (Table II.1 and Figure II.2) for more details.

2.6. Toxicity testing of different treatment solutions

The treatment solutions were from our previous work [15], which compared three ATZ degradation methods, HVED, HFUS and Fenton oxidation, and discussed the differences in ATZ degradation efficiency, metabolite generation kinetics, degradation pathways and energy consumption. However, it was unsatisfactory that there was no comparison of the toxicity of these three degradation methods. Therefore, in this work, the toxicity tests of these three ATZ degradation methods will be supplemented.

Referring to our previous work [15], the treatment solution of Fenton oxidation was prepared as follows. The initial ATZ solutions (50 mL, 20 mg/L, 0.093 mmol/L) were poured into 100-mL flat-bottom flasks with magnets, and 5 eq. equivalents of Fenton reagents (The ratio of initial $FeSO_4 \cdot 7H_2O$ or H_2O_2 molar concentration to initial ATZ molar concentration was 5 where $[FeSO_4 \cdot 7H_2O]_0 = [H_2O_2]_0 = 0.467$ mmol/L.) were added. The reaction lasted for 2 h.

The crustacean *D. magna* was used to test the potential toxicity of treatment solutions initially containing ATZ. *D. magna* were cultured according to the OCDE procedure using reconstituted M4 medium mainly containing: $NaHCO_3$ (64.8 g/L); $CaCl_2 \cdot 2H_2O$ (293.8 g/L); $MgSO_4 \cdot 7H_2O$ (123.3 g/L) and KCl (5.8 g/L) with pH between 7 and 8; hardness between 140 and 250 mg/L of $CaCO_3$ and constant oxygenation [32]. Organisms were placed into an experimental chamber with programmed temperature of $20 \pm 2^\circ C$ and artificial photoperiod of 16h:8h (light:dark). Organisms were fed daily, 5 days a week with freshwater algae *Chlorella vulgaris* (8×10^6 cells mL), and the medium was renewed every week.

All toxicity tests were conducted in a chamber under the same abiotic conditions as the culture and protocols and analyses were carried out in accordance with the international OECD Guidelines for immobilization test of *D. magna* [32]. For each replicate, 5 organisms aged less than 24 h, were placed in 20 mL of M4 medium (control) and treatment solutions diluted in M4 medium to obtain 0.1, 0.5, 1.5, 2.5 and 5 mg/L of initial Atrazine. The number of dead organisms was visually assessed after 48 h of exposure [33]. The acute toxicity to *D. magna* was defined as the average concentration that induced death in 50% of

the test organisms (LC₅₀).

3. Results and discussion

3.1. Degradation of ATZ in deionized water and tap water by HVED and HFUS

The effect of background water on ATZ degradation by HVED and HFUS was studied. [Figure 2](#) shows the degradation of ATZ in deionized water and tap water by HVED and HFUS, including four experiments “HVED ATZ DW”, “HVED ATZ TW”, “HFUS ATZ DW” and “HFUS ATZ TW”, the conditions of which are shown in [Table 1](#). The initial atrazine concentration of these solutions was 20 mg/L. The results showed that atrazine was degraded more in deionized water than in tap water, and there are differences in values under different degradation technologies HVED and HFUS. For example, after 120 min of HFUS treatment, the final concentration of ATZ solution in deionized water (9.6 mg/L) was slightly lower than that of atrazine solution in tap water (10.4 mg/L). However, since the measurement error of HPLC-HRMS was about 5%, the difference was not significant. In addition, after 10 ms of HVED treatment, the final concentration of ATZ solution in deionized water (1.8 mg/L) was much lower than that in tap water (4.4 mg/L).

It can be seen that in HVED treatment, background water had a great impact on ATZ degradation. According to the online health monitoring results of tap water quality in different cities by French government, the conductivity of tap water in Compiègne, Oise, is 780 $\mu\text{S}/\text{cm}$ at 25°C, which was updated on December 14, 2023 [34]. In comparison, the used deionized water has lower conductivity of 0.055 $\mu\text{S}/\text{cm}$ at 25°C. The liquid of high conductivity is rich in species that trap solvated electrons, inhibiting atrazine degradation [35]. Besides, the discharge reactor used has two phases, gas and liquid, and the gas phase occupies much more space than the liquid phase. The conductivity in the liquid phase has little effect on the dielectric constant of the entire space, so it has little effect on the overall discharge effect [36]. Therefore, the use of deionized water with low conductivity is more conducive to the degradation of ATZ than tap water.

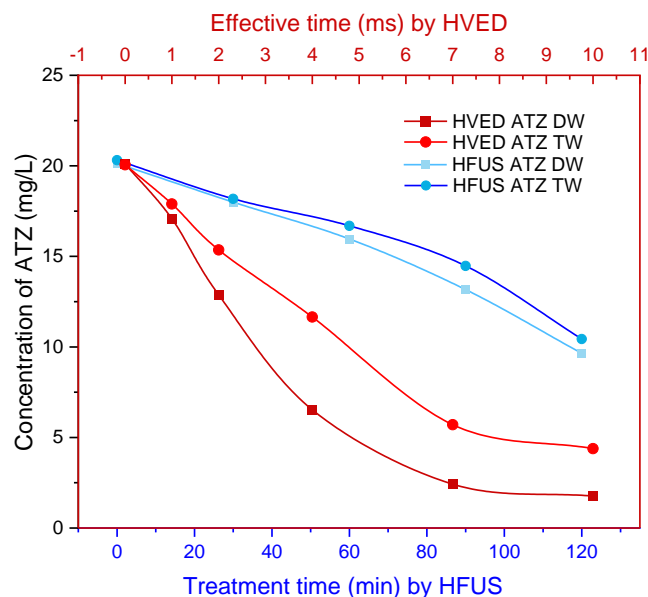


Figure 2. ATZ degradation in deionized water and tap water by HVED and HFUS, including four experiments “HVED ATZ DW”, “HVED ATZ TW”, “HFUS ATZ DW” and “HFUS ATZ TW”, the conditions of which are shown in Table 1. The initial atrazine concentration was 20 mg/L.

3.2. Normalized and statistical results of four solutions treated by HFUS and HVED

Four solutions with/without the addition of atrazine were treated by HFUS and HVED, including eight experiments “HVED ATZ DW”, “HVED ATZ TW”, “HFUS ATZ DW”, “HFUS ATZ TW”, “HVED DW”, “HVED TW”, “HFUS DW” and “HFUS TW”, the conditions of which are shown in Table 1. Figure 3 includes three principal component analysis (PCA) score plots, where (a) shows all these eight experiments, (b) shows only the four HVED-treated experiments, and (c) shows only the four HFUS-treated experiments. The PCA score plot estimates differences in metabolites (235 unassigned molecules) between sample groups of these experiments. A point represents a sample and an ellipse with 95% confidence interval represents the range of a sample group.

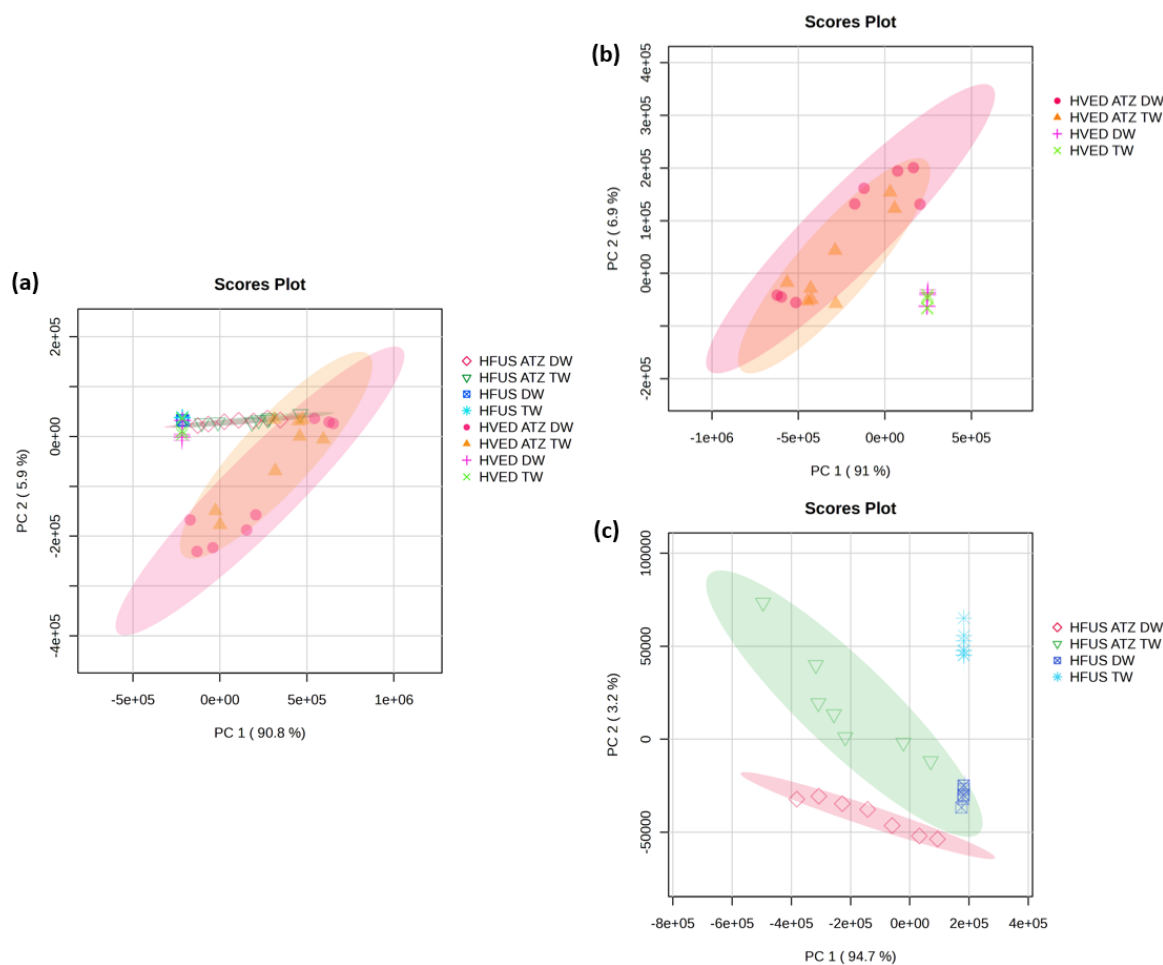


Figure 3. PCA score plot showing differences in metabolites (235 unassigned molecules) of sample groups from experiments “HVED ATZ DW”, “HVED ATZ TW”, “HFUS ATZ DW”, “HFUS ATZ TW”, “HVED DW”, “HVED TW”, “HFUS DW” and “HFUS TW”, the conditions of which are shown in Table 1. The initial atrazine concentration of experiments “HVED ATZ DW”, “HVED ATZ TW”, “HFUS ATZ DW” and “HFUS ATZ TW” was 20 mg/L.

The general distribution of sample groups from these eight experiments is shown in [Figure 3a](#). The two largest ellipses belong to experiments “HVED ATZ DW” and “HVED ATZ TW”, and they partially overlap, indicating that there are differences in the generated metabolites during the HVED treatment of ATZ in deionized water and tap water. This result is consistent with the previous large difference in degradation rates of ATZ in deionized water and tap water by HVED. In tap water, other species competed with ATZ for reactive species (e.g. hydroxyl radicals), which not only resulted in a reduction in ATZ degradation efficiency, but also resulted in a complex reaction system that contained both ATZ metabolites

and metabolites of other species.

In addition, [figure 3a](#) shows two narrow and small ellipses belonging to experiments “HFUS ATZ DW” and “HFUS ATZ TW”. These two ellipses almost overlap, and it seems that the difference in HFUS degradation metabolites of ATZ between deionized water and tap water is small. This requires more detail such as metabolite heatmaps to prove. Besides, the sample group of the other four control experiments “HVED DW”, “HVED TW”, “HFUS DW” and “HFUS TW” cannot form an ellipse, and they are concentrated near $PC2=0$. This shows that there is little difference between HVED/HFUS treatment of only deionized water and only tap water.

In order to better demonstrate the difference in atrazine degradation caused by deionized water and tap water, PCA score plots of four HVED-treated experiments ([Figure 3b](#)) and four HFUS-treated experiments ([Figure 3c](#)) were also shown. In [Figure 3b](#), the ellipses of experiments “HVED ATZ DW” and “HVED ATZ TW” almost overlap, and the sample groups of experiments “HVED DW” and experiments “HVED TW” are concentrated near the zero point. By contrast, in [Figure 3c](#), the ellipses of experiments “HFUS ATZ DW” and “HFUS ATZ TW” do not overlap, and the sample groups of deionized water and tap water are concentrated at different points. This shows that deionized water and tap water have less impact on the generation of metabolites in HVED treatment, but have a greater impact in HFUS treatment.

Due to the differences of the sample groups of experiments “HVED ATZ DW”, “HVED ATZ TW”, “HFUS ATZ DW” and “HFUS ATZ TW” in the PCA score plot ([Figure 3](#)), the atrazine metabolites analysis was performed. Six main generated metabolites of atrazine were found by HPLC-HRMS, and their information are shown in [Table 2](#). The heatmap of these six main generated metabolites of atrazine is shown in [Figure 4](#).

Table 2. Information on ATZ and its six main generated metabolites.

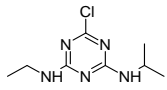
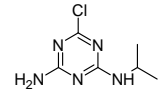
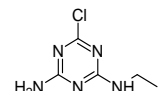
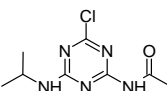
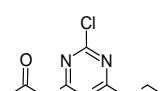
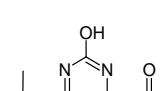
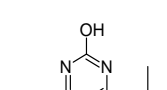
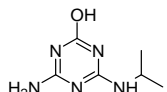
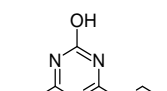
Abbreviation	Structure	Formula	Name	m/z	Retention Time (min)
ATZ		C ₈ H ₁₄ ClN ₅	Atrazine	216.1010	2.53
DEA		C ₆ H ₁₀ ClN ₅	Deethylatrazine	188.0698	1.87
DIA		C ₅ H ₈ ClN ₅	Deisopropylatrazine	174.0541	1.59
CDIT		C ₈ H ₁₂ ClN ₅ O	N-[4-Chloro-6-(isopropylamino)-1,3,5-triazin-2-yl]acetamide	230.0804	2.08
CDET		C ₇ H ₁₀ ClN ₅ O	N-[4-Chloro-6-(ethylamino)-1,3,5-triazin-2-yl]acetamide	216.0647	1.79
ODIT		C ₈ H ₁₃ N ₅ O ₂	N-[4-Hydroxy-6-(isopropylamino)-1,3,5-triazin-2-yl]acetamide	212.1142	1.19
HA		C ₈ H ₁₅ N ₅ O	Hydroxyatrazine	198.1350	1.29
DEHA		C ₆ H ₁₁ N ₅ O	Deethylhydroxyatrazine	170.1037	0.89
DIHA		C ₅ H ₉ N ₅ O	Deisopropylhydroxyatrazine	156.0880	0.67

Figure 4 shows the abundance changes of atrazine metabolites in HVED and HFUS treatments. The dechlorination-hydroxylation products HA, DIHA and DEHA were mainly produced in the electrical discharge's experiments "HVED ATZ DW" and "HVED ATZ TW". This shows that hydroxylation was the main pathway for atrazine degradation during high-voltage electrical discharge treatment. Generally, hydroxylation of atrazine was considered as a detoxification method for the treatment of atrazine-contaminated water due to the conversion into non-toxic hydroxylation products (e.g. HA) [33]. Therefore, in terms of detoxification, HVED treatment is better than HFUS treatment. Besides, impurities in tap water competed with atrazine for reactive oxygen species (hydroxy radicals), causing more HA to

be produced in deionized water than in tap water, accompanied by an increase in the production of secondary products DEHA and DIHA. The dechlorination-hydroxylation pathway is shown in [Figure 5 Pathway I](#).

In addition, the alkyl oxidation products (CDIT and CDET) and the dealkylation products (DEA and DIA), were mainly produced in ultrasound's experiments "HFUS ATZ DW" and "HFUS ATZ TW". This shows that in ultrasound treatment, the reactive species (e.g. hydroxyl radicals) preferred to attack the alkyl chain on the nitrogen atom rather than the chlorine atom on the triazine. The alkyl oxidation pathway and the dealkylation pathway are shown in [Figure 5 Pathway II and III](#). Besides, product ODIT might be from alkyl oxidation of HA in experiments "HVED ATZ DW" and "HVED ATZ TW", or from dechlorination-hydroxylation of CDIT in experiments "HFUS ATZ DW" and "HFUS ATZ TW".

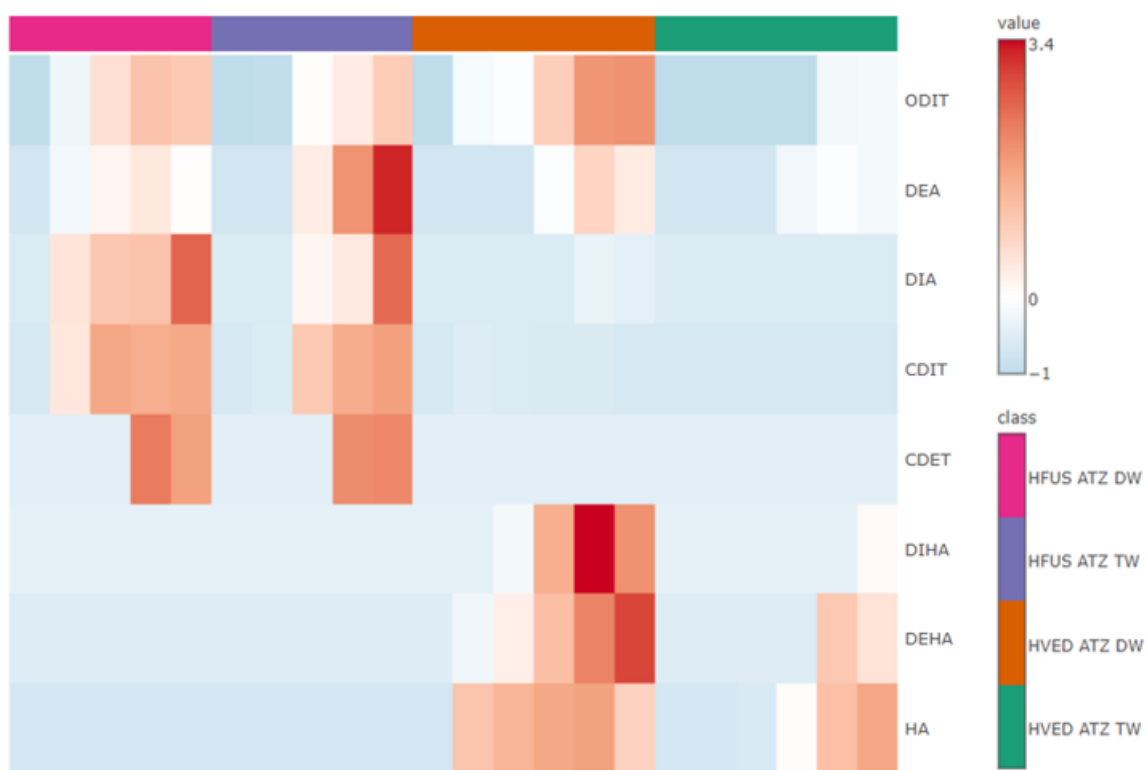


Figure 4. Heatmap of main generated atrazine metabolites of experiments "HVED ATZ DW", "HVED ATZ TW", "HFUS ATZ DW" and "HFUS ATZ TW", the conditions of which are shown in Table 1. For HVED-treated experiments, samples were taken at 0, 1, 2, 4, 7, 10 ms of effective time, corresponding to T_0 , T_1 , T_2 , T_3 , T_4 , T_5 . For HFUS-treated experiments, samples were taken at 0, 30, 60, 90, 120 min, corresponding to T_0 , T_1 , T_2 , T_3 , T_4 . The initial atrazine concentration was 20 mg/L.

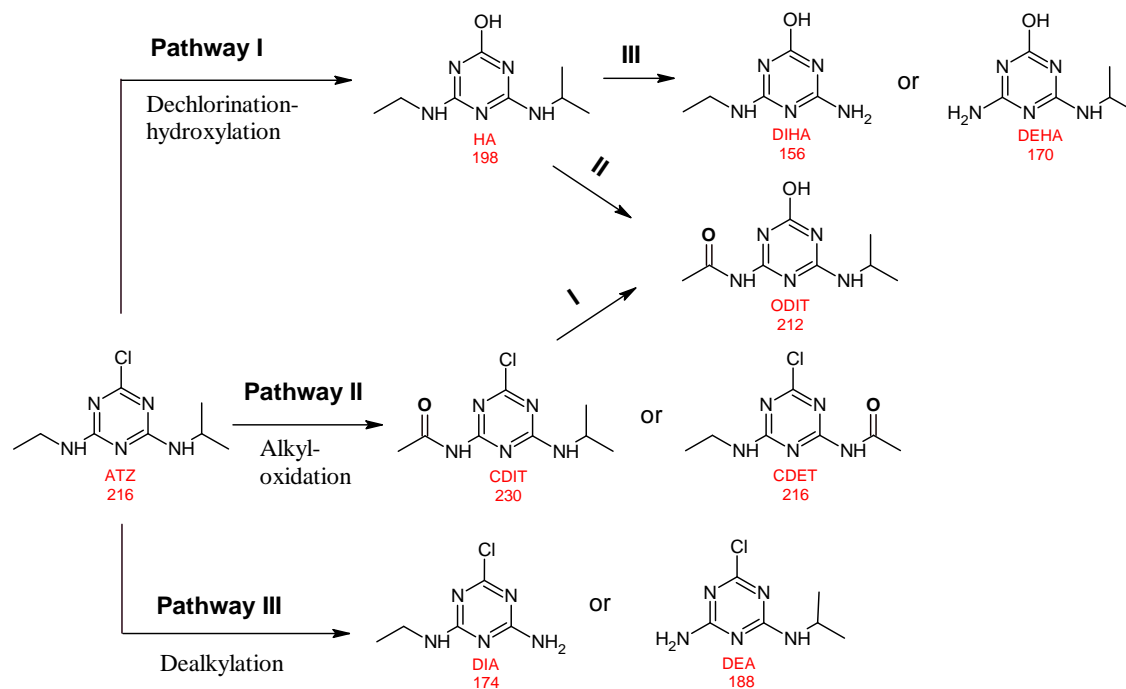


Figure 5. Proposed degradation pathway of atrazine.

3.3. Toxicity testing results of treatment solutions initially containing atrazine

This part is a complement to our previous work [15], comparing the toxicity of final treatment solutions from the experiments of atrazine degradation by three treatment technologies: HVED, HFUS, and Fenton oxidation. As shown in [Table 3](#), the acute toxicity (LC_{50}) in *Daphnia magna* varied from different treatment solutions. The atrazine solution treated by Fenton oxidation ($LC_{50} < 0.1$ mg/L) was more toxic than the blank initial atrazine solution ($LC_{50} = 3.3$ mg/L). Hydrogen peroxide used in Fenton, could be toxic for *Daphnia magna*. To study the toxic effect of Fenton reagents (Fe^{2+} and H_2O_2), only deionized water (no atrazine) was treated by Fenton oxidation, but this result was not obtained because the sample was destroyed. This part of toxicity experiment will be completed in the future. Additionally, the toxicity of atrazine solutions treated by US 525kHz and HVED were $LC_{50} > 5$ mg/L and $1.5 < LC_{50} < 2.5$ mg/L, lower than that of atrazine solution treated by Fenton oxidation. Fenton oxidation was more toxic because of the main generated metabolite ammeline (AM).

Besides, the ferrous ions reagents Fe^{2+} have an impact on the toxicity of treatment solutions. For atrazine solutions treated by US 525 kHz, adding ferrous

ions Fe^{2+} increased the toxicity. Conversely, the addition of ferrous ions Fe^{2+} reduced the toxicity of atrazine solutions treated by HVED. What's more, ferrous ions Fe^{2+} alone (without initial atrazine) shows an LC_{50} greater than other treatment conditions suggesting that the toxicity comes from atrazine or its metabolites.

Table 3. The potential toxicity of treatment solutions initially containing Atrazine.

No.	Experiments	Solution	Operation	Acute toxicity to <i>D. magna</i> ^a
1	Blank	20 mg/L (0.093 mmol/L) atrazine in deionized water	no	$LC_{50} = 3.3 \text{ mg/L}$
2	Fenton oxidation	50 ml: 20 mg/L (0.093 mmol/L) atrazine; 130 mg/L (0.467 mmol/L) $FeSO_4 \cdot 7H_2O$; 0.467 mmol/L H_2O in deionized water.	Stir for 2 h at room temperature.	$LC_{50} < 0.1 \text{ mg/L}$
3	US 525 kHz	50 ml: 20 mg/L (0.093 mmol/L) atrazine in deionized water.		$LC_{50} > 5 \text{ mg/L}$
4	US 525 kHz + Fe^{2+}	50 ml: 20 mg/L (0.093 mmol/L) atrazine; 260 mg/L (0.934 mmol/L) $FeSO_4 \cdot 7H_2O$ in deionized water.	Treat by US 525 kHz for 2h.	$2.5 < LC_{50} < 5 \text{ mg/L}$
5	US 525 kHz + Fe^{2+} (no atrazine)	50 ml: 260 mg/L (0.934 mmol/L) $FeSO_4 \cdot 7H_2O$ in deionized water.		$LC_{50} > 65 \text{ mg/L}$ (Fe^{2+})
6	HVED	250 ml: 20 mg/L (0.093 mmol/L) atrazine in deionized water.		$1.5 < LC_{50} < 2.5 \text{ mg/L}$
7	HVED + Fe^{2+}	250 ml: 20 mg/L (0.093 mmol/L) atrazine; 260 mg/L (0.934 mmol/L) $FeSO_4 \cdot 7H_2O$ in deionized water.	Treat for 16 min 40 s, in a 1 L chamber with an electric generator providing 40 kV voltage, 10 kA current, and 1 Hz frequency.	$LC_{50} = 3.3 \text{ mg/L}$
8	HVED + Fe^{2+} (no atrazine)	250 ml: 260 mg/L (0.934 mmol/L) $FeSO_4 \cdot 7H_2O$ in deionized water.		$LC_{50} = 45.9 \text{ mg/L}$ (Fe^{2+})

^a Acute toxicity (LC_{50}) in *Daphnia magna* exposed to treatment solutions with or without initial presence of atrazine.

4. Conclusion

The degradation of atrazine in tap water and atrazine in deionized water were compared, and two degradation methods, HFUS and HVED, were adopted. The degradation efficiency of atrazine in deionized water by HVED/HFUS treatment was higher than that in tap water with the same initial atrazine concentration. The samples from eight experiments “HVED ATZ DW”, “HVED ATZ TW”, “HFUS ATZ DW”, “HFUS ATZ TW”, “HVED DW”, “HVED TW”, “HFUS DW” and “HFUS TW”, were analysed by HPLC-HRMS, and the data were imported into MS-DIAL software for normalization and statistical analysis. MetaboAnalyst 6.0 was adopted to obtain the principal component analysis (PCA) score plot, in which the range of sample groups can be shown in 95% confidence interval ellipses. Based on the heatmap of ATZ metabolites, the correlation between ATZ metabolites, adopted treatment and water was obtained. The results showed that the HVED method promoted the hydroxyl substitution of atrazine to produce the less toxic hydroxyatrazine (HA). The acute toxicity (LC_{50}) in *Daphnia magna* was used to evaluate the toxicity of different treatment solutions initially containing atrazine. The results proved that the atrazine solution treated by Fenton oxidation was toxic, and the toxicity ($LC_{50} < 0.1$ mg/L) was much higher than that treated by HFUS ($LC_{50} > 5$ mg/L) and HVED ($1.5 < LC_{50} < 2.5$ mg/L), which was consistent with our previous work [14, 15]. From the perspective of environmental protection, the alternative HFUS and HVED methods are more favoured for atrazine degradation than conventional chemical oxidation methods.

V.3. Chapter conclusion

This chapter focuses on practical applications and environmental issues, and the main purpose is to evaluate the effect of real matrix (tap water) versus model matrix (deionized water) on atrazine degradation by high voltage electrical discharge (HVED) and high frequency ultrasound (HFUS) techniques. This chapter involves three parts of work:

The first part is the degradation of atrazine in tap water and deionized water by HVED and HFUS, and atrazine was quantified over time by Liquid Chromatography and High-Resolution Mass Spectrometry (HPLC-HRMS)

analytical method (validated in Chapter III). The results showed that in HVED treatment, atrazine was degraded more in deionized water than in tap water, which may be related to the conductivity of the water. By contrast, in HFUS treatment, the degradation of atrazine in tap water and deionized water showed little difference in value.

The second part is the normalized statistical analysis of the differences in metabolites between different treatments. The principal component analysis (PCA) score plots were obtained, in which the range of sample groups can be shown in 95% confidence interval ellipses. The heatmap of degradation metabolites showed that the HVED treatment promoted the hydroxyl substitution of atrazine to produce the less toxic hydroxyatrazine (HA).

The third is the toxicity test of experimental wastewater from three degradation processes HVED, HFUS and Fenton oxidation, which is a supplement to the work in Chapter IV. The acute toxicity (LC_{50}) in *Daphnia magna* was used to evaluate the toxicity of different treatment solutions initially containing atrazine. The results proved that the atrazine solution treated by Fenton oxidation ($LC_{50} < 0.1$ mg/L) was more toxic than that treated by HFUS ($LC_{50} > 5$ mg/L) and HVED ($1.5 < LC_{50} < 2.5$ mg/L). This result was consistent with the speculation of Chapter IV. Therefore, from the perspective of environmental protection, the alternative HFUS and HVED methods are more favored for atrazine degradation.

V.4. References

- [1] Europe's groundwater – A key resource under pressure, Publications Office of the European Union, Copenhagen, 2022.
- [2] Résultats du contrôle sanitaire de l'eau distribuée commune par commune, 2024.
- [3] T.B. Hayes, A. Collins, M. Lee, A. Vonk, Hermaphroditic, demasculinized frogs after exposure to the herbicide atrazine at low ecologically relevant doses, *Proceedings of the National Academy of Sciences* 99 (2002) 5476-5480.
- [4] S. Wirbisky, G. Weber, M. Sepúlveda, T. Lin, An embryonic atrazine exposure results in reproductive dysfunction in adult zebrafish and morphological alterations in their offspring, *Scientific Reports* 6 (2016) 21337.
- [5] M. Kucka, K. Pogrmic-Majkic, S. Fa, S.S. Stojilkovic, Atrazine acts as an endocrine disrupter by inhibiting cAMP-specific phosphodiesterase-4, *Toxicology and Applied Pharmacology* 265 (2012) 19-26.
- [6] C. Hopenhayn-Rich, M.L. Stump, S.R. Browning, Regional assessment of atrazine exposure and incidence of breast and ovarian cancers in kentucky, *Arch. Environ. Contam. Toxicol.* 42 (2002) 127-136.
- [7] N. Baran, A.E. Rosenbom, R. Kozel, D. Lapworth, Pesticides and their metabolites in European groundwater: Comparing regulations and approaches to monitoring in France, Denmark, England and Switzerland, *Science of The Total Environment* 842 (2022) 156696. <https://doi.org/https://doi.org/10.1016/j.scitotenv.2022.156696>.
- [8] I.S. Zektser, L.G. Everett, *Groundwater resources of the world and their use*, UNESCO, Paris, France, 2004.
- [9] N. Voulvoulis, K.D. Arpon, T. Giakoumis, The EU Water Framework Directive: From great expectations to problems with implementation, *Science of The Total Environment* 575 (2017) 358-366. <https://doi.org/https://doi.org/10.1016/j.scitotenv.2016.09.228>.
- [10] E.E. Agency, Europe's groundwater – A key resource under pressure, 2022. <https://www.eea.europa.eu/publications/europes-groundwater>. (Accessed January 24 2024).
- [11] N. Baran, N. Surdyk, C. Auterives, Pesticides in groundwater at a national scale (France): Impact of regulations, molecular properties, uses, hydrogeology and climatic conditions, *Science of The Total Environment* 791 (2021) 148137. <https://doi.org/https://doi.org/10.1016/j.scitotenv.2021.148137>.
- [12] E. Union, Directive 2006/118/EC of the European Parliament and of the Council of 12 December 2006 on the protection of groundwater against pollution and deterioration, *Official Journal of the European Communities*, 2006, pp. 19-31.

- [13] M.d.S.e.d.l. Santé, Résultats du contrôle sanitaire de l'eau distribuée commune par commune, 2024. <https://www.data.gouv.fr/fr/datasets/resultats-du-contrôle-sanitaire-de-leau-distribuee-commune-par-commune/>. (Accessed January 24 2024).
- [14] J. Hong, N. Boussetta, G. Enderlin, N. Grimi, F. Merlier, Real-Time Monitoring of the Atrazine Degradation by Liquid Chromatography and High-Resolution Mass Spectrometry: Effect of Fenton Process and Ultrasound Treatment, *Molecules*, 2022.
- [15] J. Hong, N. Boussetta, G. Enderlin, F. Merlier, N. Grimi, Degradation of herbicide atrazine in water by high voltage electrical discharge in comparison with Fenton oxidation and ultrasound treatments, *RSC Sustainability* 1(6) (2023) 1462-1470. <https://doi.org/10.1039/d3su00103b>.
- [16] J.L. Rinsky, C. Hopenhayn, V. Golla, S. Browning, H.M. Bush, Atrazine Exposure in Public Drinking Water and Preterm Birth, *Public Health Reports* 127(1) (2012) 72-80. <https://doi.org/10.1177/003335491212700108>.
- [17] R. Eisler, Atrazine Hazards to Fish, Wildlife, and Invertebrates: A Synoptic Review, Contaminant Hazard Reviews, Laurel, MD, 1989.
- [18] D.W. Gammon, C.N. Aldous, W.C. Carr Jr, J.R. Sanborn, K.F. Pfeifer, A risk assessment of atrazine use in California: human health and ecological aspects, *Pest Management Science* 61(4) (2005) 331-355. <https://doi.org/https://doi.org/10.1002/ps.1000>.
- [19] M. Kucka, K. Pogrmic-Majkic, S. Fa, S.S. Stojilkovic, R. Kovacevic, Atrazine acts as an endocrine disrupter by inhibiting cAMP-specific phosphodiesterase-4, *Toxicology and Applied Pharmacology* 265(1) (2012) 19-26. <https://doi.org/https://doi.org/10.1016/j.taap.2012.09.019>.
- [20] S.C. Stradtman, J.L. Freeman, Mechanisms of Neurotoxicity Associated with Exposure to the Herbicide Atrazine, *Toxics*, 2021.
- [21] M. Goodman, J.M. Mandel Js Fau - DeSesso, A.R. DeSesso Jm Fau - Scialli, A.R. Scialli, Atrazine and pregnancy outcomes: a systematic review of epidemiologic evidence, *Birth Defects Research Part B* 101 (2014) 215-236. <https://doi.org/10.1002/bdrb.21101>.
- [22] P.D. Winchester, J. Huskins, J. Ying, Agrichemicals in surface water and birth defects in the United States, *Acta Paediatrica* 98(4) (2009) 664-669. <https://doi.org/https://doi.org/10.1111/j.1651-2227.2008.01207.x>.
- [23] C. Hopenhayn-Rich, M.L. Stump, S.R. Browning, Regional assessment of atrazine exposure and incidence of breast and ovarian cancers in Kentucky, *Archives of Environmental Contamination and Toxicology* 42(1) (2002) 127-36. <https://doi.org/10.1007/s002440010300>.
- [24] S.E. Wirbisky, G.J. Weber, M.S. Sepúlveda, T.-L. Lin, A.S. Jannasch, J.L. Freeman, An embryonic atrazine exposure results in reproductive dysfunction in adult zebrafish and morphological alterations in their offspring, *Scientific Reports* 6(1) (2016) 21337. <https://doi.org/10.1038/srep21337>.

- [25] T.B. Hayes, A. Collins, M. Lee, M. Mendoza, N. Noriega, A.A. Stuart, A. Vonk, Hermaphroditic, demasculinized frogs after exposure to the herbicide atrazine at low ecologically relevant doses, *Proceedings of the National Academy of Sciences* 99(8) (2002) 5476-5480. <https://doi.org/10.1073/pnas.082121499>.
- [26] USEPA, Final National Level Listed Species Biological Evaluation for Atrazine, 2021. <https://www.epa.gov/endangered-species/final-national-level-listed-species-biological-evaluation-atrazine>. (Accessed January 24 2024).
- [27] Š. Klementová, L. Hornychová, M. Šorf, J. Zemanová, D. Kahoun, Toxicity of atrazine and the products of its homogeneous photocatalytic degradation on the aquatic organisms *Lemna minor* and *Daphnia magna*, *Environmental Science and Pollution Research* 26(26) (2019) 27259-27267. <https://doi.org/10.1007/s11356-019-05710-0>.
- [28] N. Hu, Y. Xu, C. Sun, L. Zhu, S. Sun, Y. Zhao, C. Hu, Removal of atrazine in catalytic degradation solutions by microalgae *Chlorella* sp. and evaluation of toxicity of degradation products via algal growth and photosynthetic activity, *Ecotoxicology and Environmental Safety* 207 (2021) 111546. <https://doi.org/https://doi.org/10.1016/j.ecoenv.2020.111546>.
- [29] W. Jia, H. Wang, Q. Wu, L. Sun, Q. Si, Q. Zhao, Y. Wu, N. Ren, W. Guo, Insight into Chinese medicine residue biochar combined with ultrasound for persulfate activation in atrazine degradation: *Acanthopanax senticosus* precursors, synergistic effects and toxicity assessment, *Science of The Total Environment* 880 (2023) 163054. <https://doi.org/https://doi.org/10.1016/j.scitotenv.2023.163054>.
- [30] Y. Wang, T. Lin, H. Chen, Degradation of atrazine by a UV-activated organic chloramines process: kinetics, degradation pathways, disinfection by-product formation, and toxicity changes, *Chemical Engineering Journal* 468 (2023) 143788. <https://doi.org/10.1016/j.cej.2023.143788>.
- [31] H. Tsugawa, T. Cajka, T. Kind, Y. Ma, B. Higgins, K. Ikeda, M. Kanazawa, J. VanderGheynst, O. Fiehn, M. Arita, MS-DIAL: data-independent MS/MS deconvolution for comprehensive metabolome analysis, *Nature Methods* 12(6) (2015) 523-526. <https://doi.org/10.1038/nmeth.3393>.
- [32] O.f.E.C.a. Development, Test No. 202: *Daphnia* sp. Acute Immobilisation Test, OECD iLibrary2004. <https://doi.org/10.1787/9789264069947-en>.
- [33] C.D.E.E.A.E.D.Q. (CEAEQ), Détermination de la toxicité : létalité (CL₅₀ 48h) chez la daphnie *Daphnia magna*. MA. 500 – *D. mag.* 1.1, Rév. 3., in: M.d.I.E.e.d.I.L.c.l.c.c.d. Québec (Ed.) Québec, 2021, p. 18.
- [34] d.I.S.e.d.S. Ministère du Travail, Qualité de l'eau potable, 2024. <https://sante.gouv.fr/sante-et-environnement/eaux/eau>. (Accessed January 24 2024).
- [35] W. Haixia, F. Zhi, X. Yanhua, Degradation of aniline wastewater using dielectric barrier discharges at atmospheric pressure, *Plasma Science and Technology* 17(3) (2015) 228.

[36] D.R. Grymonpré, A.K. Sharma, W.C. Finney, B.R. Locke, The role of Fenton's reaction in aqueous phase pulsed streamer corona reactors, Chemical Engineering Journal 82(1) (2001) 189-207. [https://doi.org/https://doi.org/10.1016/S1385-8947\(00\)00345-4](https://doi.org/https://doi.org/10.1016/S1385-8947(00)00345-4).

General Conclusion and Prospects

Pesticide residues in agricultural production remain in the soil, flow in surface water, and seep into groundwater, which seriously affects the ecosystem and human health. In the degradation of pesticides, one of the most challenging research focuses is atrazine, an herbicide widely used in farmland and roadside, due to its refractory degradation, water solubility, complex metabolism and toxicity. The degradation study of atrazine is also a reference for other pesticides (such as chloridazon). This work responds well to the Water Framework Directive proposed by the European Commission and the Sustainable Development Goals (SDGs) proposed by the United Nations.

This thesis focuses on the degradation of pesticide atrazine in water, and involves three stages, as follows:

(1) Establishment of analytical methods: A new analytical method by high performance liquid chromatography-high resolution mass spectrometry (HPLC-HRMS) was developed for the qualification and quantification of atrazine and its metabolites during degradation processes.

Real-time monitoring of the evolution of atrazine and its metabolites during Fenton reaction or US degradation processes by HPLC-HRMS was demonstrated to be feasible. In our self-designed online analysis experimental setup, automatic sampling was coupled with the HPLC-HRMS system. This avoids sample transfer and storage that leads to degradation of potentially unstable metabolites during point sampling. This online analytical method greatly improved the measurement accuracy, increased the sampling frequency, shortened the sample analysis time (4 min), and provided a good way to track each metabolite.

(2) Development of degradation technology: As an emerging technology in water treatment, high voltage electrical discharge (HVED) was adopted and compared with traditional pesticide degradation technologies Fenton oxidation and ultrasound (US) treatment.

At the same initial atrazine concentration, the effects of three degradation techniques HVED, Fenton oxidation and US on atrazine degradation were studied, and their possible degradation pathways were proposed based on the formation

kinetics of the detected 19 metabolites. Compared with the long atrazine degradation time (2h) and toxic degradation metabolite ammeline (AM) in Fenton oxidation, HVED has more efficient degradation efficiency (89%, 10 ms discharge time) and less toxic degradation metabolite Hydroxyatrazine (HA). The energy consumption of HVED was much lower than that of ultrasound when achieving same degradation rates of atrazine. The use of HVED technology has application prospects in the degradation of atrazine.

(3) Application in actual environments: Attempts were made to degrade atrazine in tap water.

The aim was to evaluate the effect of real matrix (tap water) versus model matrix (deionized water) on atrazine degradation by different techniques HVED and US treatment. The degradation efficiency of atrazine in deionized water by HVED and high frequency ultrasound (HFUS), was higher than that in tap water with the same initial atrazine concentration. Normalized statistical analysis was used to distinguish differences in atrazine metabolites during different degradation processes. The acute toxicity (LC_{50}) in *Daphnia magna* was used to evaluate the toxicity of different treatment solutions initially containing atrazine. The atrazine solution treated by Fenton oxidation ($LC_{50} < 0.1$ mg/L) was much more toxic than that treated by HFUS ($LC_{50} > 5$ mg/L) and HVED ($1.5 < LC_{50} < 2.5$ mg/L).

In summary, our self-designed online monitoring system provides new ideas for pesticide tracking through HPLC-HRMS; the degradation of atrazine in water through HVED technology was successfully achieved, and was proven to be superior to traditional water treatment methods, Fenton oxidation and US; the degradation of atrazine was applied in real matrix tap water.

However, since this thesis is still in the model research stage, there are still many problems that need to be solved, especially in terms of practical applications. The prospects are as follows:

(1) Study the degradation of other widely used pesticides such as chloridazon.

(2) Study the degradation of mixed pesticides in water.

(3) Optimize the analytical system, to expand the upper and lower detection limits and improve detection accuracy.

(4) Study the degradation of pesticide in other real matrix such as agricultural wastewater, winemaking effluent.

(5) Apply HVED technology to the medium or industrial scale wastewater treatment.

(6) Quantify H_2O_2 during US and HVED processes for the radical mechanism study.

(7) In addition to iron catalysts, other metal catalysts can also be tried.

(8) Measure the total organic carbon (TOC) for mineralization rate of atrazine.

(9) Degrade atrazine by US in a pulsed state may reduce energy consumption.

(10) Study the effect of the species in water with high conductivity on atrazine degradation during discharge. For example, add different electrolytes into treatment solutions.